THE JOURNAL

OF THE

AMERICAN CERAMIC SOCIETY

JUNE 1, 1942

MONTHLY PUBLICATION DEVOTED TO THE ARTS AND SCIENCES RELATED TO THE SILICATE INDUSTRIES

TABLE OF CONTENTS

Vol. 25 June 1, 1942 No. 10

THE JOURNAL

System CaO–FeO–Al_2O_3–SiO_2: I, Results of Quenching Experiments on Five Joins 241–74
By J. F. Schairer

An Improved Mercury Balance Volumeter 275–77
By Sidney Speil and Hewitt Wilson

Red Silver Glasses 278–80
By Edward Forst, Jr., and N. J. Kreidl

Effect of Tin in Gold Ruby Glass 280–81
By F. M. Veazie and W. A. Weyl

Preparation of Refractory and of Coal-Ash Test Cones 282
By Russell J. Smith

Publication Office: 20th & Northampton Sts., Easton, Pa.
Editorial Office: 2525 N. High St., Columbus, Ohio
Entered as second-class matter at the post office at Easton, Pa., under the act of March 3, 1879. Published monthly.
Subscription fifteen dollars ($15.00) a year. Single numbers $1.50
(Foreign and Canadian postage, 50¢ additional on subscriptions)
(Copyright 1941, American Ceramic Society, Inc.)

THE AMERICAN CERAMIC SOCIETY TRUSTEES AND OFFICERS FOR 1942–1943

President: Louis J. Trostel, General Refractories Co., Baltimore, Md.
Vice-President: M. E. Holmes, N. Y. State College of Ceramics, Alfred, N. Y.
Treasurer: C. Forrest Tefft, The Claycraft Co., Columbus, Ohio
Secretary-Editor: R. C. Purdy, 2525 North High St., Columbus, Ohio
Past-President: J. T. Littleton, Corning Glass Works, Corning, N. Y.
Past-President: J. L. Carruthers, Ohio State University, Columbus, Ohio

TRUSTEES FROM INDUSTRIAL DIVISIONS*

Art: L. E. Barringer, General Electric Co., Schenectady, N. Y. (1943)
Enamel: J. E. Hansen, Ferro Enamel Corp., Cleveland, Ohio (1943)
Glass: G. W. Morey, Geophysical Laboratory, Washington, D. C. (1944)
Materials and Equipment: J. E. Eagle, Vitro Mfg. Co., Pittsburgh, Pa. (1945)
Refractories: J. D. Sullivan, Battelle Memorial Institute, Columbus, Ohio (1943)
Structural Clay Products: Frederick Heath, Jr., Colonial Clays, Inc., Worcester, Mass. (1945)
White Wares: F. P. Hall, Onondaga Pottery Co., Syracuse, N. Y. (1944)
Institute of Ceramic Engineers: H. G. Wolfram, Porcelain Enamel & Mfg. Co., Baltimore, Md. (1944)
Ceramic Educational Council: J. W. Whittemore, Virginia Polytechnic Institute, Blacksburg, Va. (1944)

* Date of expiration of term of office in parentheses.

DIVISION OFFICERS

Art
Chairman: J. A. Foster, 9591 Sorrento Ave., Detroit, Mich.
Secretary: Marion L. Fosdick, N. Y. State College of Ceramics, Alfred, N. Y.

Enamel
Chairman: Karl Kautz, Climax Molybdenum Co., First National Bank Bldg., Canton, Ohio
Secretary: D. G. Moore, National Bureau of Standards, Washington, D. C.

Glass
Chairman: W. C. Taylor, Corning Glass Works, Corning, N. Y.
Secretary: S. R. Scholes, N. Y. State College of Ceramics, Alfred, N. Y.

Materials and Equipment
Chairman: J. F. McMahon, N. Y. State College of Ceramics, Alfred, N. Y.
Secretary: J. R. Kauffman, Allied Engineering Co., 29 Highland Drive, Milltown, N. J.

Refractories
Chairman: R. S. Bradley, A. P. Green Fire Brick Co., Mexico, Mo.
Secretary: W. R. Kerr, Armstrong Cork Co., Beaver Falls, Pa.

Structural Clay Products
Chairman: R. A. Shipley, National Fireproofing Corp., Pittsburgh, Pa.
Secretary: E. F. Theobald, Metropolitan Paving Brick Co., Canton, Ohio

White Wares
Chairman: F. C. Henderson, Hall China Co., East Liverpool, Ohio
Secretary: J. R. Beam, Universal Sanitary Mfg. Co., New Castle, Pa.

OFFICERS OF THE FELLOWS

Dean: R. B. Sosman, U. S. Steel Corp., Kearny, N. J.
Associate Dean: T. N. McVay, University of Alabama, University, Ala.
Secretary-Treasurer: R. M. King, Ohio State University, Columbus, Ohio

INSTITUTE OF CERAMIC ENGINEERS

President: H. M. Kraner, Bethlehem Steel Co., Bethlehem, Pa.
Vice-President: H. B. DuBois, Consolidated Feldspar Corp., Trenton, N. J.
Secretary: H. G. Schurecht, New York State College of Ceramics, Alfred, N. Y.

CERAMIC EDUCATIONAL COUNCIL

President: N. W. Taylor, Pennsylvania State College, State College, Pa.
Vice-President: R. M. Campbell, N. Y. State College of Ceramics, Alfred, N. Y.
Secretary: C. M. Dodd, Iowa State College, Ames, Iowa

LOCAL SECTIONS

Baltimore-Washington
Chairman: Kenneth M. Smith, Severn Clay Co., Baltimore, Md.
Secretary: W. R. Lester, Maryland Glass Corp., Baltimore, Md.

Central Ohio
Chairman: H. J. Orlowski, O.S.U. Engr. Expt. Sta., Columbus, Ohio
Secretary: A. C. Jackson, The Claycraft Co., Columbus, Ohio

Chicago
Chairman: H. G. Fisk, Armour Research Foundation, Inc., Chicago, Ill.
Secretary: C. R. Filippi, Illinois Brick Co., Chicago, Ill.

Michigan-Northwestern Ohio
Chairman: J. A. Foster, 9591 Sorrento Ave., Detroit, Mich.
Secretary: A. R. Decker, Champion Spark Plug Co., Detroit, Mich.

Northern California
Chairman: G. A. Page, Stockton Fire Brick Co., Pittsburg, Calif.
Secretary: B. W. Wyatt, N. Clark & Sons, Alameda, Calif.

Pacific-Northwest
President: M. D. Saindon, Chehalis Brick & Tile Co., Chehalis, Wash.
Secretary: W. P. Keith, Univ. of Washington, Seattle, Wash.

Pittsburgh
Chairman: G. J. Bair, Mellon Institute, Pittsburgh, Pa.
Secretary: R. M. Shremp, Lava Crucible Co., Zelienople, Pa.

Southern California
Chairman: J. E. Stevens, Emsco Refractories Co., South Gate, Calif.
Secretary: R. F. Evans, Gladding, McBean & Co., Los Angeles, Calif.

St. Louis
Chairman: H. H. Hanna, Pittsburgh Plate Glass Co., Crystal City, Mo.
Secretary: J. H. Ivery, Hydraulic Press Brick Co., St. Louis, Mo.

THE JOURNAL

OF

THE AMERICAN CERAMIC SOCIETY

Vol. 25 June 1, 1942 No. 10

THE SYSTEM CaO–FeO–Al_2O_3–SiO_2: I, RESULTS OF QUENCHING EXPERIMENTS ON FIVE JOINS*

By J. F. Schairer

Contents

I. Introduction 241
II. Limiting Systems 242
(1) CaO–FeO–SiO_2 (Fig. 1) 243
(2) CaO–Al_2O_3–SiO_2 (Fig. 2) 244
(3) FeO–Al_2O_3–SiO_2 (Figs. 3 and 4); Table I 244
(4) CaO–FeO–Al_2O_3 244
III. The Quaternary System 244
(1) Experimental Procedure 244
(2) Fe_2O_3 Content of Liquid Phase 246
(3) Glasses 246
(4) Presentation of Quaternary Data 246
(5) Joins in the Quaternary System (Figs. 5 and 6) 248
(6) Diagrams for the Joins 249
(A) Join SiO_2–Anorthite–FeO (Fig. 7); Table II 253
(B) Join Anorthite–Al_2O_3–FeO (Fig. 8); Table III 253
(C) Join $CaSiO_3$–Anorthite–FeO (Fig. 9); Table IV 255
(D) Join Gehlenite–Anorthite–FeO (Fig. 10); Table V 262
(E) Join $CaSiO_3$–Gehlenite–FeO (Fig. 11); Table VI 262
(7) Crystalline Solid Phases 263
(8) Univariant Lines and the Quaternary Invariant Points 265
(A) Univariant Lines (Fig. 12); Tables VII and VIII 265
(B) Maxima and Minima in Univariant Lines 267
(C) Tie Lines and Composition Planes 268
(D) Temperatures and Compositions of Eleven Quaternary Invariant Points 268
(9) Crystallization 272
(10) Observations of Interest to the Geologist or Petrologist 273
(11) Technologic Applications 273
IV. Summary 274

I. Introduction

Some years ago studies on the melting behavior of the silicates of ferrous iron were undertaken. Several papers presenting the melting relations of important systems with FeO or a ferrous silicate as one of the components have already appeared.[1] These laboratory investigations of silicate systems were undertaken as part of the silicate program at the Geophysical Laboratory on the fundamental chemistry of igneous rocks and rock-forming minerals.

The ultimate source of an igneous rock is its parent magma—a molten solution of complex silicates. Of the various oxides that enter into the composition of the rock-forming minerals (particularly the pyroxenes, olivines, and amphiboles), SiO_2, Al_2O_3, iron oxides, MgO, and CaO are of greatest importance. In order to obtain more definite information about the nature of

* Presented at the Forty-Third Annual Meeting, The American Ceramic Society, Baltimore, Md., April 1, 1941 (Symposium on Phase Equilibria, Refractories Division). Received December 11, 1941.

[1] (*a*) N. L. Bowen and J. F. Schairer, "System FeO–SiO_2," *Amer. Jour. Sci.*, **24** [141] 177–213 (1932); *Ceram. Abs.*, **12** [2] 83 (1933).

(*b*) N. L. Bowen, J. F. Schairer, and E. Posnjak, "System Ca_2SiO_4–Fe_2SiO_4," *Amer. Jour. Sci.*, **25** [4] 273–97 (1933).

(*c*) N. L. Bowen, J. F. Schairer, and E. Posnjak, "System CaO–FeO–SiO_2," *ibid.*, **26**, 193–284 (1933).

(*d*) N. L. Bowen and J. F. Schairer, "System MgO–FeO–SiO_2," *ibid.*, **29**, 151–217 (1935); *Ceram Abs.*, **15** [9] 288 (1936).

(*e*) N. L. Bowen and J. F. Schairer, "System Albite–Fayalite," *Proc. Nat. Acad. Sci.*, **22** [6] 345–50 (1936); *Ceram. Abs.*, **15** [10] 315 (1936).

(*f*) N. L. Bowen and J. F. Schairer, "Crystallization Equilibrium in Nepheline–Albite–Silica Mixtures with Fayalite," *Jour. Geol.*, **46** [No. 3, Part II] 397–411 (1938); *Ceram. Abs.*, **19** [2] 53 (1940).

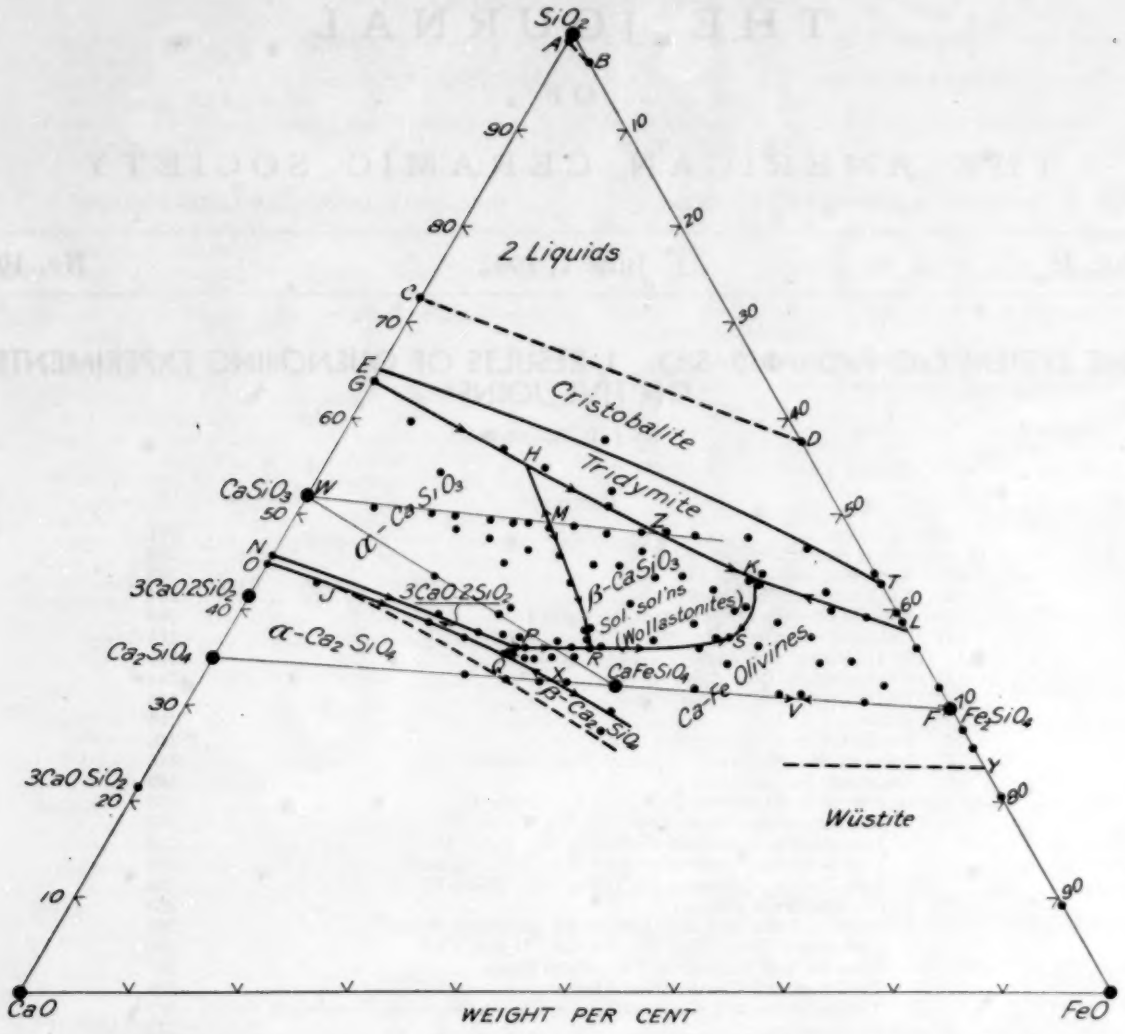

FIG. 1.—Equilibrium diagram of part of the system CaO–FeO–SiO_2 without isotherms, showing fields of stability of crystalline phases in contact with liquid. There is a small amount of Fe_2O_3 in all liquids. Diagram of Bowen, Schairer, and Posnjak.

processes involved in the crystallization of a rock magma, one by one the fundamental binary and ternary systems of rock-forming oxides have been studied, and studies of three of the quaternary systems are now in progress.

A study of the quaternary system CaO–FeO–Al_2O_3–SiO_2 was undertaken in order to obtain information about the mutual melting relations of pyroxenes, pyroxenoids, olivines, and melilites—four important groups of rock-forming minerals—and to acquire specific knowledge of their chemical compositions. Each of these mineral groups involves extensive solid solutions.

In this preliminary paper, liquidus data are presented for five planes within a regular tetrahedron used to represent the phase relations in the quaternary system. These five planes were chosen to explore that portion of the tetrahedron containing compositions of interest to igneous petrology. These results have been obtained during the past two years. Complete data for this system will require many more years, and the work has been temporarily interrupted. The geologist and petrologist are interested in the exact composition of the solid phases, particularly of the pyroxenes, pyroxenoids, olivines, and melilites. This exact information is not yet available. Much information on the coexistence of solid phases is presented, and the approximate composition of the liquid phase throughout the crystallization process may be followed. It seemed desirable at this time to place on record the liquidus data already obtained so that they might be of immediate use to the metallurgical and ceramic industries.

II. Limiting Systems

The four ternary systems CaO–FeO–SiO_2, CaO–Al_2O_3–SiO_2, FeO–Al_2O_3–SiO_2, and CaO–FeO–Al_2O_3 limit

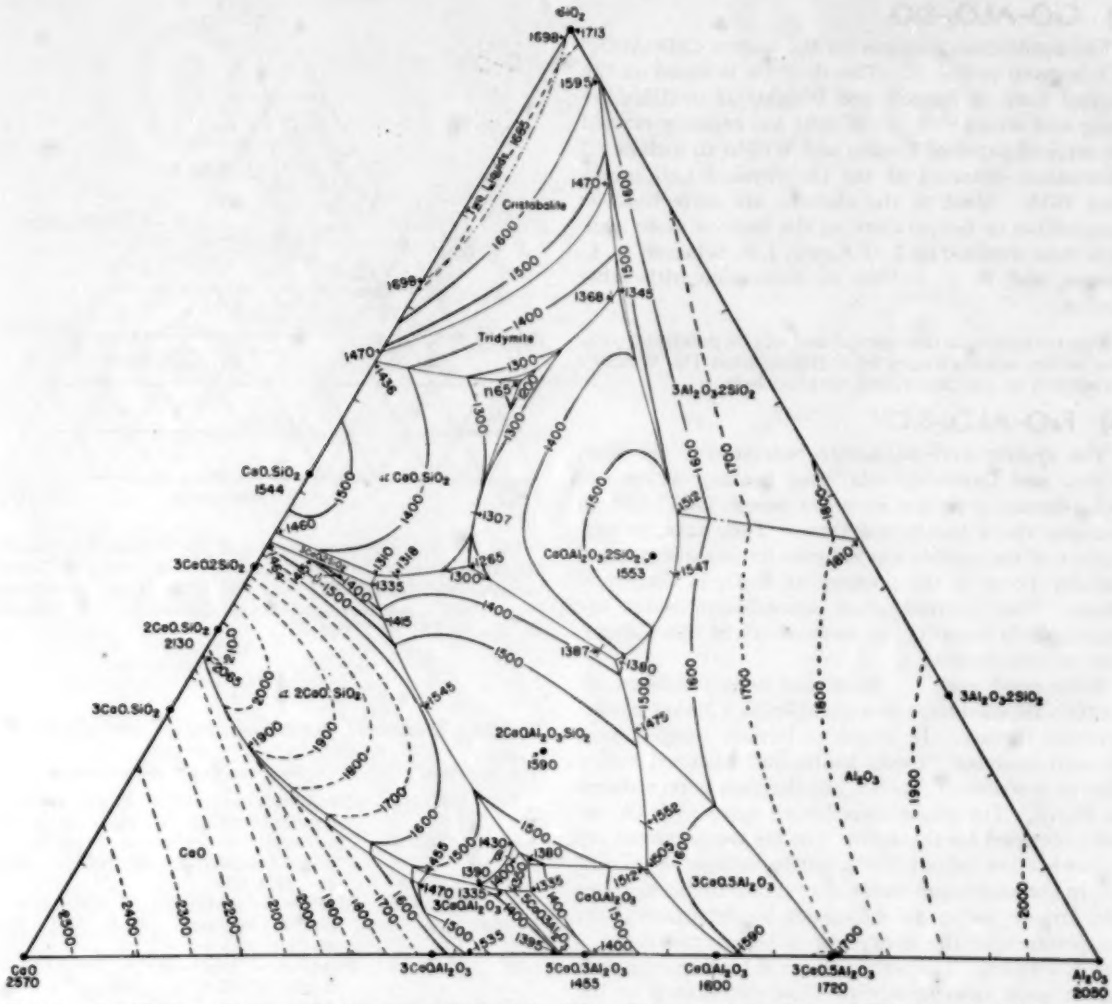

FIG. 2.—Equilibrium diagram of the system CaO–Al_2O_3–SiO_2. Diagram of Rankin and Wright revised (see text); by kind permission of F. E. Wright.

the quaternary system CaO–FeO–Al_2O_3–SiO_2. Reliable data on these ternary systems, except the last, are available.

Bowen and Schairer[2] have shown that melts of ferrous silicates are in equilibrium with metallic Fe and that equilibrium amounts of Fe_2O_3 are present in the liquid at a given temperature. The amount of Fe_2O_3 present in the liquid (small for siliceous liquids) varies with the composition of the liquid and must be determined by chemical analysis. The Fe_2O_3 content of the liquid cannot be reduced below this equilibrium amount by metallic Fe. Any attempt at reduction with the aid of a reducing agent would result only in the separation of metallic Fe from the liquid without decrease of its Fe_2O_3 content.

For a full and accurate presentation of the experimental results in the light of the above facts, it would be necessary to refer them to quinary equilibrium in the system CaO–Fe–Fe_2O_3–Al_2O_3–SiO_2. The results are much more conveniently and lucidly presented by neglecting the amount of Fe_2O_3 in the liquid, calculating the total iron as FeO, and plotting the data on planes in a tetrahedron whose apices are CaO, Al_2O_3, SiO_2, and FeO. The foregoing course has been adopted in this paper, but it must be emphasized that the liquids always contain a little ferric iron (sometimes zero within experimental error of analysis), the amount of which can be ascertained from Tables II through VI.

Throughout the paper, whenever a ternary system or a quaternary system (or a ternary or quaternary invariant point) is mentioned, the system (or point) may be treated as ternary or quaternary, respectively, only when the content of Fe_2O_3 is arbitrarily regarded as FeO.

(1) CaO–FeO–SiO_2

The equilibrium diagram[3] for the system CaO–FeO–SiO_2 is given as Fig. 1.

[2] N. L. Bowen and J. F. Schairer, "System FeO–SiO_2," *Amer. Jour. Sci.*, **24**, pp. 195–96 (1932).

[3] See reference 1 (*c*).

(2) CaO–Al_2O_3–SiO_2

The equilibrium diagram for the system CaO–Al_2O_3–SiO_2 is given as Fig. 2. This diagram is based on the original work of Rankin and Wright[4] as modified by Greig and others.[5] F. E. Wright has recently revised the original paper of Rankin and Wright to include all information obtained at the Geophysical Laboratory since 1915. Most of the changes are corrections in composition or temperature on the basis of more complete data obtained by J. W. Greig, J. F. Schairer, N. L. Bowen, and E. F. Osborn in connection with other studies.

This revision is in manuscript and will be published soon. The writer acknowledges with appreciation Dr. Wright's permission to use the revised diagram here.

(3) FeO–Al_2O_3–SiO_2

The system FeO–Al_2O_3–SiO_2 was studied by Hay, White, and Caulfield,[6] who used heating curves and molybdenum crucibles *in vacuo* below 1458° and in nitrogen above this temperature. They take no cognizance of the equilibrium between ferrous silicates and metallic Fe or of the presence of Fe_2O_3 in the liquid phase. They present phase assemblages which are incompatible according to recent work of this Laboratory on this system.

Some good work by Snow[7] has been published recently. He used large iron crucibles in a Méker muffle-type gas furnace. In preparing ternary compositions, he used analyzed Florida kaolin and Missouri burley clay as a source of Al_2O_3. His diagram is reproduced as Fig. 3. The phase assemblages agree with the results obtained by the writer, but his temperatures are somewhat low (about 100°), partly because of impurities in the kaolin and burley clay shown by his analyses but largely owing to difficulties in determining the temperature of the charge in a large crucible in a muffle furnace. The compositions of his ternary points are in good agreement with those determined in the present study.

Figure 4 is a diagram showing the liquidus relations in the system FeO–Al_2O_3–SiO_2. All liquidus determinations have been completed, but experiments at subliquidus temperatures and chemical and optical data on the solid phases are not yet complete. The compositions and temperatures of the ternary invariant points of Fig. 4 are given in Table I. The data for this system on which the diagram (Fig. 4) is based will be published in full in a later paper.

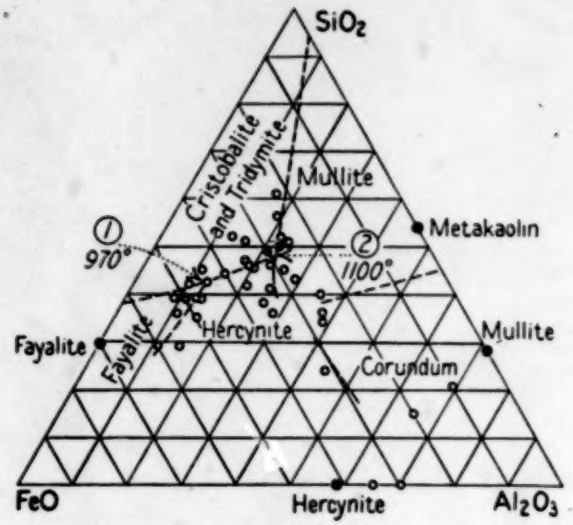

FIG. 3.—Equilibrium diagram of the system FeO–Al_2O_3–SiO_2 from Roland Bliss Snow, abstract of Doctors' Dissertations, No. 21, pp. 327–38, The Ohio State University Press (1937); see also *Jour. Amer. Ceram. Soc.*, 25 [March 15, No. 6] 151–60 (1942).

TABLE I

TERNARY INVARIANT POINTS IN SYSTEM FeO–Al_2O_3–SiO_2

Letter (Fig. 4)	Temp. °C.	Solid and liquid phases present
J	1380 ± 5	Corundum + mullite + hercynite + liquid (FeO 38 Al_2O_3 27 SiO_2 35)
K	1470 ± 5	Cristobalite + tridymite + mullite + liquid (approximately FeO 16 Al_2O_3 19 SiO_2 65)
L	1205 ± 5	Mullite + tridymite + hercynite + liquid (FeO 33.5 Al_2O_3 20.0 SiO_2 46.5)
M	1073 ± 5	Fayalite + tridymite + hercynite + liquid (FeO 47.2 Al_2O_3 12.5 SiO_2 40.3)
N	1148 ± 5	Fayalite + hercynite + wüstite + liquid (FeO 75.8 Al_2O_3 5.9 SiO_2 18.3)

(4) CaO–FeO–Al_2O_3

No data on this system have been published.

III. The Quaternary System

(1) Experimental Procedure

The method which this Laboratory has found satisfactory for the investigation of silicates containing ferrous oxide is described in full detail in previous papers.[8] Briefly, it may be said that mixtures were prepared from pure chemicals by taking silica, ferric oxide, calcium carbonate, and alumina, in the proportions calculated to give the desired composition, and melting them together in a platinum crucible three

[4] G. A. Rankin and F. E. Wright, "Ternary System CaO–Al_2O_3–SiO_2," *Amer. Jour. Sci.*, 39, 1–79 (1915).

[5] (*a*) N. L. Bowen and J. W. Greig, "System Al_2O_3–SiO_2," *Jour. Amer. Ceram. Soc.*, 7 [4] 238–54; [5] 410 (1924); (*b*) J. W. Greig, "Immiscibility in Silicate Melts," *Amer. Jour. Sci.*, 13 [73] 1–44 (1927); pp. 35–41; (*c*) N. L. Bowen, J. F. Schairer, and E. Posnjak, "System CaO–FeO–SiO_2," *ibid.*, 26, pp. 194 and 206–209 (1933).

[6] R. Hay, James White, and T. H. Caulfield, "Ternary System FeO–Al_2O_3–SiO_2," *Jour. Soc. Glass Tech.*, 21 [85] 270–80 (1937); *Ceram. Abs.*, 17 [9] 317 (1938).

[7] R. B. Snow, "Equilibrium in the System FeO–Al_2O_3–SiO_2." Abstracts of Doctors' Dissertations, No. 21, pp. 327–38, Ohio State Univ. Press (1937); *Jour. Amer. Ceram. Soc.*, 25 [March 15, No. 6] 151–60 (1942).

[8] (*a*) N. L. Bowen and J. F. Schairer, "System FeO–SiO_2," *Amer. Jour. Sci.*, 24, pp. 178–86 (1932); (*b*) N. L. Bowen, J. F. Schairer, and E. Posnjak, "System CaO–FeO–SiO_2," *ibid.*, 26, pp. 196–98 (1933).

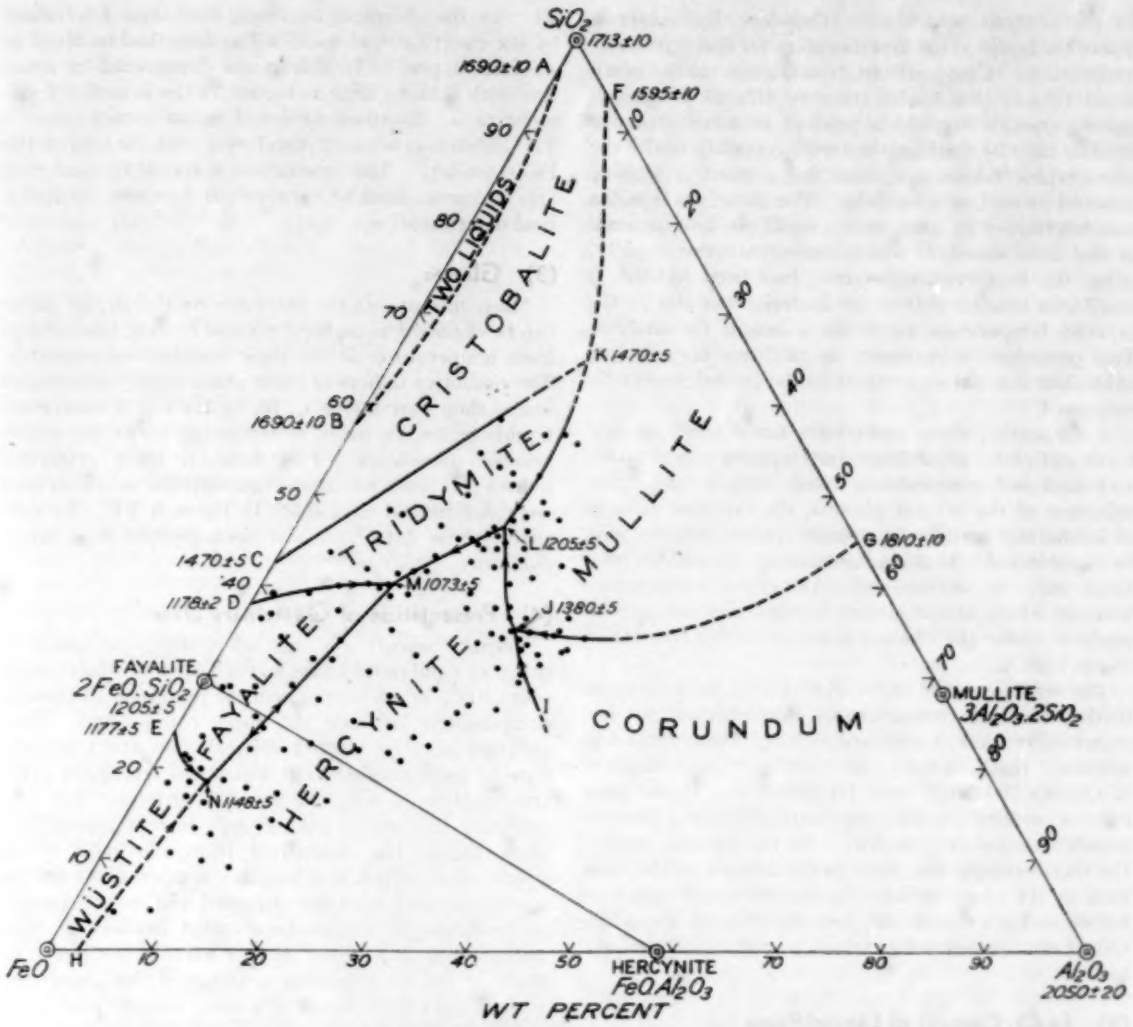

FIG. 4.—Equilibrium diagram of the system FeO–Al_2O_3–SiO_2 without isotherms, showing fields of stability of crystalline phases in contact with liquid. There is some Fe_2O_3 in all liquids. The amount is small except near the FeO apex. Unpublished diagram of J. F. Schairer; the data on which this diagram is based will be published in full in a later paper.

times in air and then three times in a Méker gas furnace with intermediate crushing of the charge between the several fusions and quenchings. Thus was obtained a charge (usually a glass) deviating somewhat from the desired product by reason of a small deficiency of iron (removed by the platinum crucible) and also the existence of some of the iron oxide in the ferric state. Small samples of this mixture with small pieces of pure Fe wire to insure intimate contact with metallic Fe were heated in iron crucibles in a stream of purified nitrogen, and the temperatures of any phase changes were determined by the method of quenching, combined with microscopic determination of the phases in the quenched product.

The small iron crucibles used in this investigation were made from pure iron sheets obtained through the courtesy of the research staff of the American Rolling Mill Company, Middletown, Ohio, whose generosity is gratefully acknowledged.

(1942)

Upon heating any iron silicate charge in an iron crucible, a change of composition occurs which is principally due to reduction of the excess ferric oxide over the equilibrium amount by the iron crucible and the consequent increase of the total iron content of the charge. This increase may partly balance, but usually more than balances, the deficiency produced by melting in platinum. In all cases it was necessary, therefore, to make a chemical analysis for FeO and Fe_2O_3 on each mixture after a run in an iron crucible at the temperature at which a change of phase was found to occur. The final composition of the mixture is not (except by accident) the composition planned but lies on a straight line (or this line produced) between the planned composition and FeO (calculating total iron as FeO).

Except for compositions very high in iron oxides, the material used in determining the liquidus temperature (temperature of completion of melting) was also used

for the analysis, which gave, therefore, the composition of the liquid at the liquidus point for that particular composition. Compositions containing more than about 75% of iron oxides are very difficult to quench rapidly enough to yield a product in which primary crystals may be distinguished with certainty under the petrographic microscope from fine-grained crystalline material formed on quenching. For these, the liquidus was determined by using only a small pinch of material in the iron crucible, which quenched very rapidly. After the liquidus temperature had been located, a small iron crucible full of the material was run at the liquidus temperature to obtain a sample for analysis. This procedure is necessary in mixtures high in iron oxide, but it is not so accurate as the procedure usually employed.

By repeating these procedures for a series of mixtures and plotting the determined liquidus temperatures and analyzed compositions (with microscopic determination of the crystal phases), the liquidus surfaces or isothermal surfaces in primary phase volumes may be constructed. In a similar manner the solidus relations may be determined. An upper temperature limit at which investigations by this method may be made is set by the melting point of the Fe crucible at about 1523°C.

The readings of the Pt vs. Pt 90 Rh 10 thermocouples used to measure temperatures were checked by frequent calibration at standard melting points defined as follows: NaCl 800.4°, Au 1062.6°, pure diopside ($CaMgSi_2O_6$) 1391.5°, and Pd 1549.5°C. In the presence of an iron crucible, the e.m.f. of such a thermocouple changes very rapidly. In the present studies, the thermocouple was never in the furnace at the same time as the iron crucible, but temperatures were read before and after each run, and the furnace was maintained at constant temperature by means of a regulator.[9]

(2) Fe_2O_3 Content of Liquid Phase

All silicates of ferrous iron, even after being held in a molten state in an iron crucible, have a portion of their iron in the ferric state. Metallic iron is incapable of further reducing the Fe_2O_3 content of these liquids. An attempt at reduction with the aid of a reducing agent would result only in the separation of metallic iron from the liquid without decrease of its Fe_2O_3 content. The amount of Fe_2O_3 present in the quaternary[10] liquids at their liquidus temperatures is a function of their composition and varies from nearly zero in quaternary liquids that contain but little iron to 11.56%[11] at the FeO (wüstite) apex of the tetrahedron.

The amount of Fe_2O_3 present in the quaternary liquids at their liquidus temperatures was determined by chemical analysis and is recorded in Tables II through VI. In the chemical analyses, FeO was determined by the Pratt method, modified as described in detail in a former paper.[12] Total iron was determined by titration with $KMnO_4$ after reduction of the iron in a Jones reductor as described in detail in an earlier paper.[13] The difference between total iron and FeO gave the Fe_2O_3 present. The amounts of CaO, Al_2O_3, and SiO_2 are, of course, fixed by synthesis and require no analytical determination.

(3) Glasses

Many mixtures in the five joins studied in this paper can be obtained as a glass by rapid cooling (quenching) from temperatures above their liquidus temperatures. The refractive indices of these glasses were determined unless they were above 1.740, by the use of immersion liquids of known index of refraction under the petrographic microscope. The data on these refractive indices are given for those compositions on which they were determined in Tables II through VI. To save space, these data have not been plotted in separate diagrams.

(4) Presentation of Quaternary Data

Ternary silicate systems are usually presented by using an equilateral triangle, each apex of which represents 100% of one component, to represent all possible compositions between the three components. Temperature may be plotted vertically on the triangular base to yield a solid model which is a triangular prism truncated by a series of liquidus surfaces. For convenience, the ternary system may be represented by a plane figure, the equilateral triangular base of the prism, upon which the liquidus temperatures for the several phases have been projected and are represented by contours of temperature called isotherms. Such ternary diagrams, either with or without isotherms, for three of the four limiting systems of the quaternary system $CaO–FeO–Al_2O_3–SiO_2$ have already been given as Figs. 1, 2, and 4.

For any such ternary system, the exact details of changes of composition of all the solid and liquid phases with change of temperature may be followed by constructing a series of isothermal planes[14] at selected temperatures. These isothermal planes are triangular sections through the triangular prism at a particular temperature, usually at or near the temperature of some important phase change or at a temperature chosen as representative of the behavior of certain solid and liquid phases over a particular range of temperatures.

A quaternary silicate system, that is, all possible mixtures of four components, may be represented by a regular tetrahedron, each apex of which represents 100% of one component. McCaffery, Oesterle, and Schapiro

---

[9] For details see N. L. Bowen and J. F. Schairer, "System FeO–SiO_2," *Amer. Jour. Sci.*, **24**, pp. 181–82 (1932).

[10] These liquids are, properly speaking, only quaternary when the Fe_2O_3 content is neglected and total iron is plotted as FeO, as has been done in this paper.

[11] N. L. Bowen and J. F. Schairer, "System FeO–SiO_2," *Amer. Jour. Sci.*, **24**, pp. 190–91 (1932).

[12] *Ibid.*, p. 185.

[13] N. L. Bowen and J. F. Schairer, "Crystallization Equilibrium in Nepheline–Albite–Silica Mixtures with Fayalite," *Jour. Geol.*, **46**, p. 400 (1938).

[14] For such a series of isothermal planes for the system CaO–FeO–SiO_2, see N. L. Bowen, J. F. Schairer, and E. Posnjak, "System CaO–FeO–SiO_2," *Amer. Jour. Sci.*, **26**, pp. 221–33 (1933).

discuss the use of the equilateral (regular) tetrahedron to represent equilibrium relations in quaternary systems.[15] They describe the geometrical relations within the tetrahedron and discuss paths of crystallization in typical cases with and without solid solutions. Their discussion of solid solution (*op. cit.*, pp. 10–12) in quaternary systems is based on a misinterpretation of Bowen's[16] classical work on solid solutions in ternary systems. Jänecke,[17] in a review article, presents the available data on a quaternary system (CaO–MgO–Al_2O_3–SiO_2) with diagrams showing the relations of geometrical solids (primary phase volumes) within the tetrahedron and a tetrahedral diagram showing the relations of the quaternary invariant points. Lea and Parker[18] discuss the use of a tetrahedron for presenting four-component polythermal condensed systems, and they describe the geometrical relations within the tetrahedron. They list many useful temperature relationships for a condensed system of four components where no solid solutions are present in the system.

The four faces of the tetrahedron representing the relations in a four-component polythermal condensed system are equilateral triangles representing the four limiting ternary systems. Each of the limiting ternary systems is divided into fields (areas with one solid phase in equilibrium with liquids whose composition lies within the area) of stability of the several solid phases, appearing in the liquidus surface, by boundary curves along which two solid phases are in equilibrium with liquids whose compositions lie on the boundary curve. These boundary curves in the limiting ternary systems become curved surfaces (quaternary divariant surfaces with two solid phases in equilibrium with liquids whose compositions lie in such a divariant surface) within the tetrahedron.

In the limiting ternary systems, three boundary curves intersect at a ternary invariant point, at a particular temperature, with three solid phases in equilibrium with only that particular liquid whose composition is represented by the ternary point. Such a point may be a ternary eutectic point, a ternary inversion[19] point, or a ternary reaction point, etc., depending upon the nature of the solid phases and the temperature distribution along the three boundary curves which meet at such a ternary invariant point. Each such ternary invariant point in the limiting ternary systems becomes a univariant line (with three solid phases in equilibrium with a liquid whose composition lies on the line) within the tetrahedron. Three curved surfaces (faces of primary phase volumes) intersect within the tetrahedron to form such a curved line. Four such univariant lines intersect within the tetrahedron at a quaternary invariant point, at a particular temperature, with four solid phases in equilibrium with only that particular liquid whose composition is represented by the point. Such a point may be a quaternary eutectic, a quaternary inversion point, or a quaternary reaction point, etc., depending upon the temperature distribution and the nature of the solid phases along the four univariant lines which meet at such a point. At such a quaternary invariant point, six curved surfaces (from four adjacent primary phase volumes) intersect in a point.

Thus, it is seen that fields (areas) of stability in the ternary triangle with one solid phase become primary phase volumes within the tetrahedron, that boundary curves (with two solid phases) become curved surfaces defining primary phase volumes within the tetrahedron, and that ternary invariant points (with three solid phases) become univariant lines within the tetrahedron. In other words, the tetrahedron is made up of a series of interlocking primary phase volumes (polyfaced geometrical figures with curved faces), each such primary phase volume representing the compositions of all quaternary liquids in equilibrium with only one solid phase. Where two primary phase volumes have a face in common, the compositions of all quaternary liquids in equilibrium with these two solid phases lie in this common face (a divariant curved surface). Where three primary phase volumes join, they have a univariant line in common. On such a curved line are the compositions of all quaternary liquids in equilibrium with these three solid phases. Where four primary phase volumes join at a point (where four univariant lines meet), this point is the composition of the only liquid in equilibrium with these four solid phases, that is, a quaternary invariant point.

Isotherms within the condensed polythermal quaternary system represented by a regular tetrahedron are a series of intersecting curved surfaces through the various primary phase volumes and cannot be represented in a simple manner on a plane diagram. However, just as triangular sections through a triangular prism may be used to present an isotherm in a ternary system,

---

[15] R. S. McCaffery, J. F. Oesterle, and Leo Schapiro, "Compositions of Blast-Furnace Slags," *Amer. Inst. Mining Met. Engrs., Tech. Pub.*, No. 19, 42 pp. (1927); pp. 2–15.

[16] N. L. Bowen, "Crystallization of Haplobasaltic, Haplodioritic, and Related Magmas," *Amer. Jour. Sci.*, **40**, 161–85 (1915).

[17] Ernst Jänecke, "Mineralogie und Phasenlehre," *Fortschr. Mineral., Krist., Petrog.*, **17** [Part II], 73–111 (1933); pp. 98–109; *Ceram. Abs.*, **14** [7] 171 (1935).

[18] F. M. Lea and T. W. Parker, "Investigations of a Portion of the Quaternary System CaO–Al_2O_3–SiO_2–Fe_2O_3: Quaternary System CaO–2CaO·SiO_2–5CaO·3Al_2O_3–4CaO·Al_2O_3·Fe_2O_3," *Trans. Roy. Soc.* [London], **A234**, 1–41 (1934); pp. 2–7; *Ceram. Abs.*, **14** [7] 173 (1935).

[19] The term "ternary inversion point" is restricted to a ternary invariant point where the inversion temperature between the two crystalline forms of the same chemical substance is independent of the composition of the liquid phase (i.e., no solid solution in either of the two crystalline forms). The inversion, therefore, does not involve a reaction between the liquid phase and the solid phases to change the chemical composition of the solid phases. For example, the point *K* (Fig. 4) is a ternary inversion point. Points *H* and *R* (Fig. 1), however, are not called ternary inversion points because at these points the inversion (pseudowollastonite (pure α-$CaSiO_3$) + liquid $\rightleftarrows$ wollastonite (solid solutions of β-$CaSiO_3$ and $FeSiO_3$) + liquid) involves reaction between wollastonite crystals and liquid to change the chemical composition of the crystals. Pure wollastonite (β-$CaSiO_3$), in the ternary system CaO–FeO–SiO_2, takes $FeSiO_3$ in solid solution, and then the inversion involves not only a change of crystal form but also of chemical composition.

so a regular tetrahedron may be used to represent an isotherm in a quaternary system. A regular tetrahedron used in this way is not easy to present as a lucid diagram.

The study of equilibrium relations in a condensed quaternary system consists of delineating the portion of the tetrahedron occupied by each primary phase volume; of determining the compositions and temperatures along the edges and at all apices of each primary phase volume; of determining the mutual relations within the tetrahedron of the many primary phase volumes involved; and of finding the locations of a sufficient number of isotherms to define adequately the liquidus and solidus temperatures within the system.

For some quaternary systems[20] of four oxides, it is possible to divide the quaternary systems into several parts, some of which are ternary or quaternary systems within the larger fundamental quaternary system, and to attack it by portions. For other quaternary systems, it is convenient to select three of the four components and add, progressively, 10, 20, 30%, etc., of the fourth component and get a series of planes through the tetrahedron parallel to one face taken as the base; or arbitrary planes through the tetrahedron may be selected for study; or combinations[21] of these methods may be used.

(5) Joins in the Quaternary System

In quaternary systems containing FeO as one of the components, certain chemical and experimental facts limit the method of attack. For any composition within the quaternary system, because of considerations presented under experimental procedure, the final composition is determined only by analysis; it is not (except accidentally) the composition planned but lies on a straight line (or a straight line produced) between the planned composition and the apex FeO. For convenience and simplicity, therefore, any line or plane in the tetrahedron which is studied should have FeO as one apex so that during the course of the experiments the composition will remain in such a line or plane and will merely move toward or away from the FeO apex along the line or in the plane, respectively.

For these reasons, five planes or joins (each having FeO as one apex) were selected to explore that portion of the tetrahedron, representing the quaternary system CaO–FeO–Al_2O_3–SiO_2, which is of geological interest. No experiments have been made in the portion of the quaternary system near the face CaO–FeO–Al_2O_3.

Figure 5 shows the positions of the five joins, SiO_2–anorthite–FeO, anorthite–Al_2O_3–FeO, $CaSiO_3$–anorthite–FeO, gehlenite–anorthite–FeO, and $CaSiO_3$–gehlenite–FeO, within the tetrahedron. The boundaries of the tetrahedron are given as heavy lines or heavy broken lines (in perspective). The five planes are given as light lines or light broken lines (in perspective).

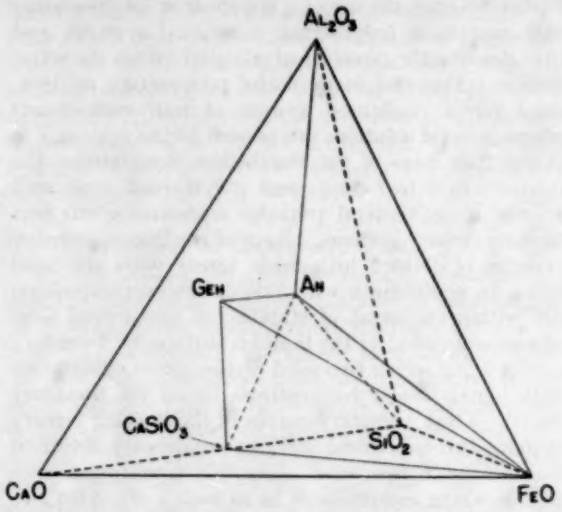

FIG. 5.—Diagram showing positions of the five joins (planes) studied within the regular (equilateral) tetrahedron CaO–FeO–Al_2O_3–SiO_2 used to represent this quaternary system. (This system is quaternary only when the small amounts of Fe_2O_3 present in liquids are treated as FeO.) *AN* = anorthite ($CaO \cdot Al_2O_3 \cdot 2SiO_2$), *GEH* = gehlenite ($2CaO \cdot Al_2O_3 \cdot SiO_2$); broken lines in perspective.

Before the experimental results on the five joins (planes joining three arbitrarily selected compositions) through the tetrahedron are presented, an explanation of the data and method of plotting such data is in order.

Two compositions in the join SiO_2–anorthite–FeO are selected for the explanation, CQ8 (the eleventh item under (*a*) of Table II) and CQ33 (the seventh item under (*c*) of Table II). The data for these are plotted in Fig. 6. In CQ33, the amount of iron subtracted by melting in platinum more than counterbalanced the iron taken up by the charge from the Fe crucible in reducing any excess Fe_2O_3 over the equilibrium amount for this composition.

In the experiments, only the relative amounts of iron oxides to other oxides can change. The ratios of the other constituents (in this case anorthite and silica) remain the same, and the final composition must lie in a straight line (for example, the line from the planned composition of CQ8 to FeO) or in a straight line produced (for example, the line from the planned composi-

[20] For example, studies on portions of CaO–MgO–Al_2O_3–SiO_2 are given by (*a*) Olaf Andersen, "System Anorthite–Forsterite–Silica," *Amer. Jour. Sci.*, **39**, 407–54 (1915).

(*b*) E. F. Osborn and J. F. Schairer, "Ternary System Pseudowollastonite–Akermanite–Gehlenite," *ibid.*, **239** [10] 715–63 (1941); *Ceram. Abs.*, **25** [2] 50 (1942).

(*c*) E. F. Osborn, "System $CaSiO_3$–Diopside–Anorthite." In completed manuscript (Nov. 15, 1941); to be published soon.

(*d*) H. F. McMurdie and Herbert Insley, "Quaternary System CaO–MgO–$2CaO \cdot SiO_2$–$5CaO \cdot Al_2O_3$," *Jour. Research Nat. Bur. Standards*, **16** [5] 467–74 (1936); R.P. 884; *Ceram. Abs.*, **15** [8] 260 (1936).

[21] Lea and Parker (*Trans. Roy. Soc.* [London], **A234**, pp. 7–41 (1934)) studied the quaternary system CaO–$2CaO \cdot SiO_2$–$5CaO \cdot 3Al_2O_3$–$4CaO \cdot Al_2O_3 \cdot Fe_2O_3$, a smaller quaternary system within the larger quaternary system CaO–Al_2O_3–SiO_2–Fe_2O_3. They studied a series of five planes parallel to the base CaO–$2CaO \cdot SiO_2$–$5CaO \cdot Al_2O_3$ with 2, 5, 10, 20, and 23% of Fe_2O_3 and also determined some additional compositions needed to define the quaternary invariant points more closely.

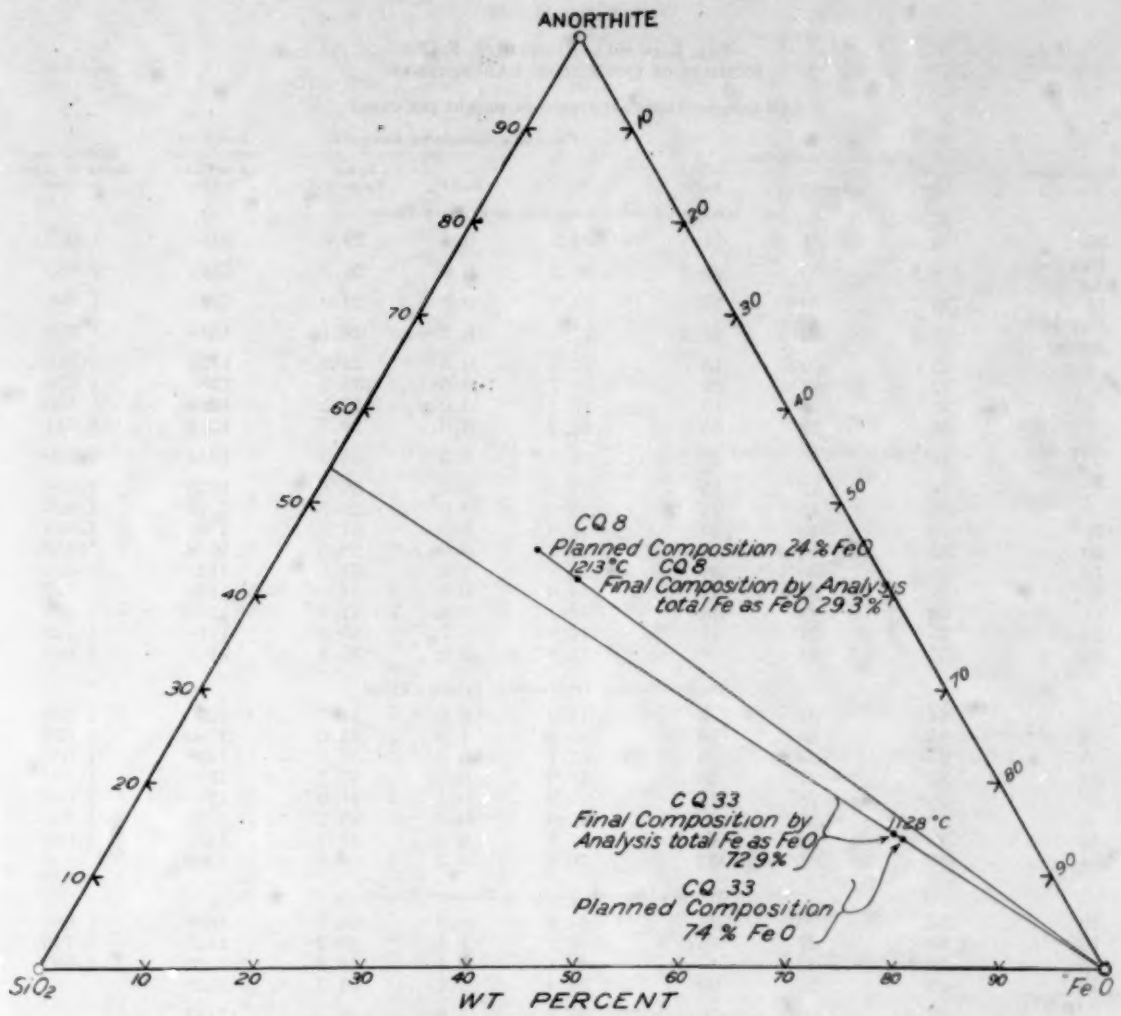

FIG. 6.—Diagram showing method of plotting experimental data given in Tables II through VI. Only the final compositions with their liquidus temperatures are plotted in Figs. 7 through 11.

tion of CQ33 to FeO produced beyond the planned composition toward the side SiO_2–anorthite). Only the final compositions with their liquidus temperatures are plotted in Figs. 7 through 11. Sometimes it was possible to obtain more than one liquidus point from the same preparation by varying either the temperature of the furnaces or the number of fusions in the gas furnace during its preparation. For example, experiments on DQ15 appear with different primary phases and different final compositions in Table IV(*f*) and (*g*), p. 258.

From the data in Tables II through VI, the composition of any point may be recalculated to the desired composition basis, such as CaO, FeO, Fe_2O_3, Al_2O_3, and SiO_2 or CaO, FeO (total Fe as FeO), Al_2O_3, and SiO_2.

(6) Diagrams for the Joins

In Figs. 7 through 11, the results on five joins studied are presented graphically. The data on which these diagrams are based are given in Tables II through VI. All data are in terms of weight per cent. Each diagram is discussed specifically under section 6 (*A*) through (*E*), pp. 253–63.

In Figs. 7 through 11, open circles represent the compositions of chemical compounds, and black dots represent the compositions of mixtures studied, whose compositions and liquidus temperatures are given in Tables II through VI. Numbers adjacent to the black dots (Figs. 7 through 11) give their liquidus temperatures in degrees Centigrade. The diagrams are divided into areas by heavy lines (or heavy dashed lines when experimental data are not sufficiently complete to give their location accurately). These *areas* in the joins labeled cristobalite or tridymite or anorthite, etc., are *traces of primary phase volumes* (with curved faces) within the tetrahedron *in the plane* (join) which the particular diagram represents. Each primary phase volume within the tetrahedron gives the compositions of all quaternary liquids (one liquid phase) in equilibrium

TABLE II

THE JOIN SiO_2–ANORTHITE–FeO
RESULTS OF QUENCHING EXPERIMENTS

(All compositions expressed in weight per cent)

Experiment No. CQ	Planned composition			Final composition by analysis			Temp. of completion of melting ±4°C.	Refractive index of glass ±0.003
	SiO_2	Anorthite	FeO	FeO	Fe_2O_3	Total Fe as FeO		
			(a) Mixtures Having Anorthite as Primary Phase					
35	5	71	24	29.2	0.4	29.6	1343	1.662
Fay 30* An 70	8.8	70	21.2	26.2	0.0	26.2	1348	1.653
14	20	70	10	19.9	0.0	19.9	1395	1.598
Fay 40 An 60	11.8	60	28.2	27.8	0.3	28.1	1335	1.658
2	25	60	15	23.8	0.0	23.8	1323	1.610
17	12	55	33	34.7	0.6	35.2	1283	1.679
1	35	55	10	17.2	0.0	17.2	1283	1.580
7	23	52	25	29.2	0.6	29.7	1278	1.641
Fay 50 An 50	14.7	50	35.3	34.9	0.4	35.3	1254	1.689
22	18	47	35	38.5	0.0	38.5	1228	1.689
8	31	45	24	28.8	0.6	29.3	1213	1.620
16	30	40	30	31.9	0.0	31.9	1180	1.638
20	25	40	35	38.6	0.0	38.6	1178	1.682
19	33	36	31	33.8	1.0	34.7	1123	1.641
41	22	35	43	44.6	0.0	44.6	1148	1.717
21	28	34	38	41.4	0.0	41.4	1128	1.681
29	25	34	41	44.9	1.7	46.4	1118	1.723
27	35	34	31	35.8	0.0	35.8	1103	1.649
			(b) Mixtures Having Tridymite as Primary Phase					
11	44	51	5	14.2	0.6	14.7	1290	1.564
4	45	45	10	19.9	1.2	21.0	1300	1.578
5	35	30	35	37.7	0.0	37.7	1138	1.651
30	35	27	38	40.8	0.3	41.1	1103	1.669
43	36	26	38	41.8	0.1	41.9	1140	1.668
6	40	20	40	42.9	0.4	43.3	1235	1.683
48	43	14	43	47.0	0.4	47.4	1383	1.688
44	42	5	53	56.6	1.3	57.8	1200	
			(c) Mixtures Having Olivine as Primary Phase					
39	33	30	37	44.0	0.0	44.0	1088	1.686
10	28	27	45	48.2	1.1	49.2	1115	1.723
15	33	22	45	46.8	0.1	46.9	1103	1.687
12	18	22	60	59.4	2.1	61.3	1128	
Fay 80 An 20	23.6	20	56.4	57.6	1.6	59.0	1143	
40	38	16	46	53.4	0.0	53.4	1130	1.721
33	12	14	74	69.0	4.3	72.9	1128	
18	15	10	75	73.4	2.8	75.9	1143	
Fay 90 An 10	26.5	10	63.5	65.1	0.7	65.7	1173	
9	40	10	50	56.5	1.7	58.0	1158	1.742
9	40	10	50	55.4	1.4	56.7	1153	1.738
32	20	5	75	71.0	4.3	74.9	1168	
44	42	5	53	58.5	0.9	59.3	1170	
			(d) Mixtures Having Hercynite as Primary Phase					
Fay 20 An 80	5.9	80	14.1	37.0	0.4	37.4	1363	1.707
37		70	30	32.6	0.0	32.6	1393	1.684
49	9	51	40	42.5	0.0	42.5	1310	1.717
13	12	41	47	48.7	1.4	50.0	1265	
Fay 60 An 40	17.7	40	42.3	41.8	0.7	42.4	1183	1.708
26		40	60	60.8	3.8	64.2	1375	
46	20	39	41	48.0	2.6	50.3	1180	1.732
Fay 70 An 30	20.6	30	49.4	51.1	1.8	52.7	1150	
38		30	70	65.2	8.5	72.8	1340	
31	12	28	60	58.6	3.9	62.1	1255	

* In preliminary experiments, eight compositions between anorthite and fayalite were made; these lie in the join SiO_2–anorthite–FeO.

TABLE II (*continued*)*

Experiment No. CQ	Planned composition			Final composition by analysis			Temp. of completion of melting ±4°C.	Refractive index of glass ±0.003
	SiO_2	Anorthite	FeO	FeO	Fe_2O_3	Total Fe as FeO		
	(*d*) Mixtures Having Hercynite as Primary Phase (*concluded*)							
45	21	27	52	53.8	3.1	56.6	1135	
25	15	25	60	60.6	3.1	63.4	1180	
24	5	20	75	68.9	6.0	74.3	1260	
52		20	80	73.9	8.3	81.4	1300	
23	12	18	70	68.2	4.8	72.5	1125	
	(*e*) Mixtures Having Wüstite as Primary Phase							
							Temp. of completion of melting, ±10°C.	
54	8	12	80	74.0	8.3	81.5	1225	
55	15	5	80	74.0	5.6	79.0	1190	

Experiment No. CQ	Planned composition			Final composition by analysis			Temp. ±4°C.	Results of microscopic examination	Refractive index of glass ±0.003
	SiO_2	Anorthite	FeO	FeO	Fe_2O_3	Total Fe as FeO			
	(*f*) Quenching Experiments on Mixtures with More Than One Solid Phase								
3		85	15	26.6	0.0	26.6	1370	Very rare anorthite and very rare hercynite in liquid	1.652
35	5	71	24	29.2	0.4	29.6	1340	Small amount anorthite and trace hercynite in liquid	
35	5	71	24	29.2	0.4	29.6	1345	All liquid	1.662
17	12	55	33	34.7	0.6	35.2	1250	Anorthite and rare hercynite in liquid	
11	44	51	5	14.2	0.6	14.7	1265	Tridymite and very rare anorthite in liquid	
28	38	46	16	22.5	0.2	22.7	1205	Very rare anorthite and very rare tridymite in liquid	1.594
27	35	34	31	35.8	0.0	35.8	1095	Anorthite and very rare tridymite in liquid	
34	26	30	44	46.3	1.7	47.8	1100	Rare olivine and rare anorthite in liquid	
34	26	30	44	46.3	1.7	47.8	1105	All liquid	1.718
39	33	30	37	44.0	0.0	44.0	1080	Rare olivine and rare anorthite in liquid	
39	33	30	37	44.0	0.0	44.0	1085	Rare olivine in liquid	
39	33	30	37	44.0	0.0	44.0	1090	All liquid	1.686
42	23	29	48	49.6	0.8	50.3	1105	Rare olivine, rare anorthite, and rare hercynite in liquid	
42	23	29	48	49.6	0.8	50.3	1110	All liquid	1.737
51	32	28	40	39.8	0.0	39.8	1070	Rare olivine, rare anorthite, and trace tridymite in liquid	
51	32	28	40	39.8	0.0	39.8	1075	Rare olivine and very rare anorthite in liquid	
51	32	28	40	39.8	0.0	39.8	1080	All liquid	1.673
45	21	27	52	53.8	3.1	56.6	1120	Hercynite and rare olivine in liquid	
45	21	27	52	53.8	3.1	56.6	1125	Hercynite in liquid	
45	21	27	52	53.8	3.1	56.6	1135	Very rare hercynite in liquid	
15	33	22	45	46.8	0.1	46.9	1085	Olivine and very rare tridymite in liquid	
23	12	18	70	68.2	4.8	72.5	1120	Olivine and hercynite in liquid	
23	12	18	70	68.2	4.8	72.5	1125	Very rare hercynite in liquid	
57	4	13	83	76.3	6.7	82.4	1260	Very rare spinel and very rare wüstite in liquid	
54	8	12	80	74.0	8.3	81.5	1120	Large amount wüstite, very rare hercynite, and very rare olivine in liquid	
55	15	5	80	74.0	5.6	79.0	1165	Wüstite and very rare olivine in liquid	
44	42	5	53	58.5	0.9	59.3	1165	Rare olivine and very rare tridymite in liquid	

* Table II concluded on p. 252.

with a single solid crystalline phase, except one near the SiO_2 apex where there are two liquid phases in equilibrium with cristobalite crystals.

The *heavy lines* in the joins are not boundary curves but are *traces of the curved boundary surfaces*, between two adjacent primary phase volumes within the tetrahedron, *in the plane* (join) which the particular diagram represents.

As these heavy lines in the joins are not boundary curves but are only traces of divariant curved surfaces (boundary surfaces between two adjacent primary phase volumes within the tetrahedron used to

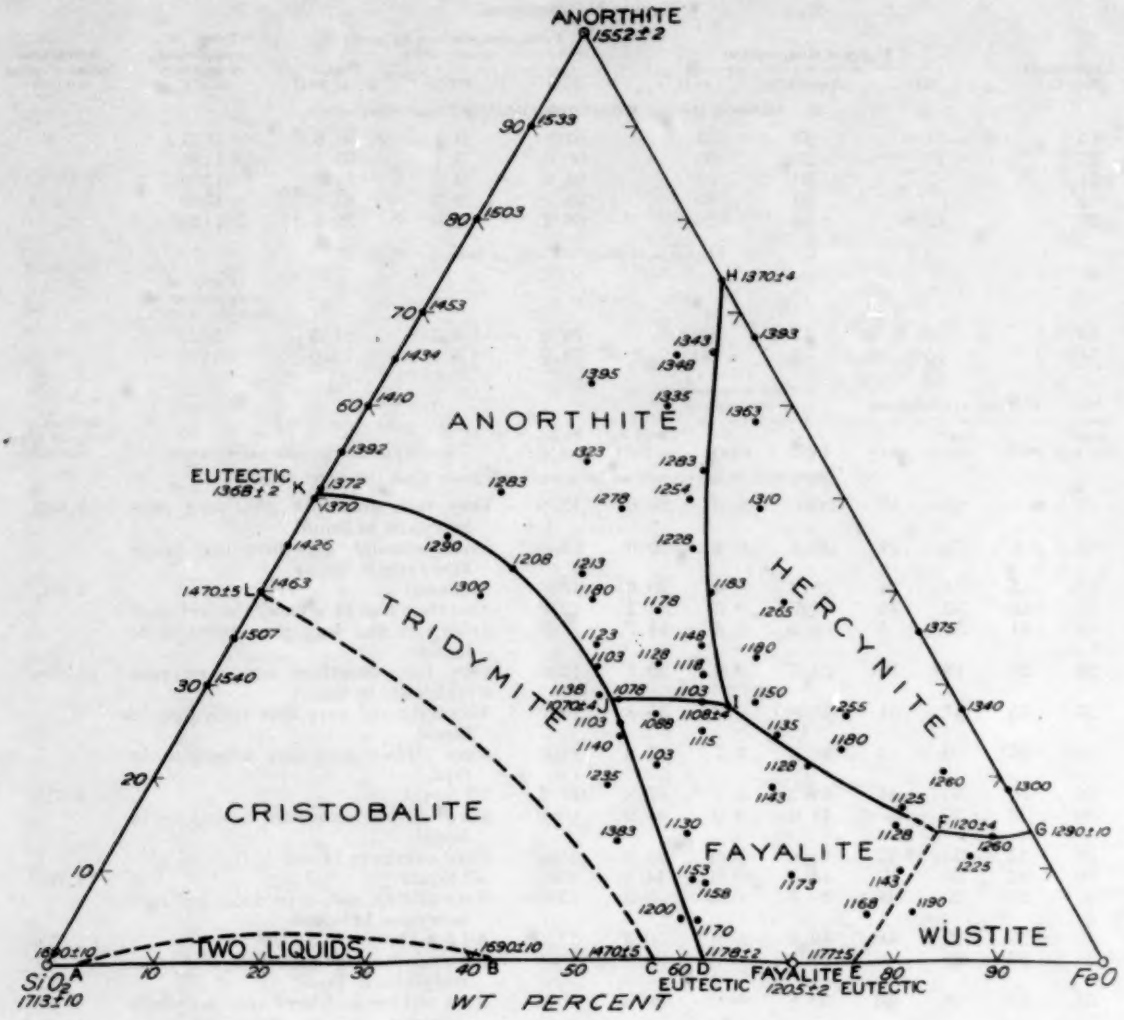

FIG. 7.—Equilibrium diagram of the join SiO_2–anorthite–FeO, showing compositions studied, primary phases, and liquidus temperatures.

TABLE II (*concluded*)

(g) Temperatures and Compositions of Lettered Points in Fig. 7

Letter (Fig. 7)	Temp. °C.	Solid and liquid phases present
A	1690 ± 10	Liquid A (FeO 3 SiO_2 97) + liquid B (FeO 42 SiO_2 58) + cristobalite (Greig)
B	1690 ± 10	Same as A (Greig)
C	1470 ± 5	Cristobalite + tridymite + liquid (FeO 57.5 SiO_2 42.5) (Bowen and Schairer)
D	1178 ± 2	Tridymite + fayalite + liquid (FeO 62.0 SiO_2 38.0) (Bowen and Schairer)
E	1177 ± 5	Fayalite + wüstite + liquid (FeO 76 SiO_2 24) (Bowen and Schairer)
F	1120 ± 4	Fayalite + wüstite + hercynite + liquid (approximately SiO_2 9 anorthite 14 FeO 77)
G	1290 ± 10	Wüstite + hercynite + liquid (approximately anorthite 14 FeO 86)
H	1370 ± 4	Hercynite + anorthite + liquid (anorthite 73.4 FeO 26.6)
I	1108 ± 4	Hercynite + anorthite + fayalite + liquid (SiO_2 22.0 anorthite 27.7 FeO 50.3)
J	1070 ± 4	Anorthite + fayalite + tridymite + liquid (SiO_2 32.5 anorthite 28.1 FeO 39.4)
K	1368 ± 2	Anorthite + tridymite + liquid (SiO_2 49.8 anorthite 50.2) (Schairer and Bowen)
L	1470 ± 5	Cristobalite + tridymite + liquid (SiO_2 60.5 anorthite 39.5) (Schairer and Bowen)

represent a condensed quaternary system) and as in this condensed system isotherms are curved surfaces within the primary phase volumes (isothermal surfaces from adjacent primary phase volumes meet in the divariant boundary surface), one of these heavy lines may cut the same isothermal surface more than once. Temperature maxima or minima may occur along such heavy lines or in the areas bounded by these lines, but they are without significance. For example, by examining the data in Table V for points near the heavy line *ZA* (Fig. 10), it is found that temperatures along *ZA* rise and then fall and *ZA* cuts an isotherm (e. g., the 1330°C. isotherm) twice.

Where three heavy lines meet at a point in the joins, these *points* are not ternary eutectics (or other ternary invariant points) but are *piercing points of lines* within the tetrahedron *in the plane* (join) which the particular diagram represents. Along these lines, three curved surfaces (faces of three adjacent primary phase volumes) intersect. Such a curved line is called a quaternary univariant line or a quintuple line. Along such univariant lines, three solid crystalline phases are in equilibrium with liquids whose compositions lie on such lines.

No quaternary invariant point lies in any of the joins studied, but these joins indicate, within approximate limits, the positions within the tetrahedron and the temperatures of several quaternary invariant points. The quaternary invariant points will be discussed in detail (section (8), p. 265) after presentation of the data on the five joins studied.

(*A*) *The Join SiO_2–Anorthite–FeO:* The experimental data for this join are given in Table II and presented graphically as Fig. 7. This join cuts the following seven primary phase volumes within the tetrahedron: Anorthite ($CaO \cdot Al_2O_3 \cdot 2SiO_2$) + liquid, hercynite ($FeO \cdot Al_2O_3$, whose composition lies outside the plane of the join) + liquid, tridymite + liquid, cristobalite + liquid, two immiscible liquids + cristobalite, fayalite[22] (olivine) + liquid, and wüstite[23] + liquid.

In Fig. 7, the data for the points *K* and *L* and other points in the binary system anorthite–SiO_2 are unpublished data of J. F. Schairer and N. L. Bowen obtained in their study of the ternary system leucite–anorthite–silica. The data for the melting point of SiO_2 and the points *A* and *B* on the side SiO_2–FeO are from Greig.[24] The data for the points *C*, *D*, and *E* are from Bowen and Schairer.[25] No value for the melting point of FeO (wüstite) is placed on the diagrams of this paper. There is still too much uncertainty as to the exact relations in the Fe–O diagram in the concentration region Fe(O)–wüstite. For discussions on this region, the reader is referred to Bowen and Schairer,[26] and to Jette and Foote[27] (with discussion by C. H. Mathewson on page 285). More recently, Chipman and Marshall[28] have determined the melting point of wüstite in presence of metallic Fe.

The nine heavy curves (*HI*, *GF*, *EF*, *FI*, *IJ*, *KJ*, *DJ*, *CL*, and *A* (dashed line) *B* of Fig. 7) are traces of the curved surfaces, along which two adjacent primary phase volumes join within the tetrahedron, in the plane SiO_2–anorthite–FeO. The points *J*, *I*, and *F* are piercing points of three univariant lines within the tetrahedron in the plane SiO_2–anorthite–FeO. Each of these points is a point (on one of the three univariant lines) which happens to lie in the plane SiO_2–anorthite–FeO. Along each of these univariant lines, three crystalline solid phases are in equilibrium with liquids whose compositions lie on the line. The phase assemblages along these three univariant lines (curved lines within the tetrahedron) are as follows:

(1) Tridymite + anorthite + fayalite + liquid. *J* (Fig. 7) lies on this line.

(2) Anorthite + fayalite + hercynite + liquid. *I* (Fig. 7) lies on this line.

(3) Fayalite + hercynite + wüstite + liquid. *F* (Fig. 7) lies on this line; the ternary eutectic fayalite + hercynite + wüstite + liquid (*l* of Table VII) in the limiting ternary system FeO–Al_2O_3–SiO_2 is one terminus of this line, and the join $CaSiO_3$–anorthite–FeO cuts this line at *U* (Fig. 9).

Each univariant line except one (which joins two ternary invariant points in different faces of the tetrahedron) leads to at least one quaternary invariant point (this is discussed more fully in section (8)). Four univariant lines meet at each quaternary invariant point. The points *J*, *I*, and *F* are, therefore, very significant because they give some information concerning the locations of several of the quaternary invariant points within the tetrahedron, and the temperatures of the points *J*, *I*, and *F* put some limit or limits on the possible temperatures of such quaternary invariant points.

(*B*) *The Join Anorthite–Al_2O_3–FeO:* The experimental data for this join are given in Table III and presented graphically as Fig. 8. This join cuts the following four primary phase volumes within the tetrahedron: Corundum (α-Al_2O_3) + liquid, anorthite +

[22] Optical data on the crystalline phases are not yet complete. Instead of pure fayalite ($2FeO \cdot SiO_2$), a lime-iron olivine might be the primary phase on this join.

[23] Wüstite is a crystalline phase of variable composition. The lowest oxide of iron does not have the stoichiometric composition required by the formula FeO but instead has a somewhat higher oxygen content and is stable over a range of compositions. This solid solution is called wüstite. Eric R. Jette and Frank Foote ("Study of the Homogeneity Limits of Wüstite (FeO) by X-Ray Methods," *Trans. Amer. Inst. Mining Met. Engrs.*, **105**, 276–89 (1933)) have shown that the iron-rich extremity of the solid solutions has the composition 76.8% of Fe. This particular solid solution is in equilibrium with metallic Fe at the melting point of the oxide.

[24] (*a*) J. W. Greig, "Immiscibility in Silicate Melts," *Amer. Jour. Sci.*, **13**, p. 12 (1927); (*b*) "On Liquid Immiscibility in the System FeO–Fe_2O_3–Al_2O_3–SiO_2," *ibid.*, **14** [84] 473–84 (1927); p. 479; *Ceram. Abs.*, **7** [2] 104 (1928).

[25] N. L. Bowen and J. F. Schairer, "System FeO–SiO_2," *Amer. Jour. Sci.*, **24**, p. 199 (1932).

[26] *Ibid.*, pp. 188–91.

[27] E. R. Jette and Frank Foote, "Study of Homogeneity Limits of Wüstite (FeO) by X-Ray Methods," *Trans. Amer. Inst. Mining Met. Engrs.*, **105**, pp. 276–84; discussion, pp. 285–89 (1933).

[28] John Chipman and Shadburn Marshall, "Equilibrium FeO + H_2 = Fe + H_2O at Temperatures up to Melting Point of Iron," *Jour. Amer. Chem. Soc.*, **62** [2] 299–305 (1940); pp. 302–303.

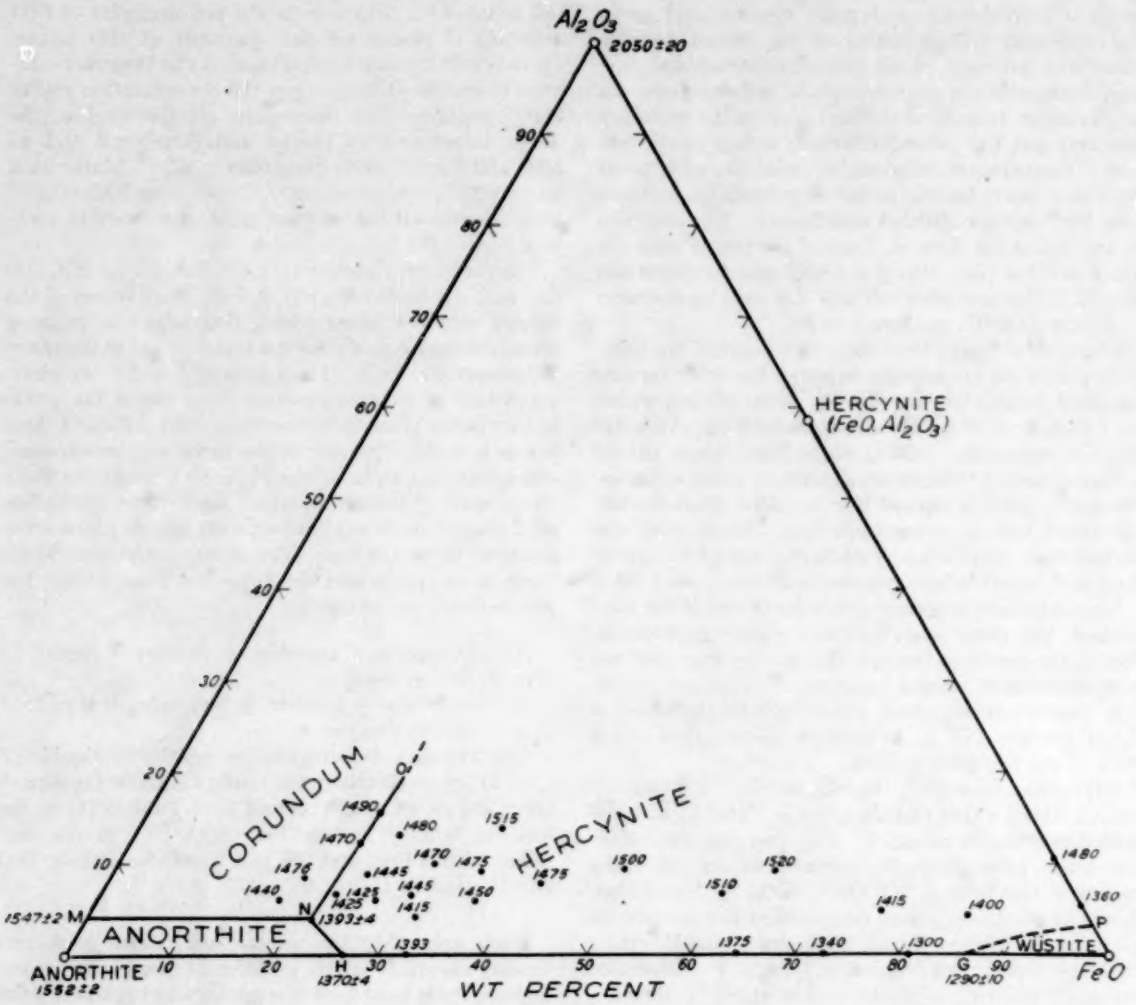

FIG. 8.—Equilibrium diagram of the join anorthite–Al_2O_3–FeO, showing compositions studied, primary phases, and liquidus temperatures.

liquid, hercynite (whose composition does not lie in this plane) + liquid, and wüstite + liquid.

In Fig. 8, the point *M* is the binary eutectic between anorthite and corundum from Rankin and Wright.[29] The data for points *H* and *G* and other points on the side anorthite–FeO have already been given in Table II. The side anorthite–FeO also forms one side of the joins SiO_2–anorthite–FeO (Fig. 7), $CaSiO_3$–anorthite–FeO (Fig. 9), and gehlenite–anorthite–FeO (Fig. 10). The melting point of Al_2O_3 is from Kanolt.[30] The point *P* (Fig. 8) is the binary eutectic between wüstite and hercynite in the system FeO–Al_2O_3. This has been determined by McIntosh, Rait, and Hay,[31] who used molybdenum crucibles. They took no cognizance of the equilibrium between the melts and metallic Fe or of the presence of Fe_2O_3 in the liquid phase. There is considerable uncertainty as to the exact composition and temperature of *P*.

The four heavy curves (*MN*, *NO*, *NH*, and *GP* of Fig. 8) are traces of the curved surfaces, along which two adjacent primary phase volumes join within the tetrahedron, in the plane anorthite–Al_2O_3–FeO. The point *N* is the piercing point of a univariant line within the tetrahedron in the plane anorthite–Al_2O_3–FeO. This point *N* is one point on the line which happens to lie in this plane. Along this univariant line, three crystalline solid phases are in equilibrium with liquids whose compositions lie on this curved line. The phase assemblage along this univariant line is anorthite + corundum + hercynite + liquid. The point *N* (1393° ± 4°C.) is a maximum on this univariant line (lettered *AK* in Fig. 12 and discussed in section (8*B*), p. 267) because it lies in the plane anorthite–Al_2O_3–FeO (which is the composition plane anorthite–Al_2O_3–hercynite

[29] G. A. Rankin and F. E. Wright, "Ternary System CaO–Al_2O_3–SiO_2," *Amer. Jour. Sci.*, **39**, p. 46 (1915).

[30] C. W. Kanolt, "Melting Points of Some Refractory Oxides," *Jour. Wash. Acad. Sci.*, **3** [11] 315–18 (1913).

[31] A. B. McIntosh, J. R. Rait, and R. Hay, "Binary System FeO–Al_2O_3," *Jour. Roy. Tech. Coll.* [Glasgow], **4** [Part I] 72–76 (1937); *Ceram. Abs.*, **17** [1] 41 (1938).

TABLE III

THE JOIN ANORTHITE–Al_2O_3–FeO
RESULTS OF QUENCHING EXPERIMENTS

(All compositions expressed in weight per cent)

Experiment No. BQ	Planned composition			Final composition by analysis			Temp. of completion of melting ±4°C.	Refractive index of glass ±0.003
	Anorthite	Al_2O_3	FeO	FeO	Fe_2O_3	Total Fe as FeO		
			(a) Mixtures Having Hercynite as Primary Phase					
19	13	5	82	73.5	11.9	84.2	1400	
18	20	5	75	69.6	7.0	75.9	1415	
16	30	10	60	56.2	8.0	63.4	1520	
17	36	7	57	52.4	8.2	59.8	1510	
14	45	10	45	45.1	3.1	47.9	1500	
15	52	8	40	40.8	0.7	41.4	1475	1.728
7	55	15	30	33.2	1.9	34.9	1515	1.696
4	60	10	30	34.1	1.1	35.1	1475	1.697
6	68	7	25	36.2	0.0	36.2	1450	1.699
6	68	7	25	29.2	0.8	29.9	1445	1.672
8	70	15	15	24.5	0.9	25.3	1480	1.653
12	72	12	16	29.8	0.4	30.2	1470	1.676
3	75	10	15	24.4	0.1	24.5	1445	1.650
5	77	5	18	31.0	0.3	31.3	1415	1.673
11	78	7	15	24.9	2.0	26.7	1425	1.653
9	84	8	8	22.5	0.0	22.5	1425	1.643
			(b) Mixtures Having Corundum as Primary Phase					
2	85	10	5	18.1	0.6	18.6	1476	1.630
10	88	7	5	17.4	0.0	17.4	1440	1.624

Experiment No. BQ	Planned composition			Final composition by analysis			Temp. ±4°C.	Results of microscopic examination	Refractive index of glass ±0.003
	Anorthite	Al_2O_3	FeO	FeO	Fe_2O_3	Total Fe as FeO			
			(c) Quenching Experiments on Mixtures with More Than One Solid Phase						
21	75	19	6	22.1	0.0	22.1	1490	Very rare corundum and very rare hercynite in liquid	1.653
20	80	15	5	22.0	0.0	22.0	1470	Very rare corundum and very rare hercynite in liquid	1.648
1	90	5	5	21.5	0.0	21.5	1390	Anorthite and hercynite in liquid	
1	90	5	5	21.5	0.0	21.5	1395	All liquid	1.638

Letter (Fig. 8)	Temp. °C.	Solid and liquid phases present
	(d) Temperatures and Compositions of Lettered Points in Fig. 8	
M	1547±2	Corundum + anorthite + liquid (anorthite 95.8 Al_2O_3 4.2) (Rankin and Wright)
N	1393±4	Corundum + anorthite + hercynite + liquid (anorthite 74.5 Al_2O_3 4.5 FeO 11.0)
O	1515±5	(Along curve, *NO*, corundum and hercynite are in equilibrium with liquids; the curve cannot be followed beyond point *O* in Fe crucibles)
P	(Not known)	Hercynite + wüstite + liquid (composition of liquid not known but is probably between 2 and 4% of Al_2O_3)

For *H* and *G*, see Table II (g), p. 252.

produced toward FeO). All compositions which lie within the area anorthite–Al_2O_3–hercynite of Fig. 8 are completely crystalline at all temperatures below *N* (1393° ± 4°C.). The point *N* (Fig. 8) is significant because it lies on a univariant line joining two quaternary invariant points and is the temperature maximum on this line (*AK*, Fig. 12). The temperature and composition of *N* yield information concerning the approximate temperatures and approximate locations within the tetrahedron of the two quaternary invariant points anorthite + corundum + hercynite + gehlenite + liquid (*K* of Fig. 12) and anorthite + corundum + mullite + hercynite + liquid (*A* of Fig. 12).

The line *NO* (Fig. 8) could not be followed beyond *O* because the practical upper temperature limit of experiments, when Fe crucibles are used, is 1510° ± 5°C.

(*C*) *The Join $CaSiO_3$–Anorthite–FeO:* The experimental data for this join are given in Table IV and presented graphically as Fig. 9. This join cuts the following seven primary phase volumes within the tetrahedron: Anorthite + liquid, hercynite ($FeO \cdot Al_2O_3$, whose composition does not lie in this plane) + liquid, wüstite + liquid, melilite[32] + liquid, olivine[33] + liquid, α-$CaSiO_3$

[32] The general term melilite is used advisedly instead of gehlenite for the tetragonal crystals in equilibrium with these melts. Their composition does not lie in this plane. Chemical and optical data are not yet completed on the solid phases of the quaternary system. It is not known yet to what extent iron-akermanite ($Ca_2FeSi_2O_7$) goes into solid solution with gehlenite ($Ca_2Al_2SiO_7$) in the crystals.

[33] The general term olivine is used because the exact composition of the crystals is not known. Optical and chemical data on the solid phases are not yet completed. The crystals are probably solid solutions of $CaFeSiO_4$ and Fe_2SiO_4 called lime-iron olivines.

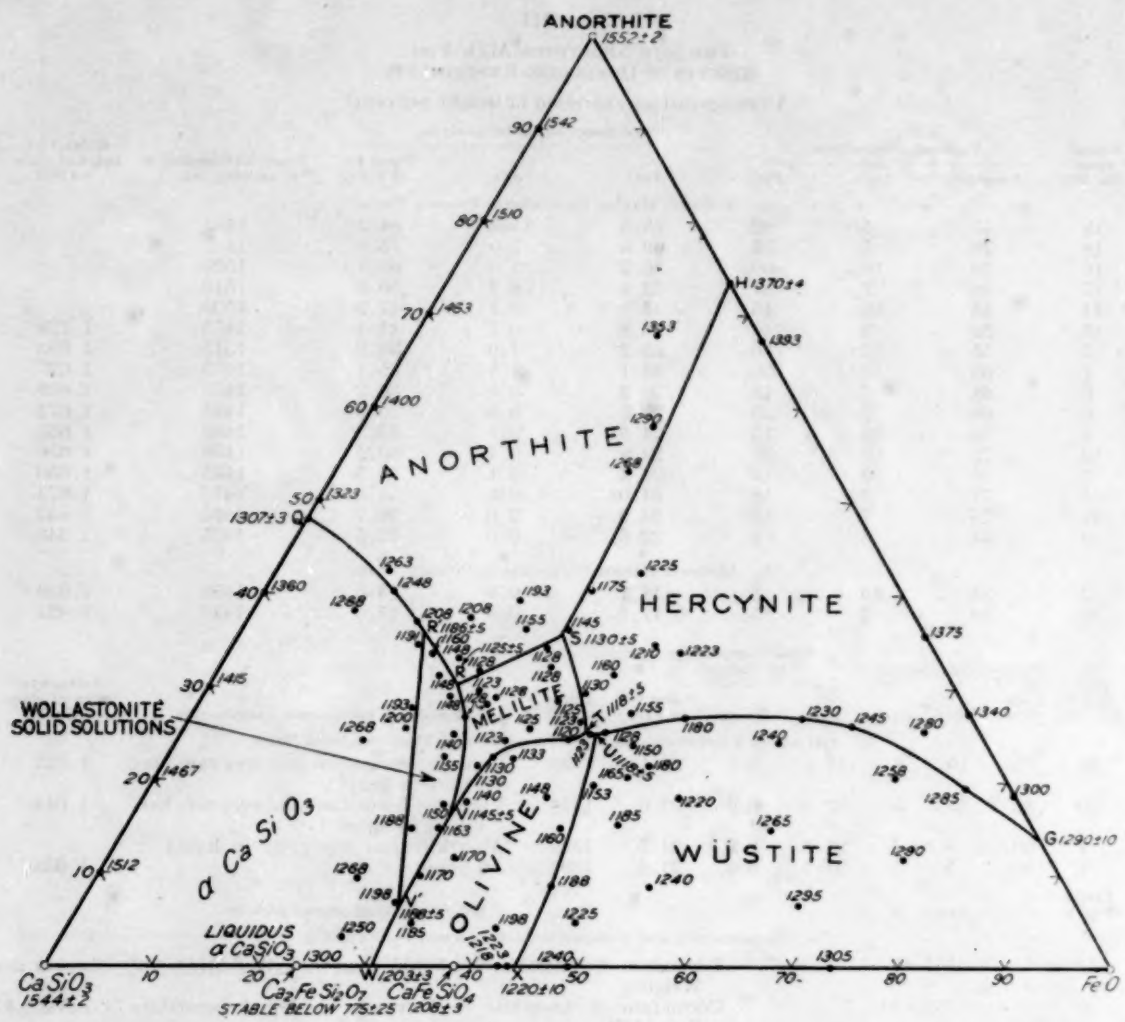

FIG. 9.—Equilibrium diagram of the join $CaSiO_3$–anorthite–FeO, showing compositions studied, primary phases, and liquidus temperatures.

+ liquid, and wollastonite (β-$CaSiO_3$ solid solutions) + liquid.

In Fig. 9, the data for the point *Q* and other points in the binary system $CaSiO_3$–anorthite are those of Osborn.[34] The data for points *H* and *G* and other points on the side anorthite–FeO have already been given in Table II. The side anorthite–FeO also forms one side of the joins SiO_2–anorthite–FeO (Fig. 7), anorthite–Al_2O_3–FeO (Fig. 8), and gehlenite–anorthite–FeO (Fig. 10). Data for the point *W* and other points in the binary system $CaSiO_3$–$CaFeSiO_4$ are from Bowen, Schairer, and Posnjak.[35] Data for the point *X* and other points between $CaFeSiO_4$ and FeO on the side $CaSiO_3$–FeO are given in Table IV.

The thirteen heavy curves (*QR'*, *R'R*, *RV*, *R'V'*, *WV'*, *V'V*, *VT*, *XU*, *UT*, *GU*, *ST*, *HS*, and *RS* of Fig. 9) are traces of the curved surfaces, along which two adjacent primary phase volumes join within the tetrahedron, in the plane $CaSiO_3$–anorthite–FeO. The points *R*, *R'*, *V*, *V'*, *U*, *T*, and *S* are piercing points of seven univariant lines, within the tetrahedron, in the plane $CaSiO_3$–anorthite–FeO. Each of these points is a point (on one of the seven univariant lines) which happens to lie in the plane $CaSiO_3$–anorthite–FeO. Along each of these seven curved univariant lines, three crystalline solid phases are in equilibrium with liquids whose compositions lie on one of the lines. The phase assemblages along these seven univariant lines are as follows:

(1) Pseudowollastonite (α-$CaSiO_3$) + wollastonite (β-$CaSiO_3$ solid solutions) + anorthite + liquid. *R'* (Fig. 9) lies on this line.

(2) Wollastonite (β-$CaSiO_3$ solid solutions) +

[34] E. F. Osborn, see reference 20 (*c*), p. 248.

[35] N. L. Bowen, J. F. Schairer, and E. Posnjak, "System CaO–FeO–SiO_2," *Amer. Jour. Sci.*, 26, pp. 211–12 (1933).

TABLE IV

THE JOIN $CaSiO_3$–ANORTHITE–FeO
RESULTS OF QUENCHING EXPERIMENTS

(All compositions expressed in weight per cent)

Experiment No. DQ	Planned composition			Final composition by analysis			Temp. of completion of melting ±4°C.	Refractive index of glass ±0.003
	$CaSiO_3$	Anorthite	FeO	FeO	Fe_2O_3	Total Fe as FeO		
			(a) Mixtures Having Anorthite as Primary Phase					
45	10	70	20	22.6	0.0	22.6	1353	1.649
44	15	60	25	27.1	0.1	27.2	1290	1.674
4	20	55	25	27.5	0.0	27.5	1268	1.674
7	50	45	5	11.3	0.1	11.4	1263	1.630
34	37	40	23	23.4	1.0	24.3	1193	1.677
10	45	40	15	19.9	1.0	20.8	1208	1.656
48	38	37	25	26.4	0.1	26.5	1155	1.686
35	45	33	22	21.9	0.0	21.9	1148	1.673
62	44	32	24	24.6	0.0	24.6	1128	1.681
			(b) Mixtures Having Hercynite as Primary Phase					
18	24	43	33	34.0	0.2	34.2	1225	1.709
47	30	42	28	30.4	0.0	30.4	1175	1.693
32	30	40	30	38.2	1.6	39.6	1210	1.738
46	34	37	29	30.2	0.1	30.3	1145	1.698
5	25	35	40	40.7	1.7	42.2	1223	
29	34	34	32	36.3	1.0	37.2	1160	1.732
70	37	31	32	34.1	1.8	35.7	1130	1.726
11	35	30	35	40.0	1.1	41.0	1155	
59	5	25	70	63.2	7.1	69.6	1280*	
			(c) Mixtures Having Melilite as Primary Phase					
69	37	35	28	27.5	2.4	29.7	1128	1.703
23	40	35	25	31.0	0.0	31.0	1128	1.706
74	47	31	22	25.0	0.9	25.8	1123	1.687
49	47	31	22	27.2	0.4	27.6	1128	1.694
22	40	30	30	32.5	1.0	33.4	1125	1.714
73	48	30	22	27.1	0.0	27.1	1128	1.688
28	46	28	26	30.9	1.4	32.2	1125	1.712
26	38	27	35	37.0	0.0	37.0	1123	1.732
39	48	26	26	30.1	0.8	30.8	1123	1.712
63	50	22	28	28.9	0.8	29.6	1130	1.708
			(d) Mixtures Having Olivine as Primary Phase					
67	45	22	33	31.4	1.2	32.5	1133	1.718
66	46	19	35	35.6	2.4	37.8	1148	
24	53	18	29	28.9	1.8	30.5	1140	1.709
6	45	15	40	38.7	2.3	40.8	1160	
25	58	12	30	30.6	1.9	32.3	1170	1.728
17	62	10	28	29.4	0.7	30.0	1170	1.718
8	68	5	27	30.7	1.4	32.0	1185	1.724
68	55	4	41	36.5	4.0	40.1	1198	
85	56		44	39.2	4.4	43.2	1223	
54	58		42	38.6	4.2	42.4	1218	
			(e) Mixtures Having Wüstite as Primary Phase				Temp. of completion of melting, °C.	
43	20	25	55	51.5	5.7	56.6	1240±10	
20	35	25	40	40.2	3.1	43.0	1150± 5	
33	38	25	37	43.0	3.1	45.8	1180± 5	
27	40	23	37	41.9	2.6	44.2	1165± 5	
65	10	20	70	63.9	6.0	69.3	1258±10	
12	35	20	45	45.6	5.0	50.1	1220±10	
19	40	20	40	39.7	1.8	41.3	1153± 5	
40	43	17	40	43.9	2.3	46.0	1185± 5	
60	25	15	60	55.1	6.1	60.6	1265±10	
84	13	11	76	68.5	6.7	74.6	1290±10	
31	46	10	44	47.4	5.3	52.2	1240±10	
81	28	7	65	60.4	7.8	67.4	1295±10	
42	50	5	45	43.3	4.4	47.3	1225±10	
83	25		75	67.8	6.7	73.8	1305±10	
30	55		45	45.1	4.3	49.0	1240±10	

* Temp. of completion of melting ±10°C.

TABLE IV (*continued*)

Experiment No. DQ	Planned composition			Final composition by analysis			Temp. of completion of melting ±4°C.	Refractive index of glass ±0.00.3
	$CaSiO_3$	Anorthite	FeO	FeO	Fe_2O_3	Total Fe as FeO		
			(*f*) Mixtures Having Pseudowollastonite as Primary Phase					
3	55	40	5	9.4	0.0	9.4	1288	1.623
15	49	35	16	17.7	0.0	17.7	1191	1.652
53	54	29	17	20.5	0.3	20.8	1193	1.668
52	55	26	19	20.1	0.9	20.9	1200	1.669
2	60	25	15	17.2	0.1	17.3	1268	1.659
1	70	10	20	24.7	0.0	24.7	1268	1.689
79	66	7	27	27.6	2.0	29.4	1198	1.717
37	70	3	27	25.1	1.2	26.2	1250	1.708
			(*g*) Mixtures Having Wollastonite Solid Solutions as Primary Phase					
15	49	35	16	19.2	0.0	19.2	1160	1.658
61	49	32	19	20.8	0.2	21.0	1148	1.673
38	51	31	18	23.1	0.0	23.1	1148	1.678
14	50	25	25	25.7	0.2	25.9	1140	1.689
51	53	23	24	25.5	0.6	26.0	1155	1.689
77	56	18	26	28.3	0.2	28.5	1150	1.704
78	57	15	28	27.7	2.2	29.7	1163	1.707
9	60	15	25	25.6	0.6	26.1	1188	1.697

Experiment No. DQ	Planned composition			Final composition by analysis			Temp. °C.	Results of microscopic examination	Refractive index of glass ±0.003
	$CaSiO_3$	Anorthite	FeO	FeO	Fe_2O_3	Total Fe as FeO			
				(*h*) Quenching Experiments on Mixtures with More Than One Solid Phase					
44	15	60	25	27.1	0.1	27.2	1265 ± 4	Anorthite and very rare hercynite in liquid	
4	20	55	25	27.5	0.0	27.5	1225 ± 4	Anorthite and very rare hercynite in liquid	
16	51	43	6	11.9	0.1	12.0	1245 ± 4	Rare anorthite and rare pseudowollastonite in liquid	
16	51	43	6	11.9	0.1	12.0	1250 ± 4	All liquid	1.631
47	30	42	28	30.4	0.0	30.4	1165 ± 4	Rare anorthite and rare hercynite in liquid	
80	49	38	13	15.5	0.6	16.0	1205 ± 4	Rare anorthite and very rare pseudowollastonite in liquid	1.646
46	34	37	29	30.2	0.1	30.3	1135 ± 4	Hercynite and very rare anorthite in liquid	
46	34	37	29	30.2	0.1	30.3	1123 ± 4	Hercynite, anorthite, and very rare melilite in liquid	
15	49	35	16	17.7	0.0	17.7	1185 ± 4	Pseudowollastonite and rare wollastonite in liquid	
15	49	35	16	17.7	0.0	17.7	1190 ± 4	Very rare pseudowollastonite in liquid	1.652
69	37	35	28	27.5	2.4	29.7	1110 ± 4	Melilite, very rare anorthite, very rare hercynite in liquid	
62	44	32	24	24.6	0.0	24.6	1125 ± 4	Anorthite and very rare melilite in liquid	
61	49	32	19	20.8	0.2	21.0	1138 ± 4	Wollastonite and very rare anorthite in liquid	
70	37	31	32	34.1	1.8	35.7	1123 ± 4	Hercynite and very rare melilite in liquid	
38	51	31	18	23.1	0.0	23.1	1127 ± 4	Wollastonite and very rare melilite in liquid	
74	47	31	22	25.0	0.9	25.8	1118 ± 4	Melilite, very rare wollastonite, and very rare anorthite in liquid	
53	54	29	17	20.5	0.3	20.8	1185 ± 4	Wollastonite and very rare pseudowollastonite in liquid	
53	54	29	17	20.5	0.3	20.8	1190 ± 4	Pseudowollastonite and rare wollastonite in liquid	
53	54	29	17	20.5	0.3	20.8	1195 ± 4	All liquid	1.668
28	46	28	26	30.9	1.4	32.2	1113 ± 4	Melilite and very rare olivine in liquid	
55	17	28	55	52.9	5.1	57.5	1230 ± 10	Very rare hercynite and very rare wüstite in liquid	
36	27	27	46	43.7	2.8	46.2	1180 ± 10	Very rare hercynite and very rare wüstite in liquid	
26	38	27	35	37.0	0.0	37.0	1120 ± 4	Rare melilite and very rare hercynite in liquid	

TABLE IV (*concluded*)

Experiment No. DQ	Planned composition: $CaSiO_3$	Planned composition: Anorthite	Planned composition: FeO	Final composition by analysis: FeO	Final composition by analysis: Fe_2O_3	Final composition by analysis: Total Fe as FeO	Temp. °C.	Results of microscopic examination	Refractive index of glass ±0.003
				(h) Quenching Experiments on Mixtures with More Than One Solid Phase (*concluded*)					
64	48	27	25	25.7	0.1	25.8	1125 ± 4	Rare wollastonite and rare melilite in liquid	
64	48	27	25	25.7	0.1	25.8	1130 ± 4	All liquid	1.688
76	38	26	36	37.4	0.8	38.1	1120 ± 4	Rare olivine and rare hercynite in liquid	
76	38	26	36	37.4	0.8	38.1	1125 ± 4	All liquid	
39	48	26	26	30.1	0.8	30.8	1118 ± 4	Melilite and very rare olivine in liquid	
52	55	26	19	20.1	0.9	20.9	1195 ± 4	Pseudowollastonite and rare wollastonite in liquid	
52	55	26	19	20.1	0.9	20.9	1200 ± 4	Very rare pseudowollastonite in liquid	1.669
58	11	25	64	55.7	7.6	62.5	1245 ± 10	Very rare hercynite and very rare wüstite in liquid	
21	40	25	35	36.7	0.1	36.8	1120 ± 4	Very rare olivine and very rare melilite in liquid	1.729
21	40	25	35	36.7	0.1	36.8	1113 ± 4	Melilite, olivine, and very rare hercynite in liquid	
14	50	25	25	25.7	0.2	25.9	1128 ± 4	Wollastonite and very rare melilite in liquid	
57	48	23	29	29.3	1.2	30.4	1130 ± 4	Very rare melilite and very rare olivine in liquid	1.708
51	53	23	24	25.5	0.6	26.0	1128 ± 4	Wollastonite and very rare melilite in liquid	
63	50	22	28	28.9	0.8	29.6	1128 ± 4	Rare melilite and very rare olivine in liquid	
19	40	20	40	39.7	1.8	41.3	1135 ± 5	Wüstite and very rare olivine in liquid	
82	4	19	77	70.0	7.3	76.6	1285 ± 4	Very rare hercynite and very rare wüstite in liquid	
24	53	18	29	28.9	0.7	30.5	1137 ± 4	Rare olivine and very rare melilite in liquid	
77	56	18	26	28.3	0.2	28.5	1143 ± 4	Wollastonite and very rare melilite in liquid	
78	57	15	28	27.7	2.2	29.7	1155 ± 4	Wollastonite and very rare olivine in liquid	
17	62	10	28	29.4	0.7	30.0	1163 ± 4	Olivine and very rare wollastonite in liquid	
56	50	9	41	39.9	3.4	43.0	1185 ± 4	Rare olivine and rare wüstite in liquid	
56	50	9	41	39.9	3.4	43.0	1190 ± 4	All liquid	
79	66	7	27	27.6	2.0	29.4	1180 ± 4	Wollastonite, pseudowollastonite, and rare olivine in liquid	
79	66	7	27	27.6	2.0	29.4	1185 ± 4	Pseudowollastonite and rare wollastonite in liquid	
79	66	7	27	27.6	2.0	29.4	1190 ± 4	Pseudowollastonite in liquid	

Letter (Fig. 9)	Temp. °C.	Solid and liquid phases present
		(i) Temperatures and Compositions of Lettered Points in Fig. 9
Q	1307 ± 3	Anorthite + pseudowollastonite + liquid ($CaSiO_3$ 52 anorthite 48) (Osborn)
R	1125 ± 5	Wollastonite + anorthite + melilite + liquid ($CaSiO_3$ 46.2 anorthite 30.6 FeO 23.2)
R'	1186 ± 5	Pseudowollastonite + wollastonite + anorthite + liquid ($CaSiO_3$ 47.0 anorthite 35.5 FeO 17.5)
S	1130 ± 5	Hercynite + melilite + anorthite + liquid ($CaSiO_3$ 34.3 anorthite 35.5 FeO 30.2)
T	1118 ± 5	Hercynite + melilite + olivine + liquid ($CaSiO_3$ 37 anorthite 25 FeO 38)
U	1118 ± 5	Hercynite + wüstite + olivine + liquid ($CaSiO_3$ 36 anorthite 25 FeO 39)
V	1145 ± 5	Wollastonite + olivine + melilite + liquid ($CaSiO_3$ 54.0 anorthite 16.5 FeO 29.5)
V'	1188 ± 5	Pseudowollastonite + wollastonite + olivine + liquid ($CaSiO_3$ 64 anorthite 6 FeO 30)
W	1203 ± 3	Pseudowollastonite + $CaFeSiO_4$ + liquid ($CaSiO_3$ 69.4 FeO 30.6) (Bowen, Schairer, and Posnjak)
X	1220 ± 10	Olivine + wüstite + liquid ($CaSiO_3$ 56 FeO 44)

For *H* and *G* see Table II (g)

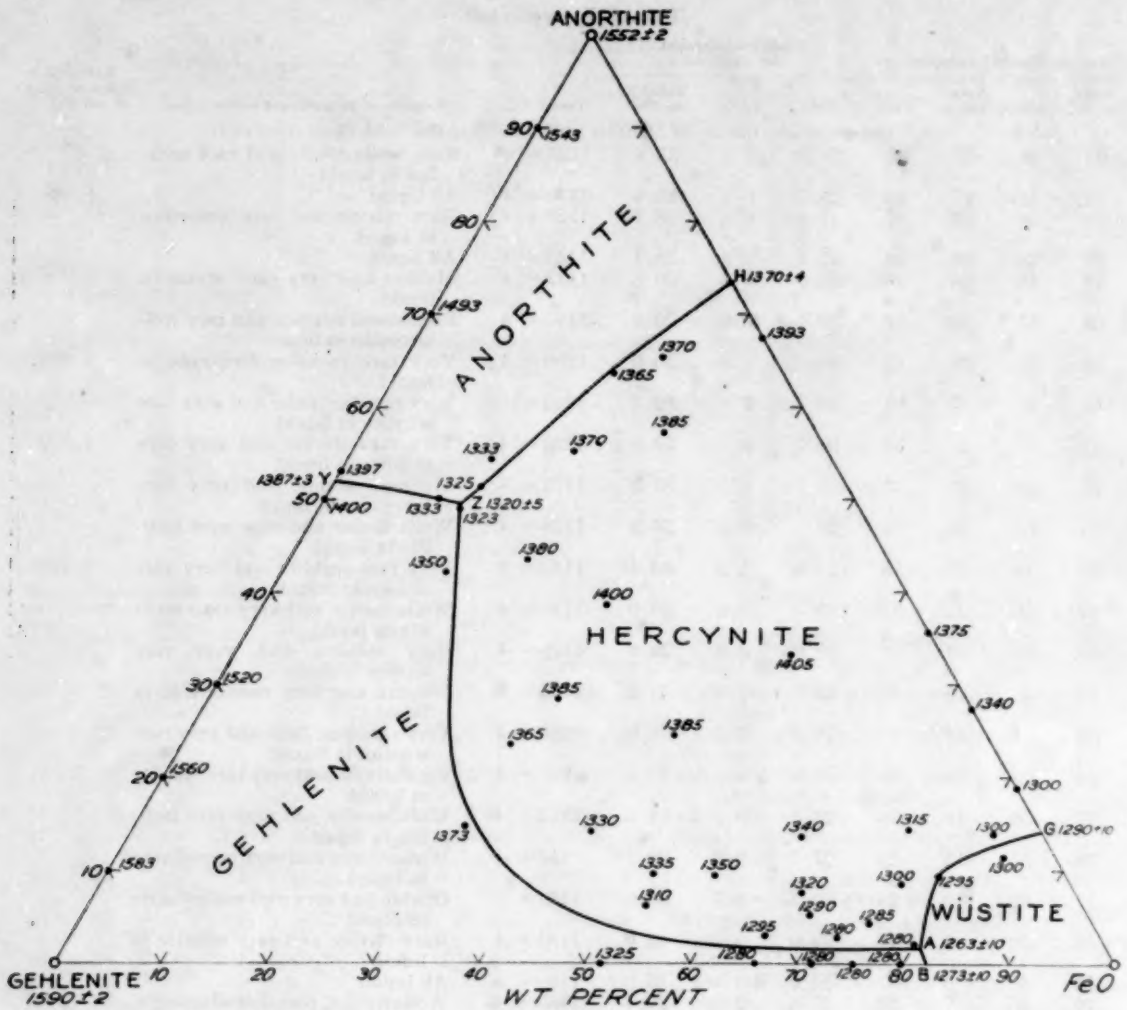

FIG. 10.—Equilibrium diagram of the join gehlenite–anorthite–FeO, showing compositions studied, primary phases, and liquidus temperatures.

anorthite + melilite + liquid. *R* (Fig. 9) lies on this line.

(3) Pseudowollastonite (α-$CaSiO_3$) + wollastonite (β-$CaSiO_3$ solid solutions) + olivine (solid solutions) + liquid. *V'* (Fig. 9) lies on this line, and the ternary reaction point pseudowollastonite + wollastonite (solid solutions) + olivine (solid solutions) + liquid *e* (of Table VII) in the limiting system CaO–FeO–SiO_2 is one terminus of this line.

(4) Wollastonite (β-$CaSiO_3$ solid solutions) + olivine (solid solutions) + melilite + liquid. *V* (Fig. 9) lies on this line.

(5) Anorthite + hercynite + melilite + liquid. *S* (Fig. 9) lies on this line and the join gehlenite–anorthite–FeO cuts this line at *Z* (Fig. 10).

(6) Olivine (solid solution) + hercynite + melilite + liquid. *T* (Fig. 9) lies on this line.

(7) Olivine (solid solution) + wüstite + hercynite + liquid. *U* (Fig. 9) lies on this line; the join SiO_2–anorthite–FeO cuts this line at *F* (Fig. 7); and the ternary eutectic fayalite + wüstite + hercynite + liquid (*l* of Table VII) in the limiting system FeO–Al_2O_3–SiO_2 is one terminus of this line.

Each such curved univariant line within the tetrahedron has two termini, (1) at two quaternary invariant points, (2) at one ternary invariant point and one quaternary invariant point, or (3) at two ternary invariant points in different faces of the tetrahedron. Each such univariant line may or may not have a temperature maximum or minimum at some point along the line. This temperature distribution and the factors on which it depends will be discussed in section (8*D*). By noting which of the joins studied cut the different univariant lines and the probable termini of such lines, much information concerning the location and approximate temperatures of quaternary invariant

TABLE V

THE JOIN GEHLENITE–ANORTHITE–FeO
RESULTS OF QUENCHING EXPERIMENTS

(All compositions expressed in weight per cent)

Experiment No. AQ	Planned composition			Final composition by analysis			Temp. of completion of melting °C.	Refractive index of glass ±0.003
	Gehlenite	Anorthite	FeO	FeO	Fe_2O_3	Total Fe as FeO		
			(a) Mixtures Having Hercynite as Primary Phase					
17	17	69	14	19.8	0.7	20.4	1365 ± 5	1.647
13	11	69	20	23.0	1.3	24.2	1370 ± 5	1.654
4	15	60	25	27.2	1.7	28.7	1385 ± 5	1.678
12	25	58	17	20.7	0.3	21.0	1370 ± 5	1.654
9	35	45	20	21.8	1.0	22.7	1380 ± 5	1.673
2	30	40	30	30.7	1.9	32.4	1400 ± 5	1.707
8	15	35	50	48.8	4.2	52.6	1405 ± 5	
18	42	31	27	30.7	2.6	33.0	1385 ± 5	1.713
21	48	25	27	29.5	1.7	31.0	1365 ± 5	1.722
6	30	25	45	42.4	4.0	46.0	1385 ± 5	
10	45	15	40	38.9	5.0	43.4	1330 ± 5	
7	25	15	60	58.2	6.1	63.7	1340 ± 10	
16	13	15	72	66.1	8.0	73.3	1315 ± 10	
25	5	15	80	70.8	0.4	81.2	1300 ± 10	
29	44	11	45	46.8	5.6	51.8	1335 ± 10	
14	35	10	55	49.1	9.2	57.4	1350 ± 10	
15	27	8	65	58.1	9.6	66.7	1320 ± 10	
24	15	8	77	67.2	9.1	75.4	1300 ± 10	
20	40	6	54	46.0	7.4	52.7	1310 ± 10	
23	25	5	70	63.2	5.9	68.5	1290 ± 10	
35	20	4	76	67.0	8.3	74.5	1285 ± 10	
27	32	3	65	55.5	11.0	65.4	1295 ± 10	
32	26	3	71	64.2	8.9	72.2	1280 ± 10	
36	21	2	77	68.4	12.9	80.0	1280 ± 10	
			(b) Mixtures Having Anorthite* or Gehlenite† or Wüstite‡ as Primary Phase					
19	34	58	8	13.6	0.2	13.8	1333 ± 5	1.638
3	45	45	10	15.3	0.0	15.3	1350 ± 5	1.647
33	55	15	30	28.3	3.1	31.1	1373 ± 5	1.729
1	50		50	46.1	5.7	51.2	1325 ± 10	
5	35		65	56.9	10.1	66.0	1280 ± 10	
22	30		70	63.2	9.1	71.4	1280 ± 10	
34	25		75	67.5	8.6	75.2	1280 ± 10	
37	20		80	69.1	11.9	79.8	1280 ± 10	
30	5	12	83	73.2	11.6	83.6	1300 ± 10	

* Anorthite primary phase for No. 19.
† Gehlenite primary phase for No. 3 through 37.
‡ Wüstite primary phase for No. 30.

Experiment No. AQ	Planned composition			Final composition by analysis			Temp. °C.	Results of microscopic examination	Refractive index of glass ±0.003
	Gehlenite	Anorthite	FeO	FeO	Fe_2O_3	Total Fe as FeO			
			(c) Quenching Experiments on Mixtures with More Than One Solid Phase						
17	17	69	14	19.8	0.7	20.4	1360 ± 5	Anorthite and very rare hercynite in liquid	
26	37	55	8	13.7	0.8	14.4	1325 ± 5	Very rare hercynite and very rare anorthite in liquid	1.639
28	43	55	2	10.9	0.0	10.9	1330 ± 5	Gehlenite and anorthite in liquid	
28	43	55	2	10.9	0.0	10.9	1335 ± 5	All liquid	1.633
11	40	52	8	13.3	0.0	13.3	1315 ± 5	Gehlenite, hercynite, and very rare anorthite in liquid	
11	40	52	8	13.3	0.0	13.3	1320 ± 5	Rare gehlenite and rare hercynite in liquid	1.637
33	55	15	30	28.3	3.1	31.1	1365 ± 5	Gehlenite and very rare hercynite in liquid	
31	10	8	82	70.6	8.7	78.4	1295 ± 10	Very rare hercynite and very rare wüstite in liquid	
20	40	6	54	46.0	7.5	52.7	1290 ± 10	Hercynite and very rare gehlenite in liquid	
27	32	3	65	55.5	11.0	65.4	1280 ± 10	Hercynite and very rare gehlenite in liquid	
32	26	3	71	64.2	8.9	72.2	1275 ± 10	Hercynite and rare gehlenite in liquid	
36	21	2	77	68.4	12.9	80.0	1265 ± 10	Hercynite, gehlenite, and wüstite in liquid	

TABLE V (*concluded*)

Experiment No. AQ	Planned composition: Gehlenite	Planned composition: Anorthite	Planned composition: FeO	Final composition by analysis: FeO	Final composition by analysis: Fe_2O_3	Final composition by analysis: Total Fe as FeO	Temp. °C.	Results of microscopic examination
				(*c*) Quenching Experiments on Mixtures with More Than One Solid Phase (*concluded*)				
36	21	2	77	68.4	12.9	80.0	1270 ± 10	Hercynite and gehlenite in liquid
36	21	2	77	68.4	12.9	80.0	1275 ± 10	Rare hercynite and rare gehlenite in liquid
36	21	2	77	68.4	12.9	80.0	1280 ± 10	Very rare hercynite in liquid
37	20		80	69.1	11.9	79.8	1270 ± 10	Wüstite and gehlenite in liquid
37	20		80	69.1	11.9	79.8	1275 ± 10	Gehlenite in liquid

Letter (Fig. 9)	Temp. °C.	Solid and liquid phases present
		(*d*) Temperatures and Compositions of Lettered Points in Fig. 9
Y	1387 ± 3	Gehlenite + anorthite + liquid (gehlenite 48 anorthite 52) (Osborn)
Z	1320 ± 5	Gehlenite + anorthite + hercynite + liquid (gehlenite 37.3 anorthite 49.6 FeO 13.1)
A	1263 ± 10	Gehlenite + hercynite + wüstite + liquid (approximately gehlenite 17.8 anorthite 1.4 FeO 80.8)
B	1273 ± 10	Gehlenite + wüstite + liquid (approximately gehlenite 18 FeO 82)

For *H* and *G* see Table II (*g*), p. 252.

points may be deduced from knowledge of only five joins (planes) through the tetrahedron.

For example, note the close proximity (almost within experimental error) of the points *U* and *T* (Fig. 9) in composition and temperature. *U* is the piercing point of the univariant line *IJ* (Fig. 12) along which olivine + wüstite + hercynite + liquid are in equilibrium within the tetrahedron. *T* is the piercing point of the univariant line *IJ* (Fig. 12) along which olivine + hercynite + melilite + liquid are in equilibrium within the tetrahedron. When a fourth solid crystalline phase is added to each of these (melilite to the first and wüstite to the second), the quaternary eutectic point (*J*, Fig. 12) olivine + hercynite + melilite + wüstite + liquid is reached. This quaternary point must be located in the volume gehlenite–anorthite–$CaSiO_3$–FeO, very near the plane $CaSiO_3$–anorthite–FeO, at a composition very close to the compositions of *U* and *T*, and at a temperature close to (but lower than) the temperatures of *U* and *T*.

(*D*) *The Join Gehlenite–Anorthite–FeO:* The experimental data for this join are given in Table V and presented graphically as Fig. 10. This join cuts the following four primary phase volumes within the tetrahedron: Anorthite + liquid, gehlenite[36] + liquid, hercynite ($FeO \cdot Al_2O_3$, whose composition lies outside the plane of this join) + liquid, and wüstite + liquid.

In Fig. 10, the data for the point *Y* and other points in the binary system gehlenite–anorthite are from unpublished data of E. F. Osborn of this Laboratory. These data are more complete than (but check very closely with) the data of Rankin and Wright for the system CaO–Al_2O_3–SiO_2. The data for points *H* and *G* and other points on the side anorthite–FeO have already been given in Table II. The side anorthite–FeO also forms one side of the joins SiO_2–anorthite–FeO (Fig. 7), anorthite–Al_2O_3–FeO (Fig. 8), and $CaSiO_3$–anorthite–FeO (Fig. 9). Data for the point *B* (Fig. 10) and other points on the side gehlenite–FeO are given in Table V.

The five heavy curves (*YZ*, *HZ*, *ZA*, *BA*, and *GA* of Fig. 10) are traces of the curved surfaces, along which two adjacent primary phase volumes join within the tetrahedron, in the plane gehlenite–anorthite–FeO. The points *Z* and *A* are piercing points of two univariant lines, within the tetrahedron, in the plane gehlenite–anorthite–FeO. Along each of these curved univariant lines, three crystalline solid phases are in equilibrium with liquids whose compositions lie on one of these lines. The phase assemblages along the two univariant lines are as follows:

(1) Gehlenite (melilite) + anorthite + hercynite + liquid. *Z* (Fig. 10) lies on this line, and the join $CaSiO_3$–anorthite–FeO cuts this line at *S* (Fig. 9).

(2) Gehlenite (melilite) + hercynite + wüstite + liquid. *A* (Fig. 10) lies on this line.

(*E*) *The Join $CaSiO_3$–Gehlenite–FeO:* The experimental data for this join are given in Table VI and presented graphically as Fig. 11. This join cuts the following four primary phase volumes within the tetrahedron: α-$CaSiO_3$ + liquid, melilite + liquid, olivine + liquid, and wüstite + liquid.

In Fig. 11, a light line joins the compositions of gehlenite ($2CaO \cdot Al_2O_3 \cdot SiO_2$ or $Ca_2Al_2SiO_7$) and iron-akermanite ($2CaO \cdot FeO \cdot 2SiO_2$ or $Ca_2FeSi_2O_7$). Bowen, Schairer, and Posnjak[37] have shown that the iron analog of akermanite is stable only at temperatures below 775° ± 25°C., and above that temperature it is decomposed into β-$CaSiO_3$ and the lime–iron olivine $CaFeSiO_4$. These authors suggest that although iron–akermanite itself is stable only below 775°, when it enters into solid solution with other melilite molecules that are stable at high temperatures (such as gehlenite), the resulting solid solutions should have their range of stability extended to higher temperatures. No information on this point is available at this time because the study of

[36] Pure gehlenite has the composition $2CaO \cdot Al_2O_3 \cdot SiO_2$. Optical and chemical data are not yet complete on the tetragonal crystals in equilibrium with these melts. They may be melilite crystals (solid solutions of gehlenite and iron–akermanite, $2CaO \cdot FeO \cdot 2SiO_2$).

[37] N. L. Bowen, J. F. Schairer, and E. Posnjak, "System CaO–FeO–SiO_2," *Amer. Jour. Sci.*, **26**, pp. 211–12 and p. 276 (1933).

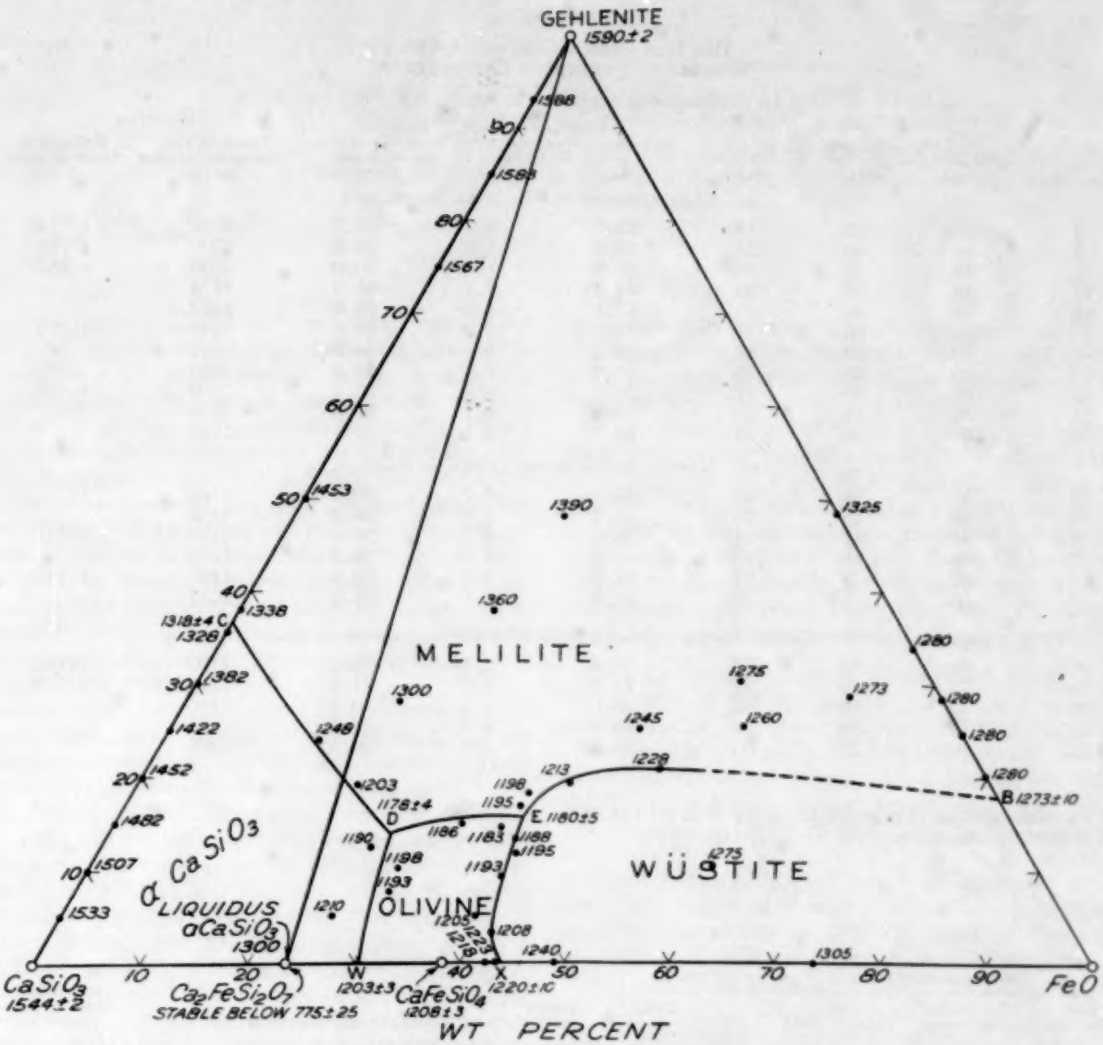

FIG. 11.—Equilibrium diagram of the join $CaSiO_3$–gehlenite–FeO, showing compositions studied, primary phases, and liquidus temperatures.

the chemical and optical properties of the crystalline phases in the quaternary melts is not yet complete.

In Fig. 11, the data for the point *C* and other points in the binary system $CaSiO_3$–gehlenite are from Osborn and Schairer.[38] The data for the point *B* and other points in the side gehlenite–FeO, which is also common to the join gehlenite–anorthite–FeO (Fig. 10), have already been given in Table V. The source of the data for the points *W* and *X* and other points in the side $CaSiO_3$–FeO has already been given in section (6*C*), p. 255.

The five heavy curves (*CD*, *WD*, *DE*, *XE*, and *BE* of Fig. 11) are traces of the curved surfaces, along which two adjacent primary phase volumes join within the tetrahedron, in the plane $CaSiO_3$–gehlenite–FeO. The points *D* and *E* are piercing points of two univariant lines, within the tetrahedron, in the plane $CaSiO_3$–gehlenite–FeO. Each of these is a point (on one of the two univariant lines) which happens to lie in the plane $CaSiO_3$–gehlenite–FeO. Along each of these two curved univariant lines, three crystalline solid phases are in equilibrium with liquids whose compositions lie on one of these lines. The phase assemblages along the two univariant lines are as follows:

(1) α-$CaSiO_3$ + melilite + olivine + liquid. *D* (Fig. 11) lies on this line.

(2) Melilite + olivine + wüstite + liquid. *E* (Fig. 11) lies on this line.

(7) Crystalline Solid Phases

Seven crystalline solids of fixed composition are found in the portion of the quaternary system studied,

[38] E. F. Osborn and J. F. Schairer, "Ternary System Pseudowollastonite–Akermanite–Gehlenite," *Amer. Jour. Sci.*, **239** [10] pp. 715–63 (1941).

TABLE VI

THE JOIN $CaSiO_3$–GEHLENITE–FeO
RESULTS OF QUENCHING EXPERIMENTS

(All compositions expressed in weight per cent)

Experiment No. EQ	Planned composition			Final composition by analysis			Temp. of completion of melting ±4°C.	Refractive index of glass ±0.003
	$CaSiO_3$	Gehlenite	FeO	FeO	Fe_2O_3	Total Fe as FeO		
			(a) Mixtures Having Melilite as Primary Phase					
4	30	55	15	22.7	3.3	25.7	1390	1.714
3	40	40	20	22.4	1.8	24.0	1360	1.708
1	55	30	15	18.9	1.2	20.0	1300	1.687
12	18	30	52	44.9	7.1	51.3	1275	
18	9	30	61	52.4	11.6	62.8	1273	
11	64	25	11	14.4	0.2	14.6	1248	1.672
6	30	25	45	40.2	4.6	44.3	1245	
17	20	25	55	47.4	7.6	54.2	1260	
25	63	20	17	20.5	0.2	20.7	1203	1.693
21	46	19	35	32.7	5.1	37.3	1198	
22	49	18	33	32.5	5.1	37.1	1195	
			(b) Mixtures Having Olivine as Primary Phase					
23	56	16	28	31.1	1.7	32.6	1186	1.732
5	50	15	35	33.2	3.8	36.6	1183	
9	65	11	24	26.1	3.2	29.0	1198	1.717
7	55	10	35	36.7	2.8	39.2	1193	
8	65	8	27	28.3	1.2	29.4	1193	1.719
13	56	5	39	36.4	3.1	39.2	1205	
			(c) Mixtures Having Pseudowollastonite* or Wüstite† as Primary Phase					
20	65	13	22	23.4	2.0	25.2	1190	1.702
16	71	5	24	24.5	0.9	25.3	1210	1.708
10	50	12	38	36.6	3.1	39.4	1195	
14	39	19	42	36.4	4.8	40.7	1213	
26	30	10	60	55.2	3.8	58.6	1275	

* Pseudowollastonite primary phase for Nos. 20 and 16.
† Wüstite primary phase for Nos. 10, 14, and 26.

Experiment No. EQ	Planned composition			Final composition by analysis			Temp. ±4°C.	Results of microscopic examination	Refractive index of glass ±0.003
	$CaSiO_3$	Gehlenite	FeO	FeO	Fe_2O_3	Total Fe as FeO			
			(d) Quenching Experiments on Mixtures with More than One Solid Phase						
16	71	5	24	24.5	0.9	25.3	1185	Pseudowollastonite and olivine in liquid	
16	71	5	24	24.5	0.9	25.3	1190	Pseudowollastonite in liquid	
8	65	8	27	28.3	1.2	29.4	1170	Olivine and very rare melilite in liquid	
9	65	11	24	26.1	3.2	29.0	1178	Olivine and very rare melilite in liquid	
2	65	15	20	25.0	2.0	26.8	1175	Rare olivine, rare melilite, and rare pseudowollastonite in liquid	
2	65	15	20	25.0	2.0	26.8	1180	All liquid	1.704
11	64	25	11	14.4	0.2	14.6	1240	Melilite and very rare pseudowollastonite in liquid	
23	56	16	28	31.1	1.7	32.6	1180	Rare olivine and rare melilite in liquid	
23	56	16	28	31.1	1.7	32.6	1185	Very rare olivine in liquid	1.732
24	55	3	42	39.1	2.9	41.7	1205	Rare olivine and rare wüstite in liquid	
24	55	3	42	39.1	2.9	41.7	1210	All liquid	
10	50	12	38	36.6	3.1	39.4	1185	Olivine and wüstite in liquid	
10	50	12	38	36.6	3.1	39.4	1190	Wüstite in liquid	
19	50	14	36	34.2	5.2	38.9	1185	Rare olivine and rare wüstite in liquid	
19	50	14	36	34.2	5.2	38.9	1190	All liquid	
22	49	18	33	32.5	5.1	37.1	1180	Melilite and rare olivine in liquid	
22	49	18	33	32.5	5.1	37.1	1185	Melilite in liquid	
21	46	19	35	32.7	5.1	37.3	1190	Melilite and rare wüstite in liquid	
21	46	19	35	32.7	5.1	37.3	1195	Rare melilite in liquid	
14	39	19	42	36.4	4.8	40.7	1200	Wüstite and rare melilite in liquid	
14	39	19	42	36.4	4.8	40.7	1205	Wüstite in liquid	
15	31	21	48	42.0	7.2	48.5	1225	Rare melilite and rare wüstite in liquid	
15	31	21	48	42.0	7.2	48.5	1230	All liquid	

TABLE VI (*concluded*)

Letter (Fig. 10)	Temp. °C.	Solid and liquid phases present
	(*e*)	Temperatures and Compositions of Lettered Points in Fig. 10
C	1318 ± 4	α-$CaSiO_3$ + gehlenite + liquid ($CaSiO_3$ 63.3 gehlenite 36.7) (Osborn and Schairer)
D	1178 ± 4	α-$CaSiO_3$ + melilite + olivine + liquid ($CaSiO_3$ 59.8 gehlenite 13.4 FeO 26.8)
E	1180 ± 5	Olivine + melilite + wüstite + liquid ($CaSiO_3$ 46.1 gehlenite 15.7 FeO 38.2)

For *B*, see Table V (*d*), p. 262.
For *W* and *X*, see Table IV (*i*), p. 259.

namely, corundum, mullite,[39] tridymite, cristobalite, α-$CaSiO_3$ (pseudowollastonite), and anorthite. The crystalline solid phases wüstite, olivine, wollastonite (β-$CaSiO_3$ with $FeSiO_3$ and possibly some molecule containing Al_2O_3), and probably melilite (gehlenite with other melilite compounds) are not of fixed composition in this system but are solid solutions. The composition of wüstite has been discussed by Bowen and Schairer[40] and by Jette and Foote.[41] The compositions of melilites in systems containing FeO have been discussed by Bowen, Schairer, and Posnjak.[42] Inasmuch as data on the chemical composition and optical properties of the solid phases are not yet complete, no additional information on the composition of the melilites is recorded here.

In the limiting ternary system CaO–FeO–SiO_2, Bowen, Schairer, and Posnjak reported in detail on the chemical compositions and optical properties of three sets of solid solutions occurring as crystalline phases in that system, namely, the olivines (lime–iron olivines), the wollastonites, and the hedenbergites, the last occurring in the ternary system only at temperatures below which liquid was present. No additional information is given at this time on these three sets of solid solutions. The wollastonites appear only as a small area on one join, and hedenbergites do not appear at liquidus temperatures on any of the five joins reported here. Optical and chemical data for the wollastonite solid solution crystals are incomplete and are not reported here. Olivines appear on three of the joins studied, namely, SiO_2–anorthite–FeO, $CaSiO_3$–anorthite–FeO, and $CaSiO_3$–gehlenite–FeO, but data on their chemical composition and optical properties are incomplete and are not recorded here.

(8) Univariant Lines and the Quaternary Invariant Points

The data already presented yield some information about eleven of the quaternary invariant points in the system. Data on the rest of the quaternary invariant points are still lacking. The determination of these requires a study of the limiting ternary system CaO–FeO–Al_2O_3 and of other joins nearer that face of the tetrahedron.

(*A*) *Univariant Lines:* In Figs. 7 through 11, where three heavy curves meet at a point (*F*, *I*, and *J* of Fig. 7; *N* of Fig. 8; *S*, *T*, *U*, *R*, *R'*, *V*, and *V'* of Fig. 9; *Z* and *A* of Fig. 10; and *D* and *E* of Fig. 11), each such point lies on a quaternary univariant line within the tetrahedron. Along each of these curved lines three solid crystalline phases are in equilibrium with liquids whose compositions lie on the line. Each such curved univariant line within the tetrahedron may connect:

(1) Two ternary invariant points which lie in different faces of the tetrahedron. There is one such univariant line in the portion of the tetrahedron discussed in this paper. It connects the ternary inversion point cristobalite + tridymite + mullite + liquid (1470° ± 5°C.) in the ternary system CaO–Al_2O_3–SiO_2 and the ternary inversion point cristobalite + tridymite + mullite + liquid (1470° ± 5°) in the ternary system FeO–Al_2O_3–SiO_2. There is no change of temperature (no solid solution of other substances in SiO_2) along this curved univariant line on which lie the compositions of all quaternary liquids in equilibrium with two of the forms of SiO_2, tridymite and cristobalite, and with mullite. This univariant line is not found in Fig. 12, which depicts only the interrelations of the univariant lines connecting the ternary and quaternary invariant points.

(2) Ternary invariant point from one of the four faces of the tetrahedron and a quaternary invariant point within the tetrahedron. Twelve univariant lines of this type are shown in Fig. 12 (*aH*, *bG*, *cD*, *dD*, *eE*, *fC*, *gB*, *hB*, *iA*, *jA*, *kK*, and *lJ*).

(3) Two quaternary points within the tetrahedron. Eighteen univariant lines of this type are shown in Fig. 12 (*AK*, *AB*, *BC*, *EC*, *DE*, *DG*, *GH*, *EF*, *GF*, *HF*, *FI*, *CI*, *IK*, *IJ*, and *pH*, *nJ*, *oJ*, and *mK*. These last four connect quaternary invariant points of Fig. 12 with other quaternary invariant points not discussed in this paper.

When a univariant line joins a ternary invariant point (in one of the limiting ternary systems) and a quaternary invariant point (within the tetrahedron), the temperature along this univariant line must fall from the ternary invariant point toward the quaternary point unless within the tetrahedron another substance or substances not present at the ternary invariant point

[39] For possible solid solution in mullite see H. P. Rooksby and J. H. Partridge, "X-Ray Study of Natural and Artificial Mullites," *Jour. Soc. Glass Tech.*, **23**, 338–46 (1939); *Ceram. Abs.*, **19** [8] 181 (1940). Schairer and Osborn are making a chemical and optical study of mullite crystals from melts in the system FeO–Al_2O_3–SiO_2.

[40] N. L. Bowen and J. F. Schairer, "System FeO–SiO_2," *Amer. Jour. Sci.*, **24**, pp. 188–91 (1932).

[41] E. R. Jette and Frank Foote, see reference 23, p. 253.

[42] N. L. Bowen, J. F. Schairer, and E. Posnjak, "System CaO–FeO–SiO_2," *Amer. Jour. Sci.*, **26**, p. 276 (1933).

enters into solid solution with one or more of the three solid phases present along the univariant line. At the ternary reaction points *a*, *c*, and *e* (Fig. 12) from the limiting ternary system CaO–FeO–SiO_2, wollastonite (solid solution) is one of the crystalline phases. The wollastonite crystals are solid solutions of $CaSiO_3$ and $FeSiO_3$ (binary solid solutions within the ternary system) and at each of these three points, *a*, *c*, and *e*, the wollastonite solid solution has a different composition (see Table VII). If along the univariant lines, *aH* or *cD* or *eE*, a third substance whose composition lies outside the face CaO–FeO–SiO_2 (for example, a molecule containing Al_2O_3) should enter into solid solution in the wollastonite crystals, these solid solutions become ternary solid solutions within the quaternary system and the temperature along *aH* or *cD* or *eE* might rise toward the quaternary point. From chemical analyses of the natural pyroxenes called augites (which, however, contain MgO and are much more complex than these mixtures under discussion) from igneous rocks, it is known that a considerable amount of Al_2O_3 is present in augite crystals. The relations of the aluminous pyroxenes (augites) to the wollastonites are unknown, and because the data on the composition of the wollastonite crystals within the quaternary system CaO–FeO–Al_2O_3–SiO_2 are not available, for purposes of discussion it is assumed that the wollastonite solid solutions remain binary, and the temperatures are shown falling toward the quaternary invariant points along *aH*, *cD*, and *eE* of Fig. 12.

All the univariant lines within the tetrahedron are curved lines. For simplicity, they are shown as straight lines in Fig. 12, which is not spatial but merely depicts the relations of quaternary invariant points to one another and to certain ternary invariant points without regard for their spatial relations in the tetrahedron. The lengths of the univariant lines of Fig. 12 are arbitrary and without significance.

Figure 12 has been constructed to show the probable relations between the eleven quaternary invariant points[43] on which approximate information is now available. Four lines are shown which meet at each quaternary invariant point labeled with a capital letter (*A* through *J*). They are curved univariant lines within the tetrahedron, and the three solid crystalline phases in equilibrium with liquids whose composition lies on the line are listed on each line. The four solid crystalline phases at each quaternary invariant point are listed. Arrows on the lines indicate the direction of falling temperature, and some lines show a temperature maximum (eight are shown in *AK*, *EC*, *CI*, *IK*, *IJ*, *FI*, *GH*, and *DG*) or a temperature minimum (one is shown in *HF*). Some of the lines have one terminus at a ternary invariant point (labeled with small letters, *a* through *l*), and their temperatures and the limiting ternary system in which they occur are indicated in Fig. 12. The temperatures and compositions of the ternary invariant points of Fig. 12 are given in Table VII. The ternary and quaternary invariant points do not lie in a plane. Only their relations to one another are shown in Fig. 12, which is not intended to depict their spatial relations.

Table VIII gives the fifteen points in the five joins studied, which have three solid crystalline phases in equilibrium with liquid, and indicates on which univariant line of Fig. 12 each of these points lies. The temperatures and compositions of these fifteen points (Table VIII) from the five joins, the temperatures and compositions of the ternary invariant points (Table VII)

TABLE VII

TEMPERATURES AND COMPOSITIONS OF TERNARY INVARIANT POINTS OF FIGURE 12

Letter (Fig. 12)	Temp. °C.	Solid and liquid phases present
a	1193 ± 3	α-$CaSiO_3$ + wollastonite ($CaSiO_3$ 97 $FeSiO_3$ 3) + olivine (Ca_2SiO_4 43 Fe_2SiO_4 57) + liquid (CaO 30 FeO 34 SiO_2 36) (Bowen, Schairer, and Posnjak)
b	1265 ± 5	α-$CaSiO_3$ + anorthite + gehlenite + liquid (CaO 38.1 Al_2O_3 20.0 SiO_2 41.9) (Rankin and Wright)
c	1272 ± 3	α-$CaSiO_3$ + wollastonite ($CaSiO_3$ 93 $FeSiO_3$ 7) + tridymite + liquid (CaO 26.5 FeO 18.5 SiO_2 55) (Bowen, Schairer, and Posnjak)
d	1165 ± 5	α-$CaSiO_3$ + anorthite + tridymite + liquid (CaO 23.3 Al_2O_3 14.8 SiO_2 61.9) (Rankin and Wright)
e	1105 ± 3	Wollastonite ($CaSiO_3$ 28 $FeSiO_3$ 72) + olivine (Ca_2SiO_4 4 Fe_2SiO_4 96) + tridymite + liquid (CaO 11.5 FeO 45.5 SiO_2 43) (Bowen, Schairer, and Posnjak)
f	1073 ± 5	Olivine + tridymite + hercynite + liquid (FeO 47.2 Al_2O_3 12.5 SiO_2 40.3) (Schairer)
g	1345 ± 5	Mullite + anorthite + tridymite + liquid (CaO 9.1 Al_2O_3 18.8 SiO_2 72.1) (Rankin and Wright revised)
h	1205 ± 5	Mullite + hercynite + tridymite + liquid (FeO 33.5 Al_2O_3 20 SiO_2 46.5) (Schairer)
i	1380 ± 5	Corundum + mullite + hercynite + liquid (FeO 38 Al_2O_3 27 SiO_2 35) (Schairer)
j	1512 ± 5	Corundum + mullite + anorthite + liquid (CaO 15.7 Al_2O_3 36.5 SiO_2 47.8) (Rankin and Wright revised)
k	1380 ± 5	Gehlenite + anorthite + corundum + liquid (CaO 29.3 Al_2O_3 39.0 SiO_2 31.7) (Rankin and Wright)
l	1148 ± 5	Olivine + hercynite + wüstite + liquid (FeO 75.8 Al_2O_3 5.9 SiO_2 18.3) (Schairer)

[43] There is the possibility of additional quaternary invariant points with four solid phases in equilibrium with liquid in the region of the tetrahedron depicted diagrammatically in Fig. 12.

In their study of CaO–FeO–SiO_2, Bowen, Schairer, and Posnjak (*Amer. Jour. Sci.*, **26**, p. 213 (1933)) give the relations along the metasilicate join $CaSiO_3$–$FeSiO_3$, showing a series of hedenbergite solid solutions none of which is in equilibrium with liquids in the ternary system. The maximum temperature for the existence of a hedenbergite solid solution in the ternary system is 980°. The lowest temperature at which liquid is present in the ternary system is 1093°. If the temperatures along *HF* (Fig. 12) were low enough, hedenbergite solid solutions might be in equilibrium with liquids in the quaternary system, and additional quaternary invariant points with four crystalline solid phases and a liquid are possible. None of the five joins studied is near enough to this region to give the desired information on this possibility.

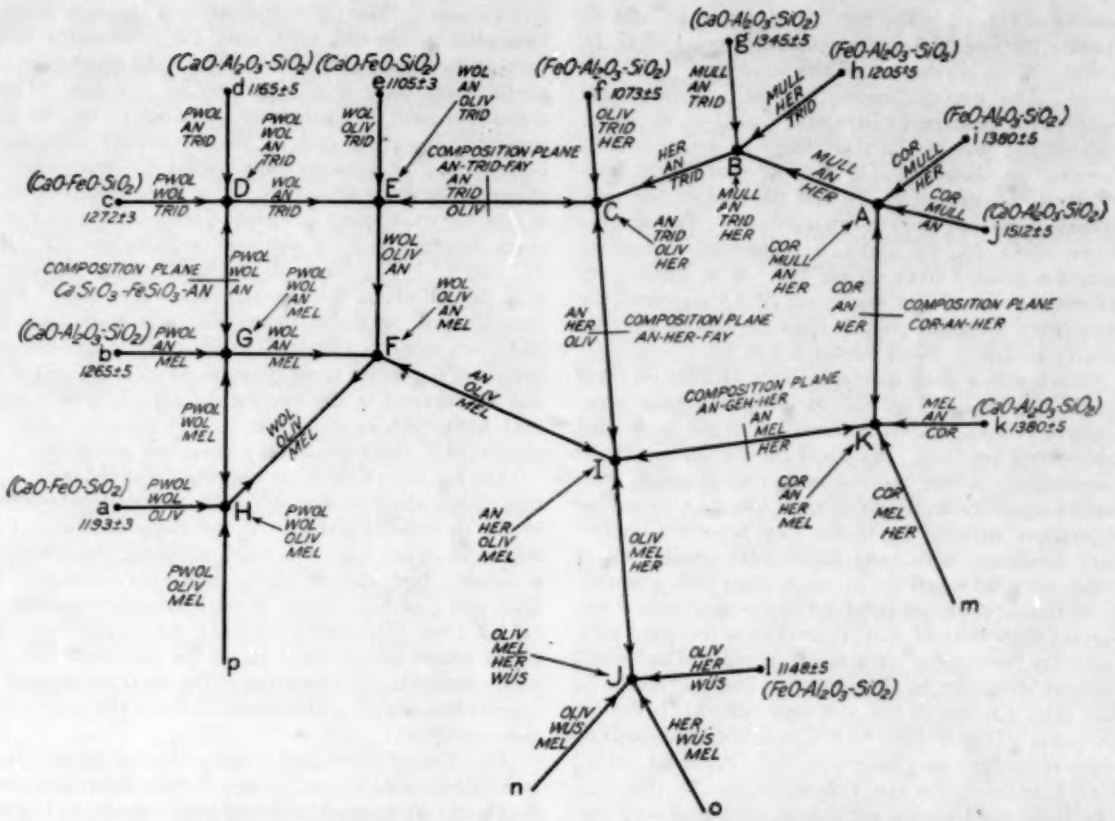

FIG. 12.—Diagram showing relations between univariant lines, ternary invariant points in the limiting systems (small letters), and quaternary invariant points (capital letters). These lines and points do not lie in a plane. Only their relations to one another are shown in this diagram, which is not intended to depict their spatial relations. The lengths of the univariant lines of this figure are arbitrary and without significance. Abbreviations for solid phases along the lines and at the points: *AN* = anorthite, *COR* = corundum, *FAY* = fayalite, *GEH* = gehlenite, *HER* = hercynite, *MEL* = melilite, *MUL* = mullite, *OLIV* = olivine, *PWOL* = pseudowollastonite, *TRID* = tridymite, *WOL* = wollastonite, and *WÜS* = wüstite.

TABLE VIII

LOCATIONS OF SIGNIFICANT POINTS IN THE FIVE JOINS ON UNIVARIANT LINES OF FIG. 12.

Letter	Figure No.	Temp. °C.	Three solid phases	Line (Fig. 12) in which lettered point lies
F	7	1120 ± 4	Olivine + hercynite + wüstite	*lJ*
I	7	1108 ± 4	Anorthite + hercynite + olivine	*CI*
J	7	1070 ± 4	Anorthite + tridymite + olivine	*EC*
N	8	1393 ± 4	Corundum + anorthite + hercynite	*AK*
R'	9	1186 ± 5	Pseudowollastonite + wollastonite + anorthite	*DG*
R	9	1125 ± 5	Wollastonite + anorthite + melilite	*GF*
S	9	1130 ± 5	Anorthite + melilite + hercynite	*IK*
T	9	1118 ± 5	Olivine + melilite + hercynite	*IJ*
U	8	1118 ± 5	Olivine + hercynite + wüstite	*lJ*
V'	9	1188 ± 5	Pseudowollastonite + wollastonite + olivine	*aH*
V	9	1145 ± 5	Wollastonite + olivine + melilite	*HF*
Z	10	1320 ± 5	Anorthite + melilite + hercynite	*IK*
A	10	1263 ± 10	Hercynite + wüstite + melilite	*oJ*
D	11	1178 ± 4	Pseudowollastonite + olivine + melilite	*pH*
E	11	1180 ± 5	Olivine + wüstite + melilite	*nJ*

from three of the limiting ternary systems, and certain deductions on the presence of maxima in the univariant lines which are related to the composition planes (discussed later) place a limit or limits on the temperatures and possible compositions of the eleven quaternary in variant points shown in Fig. 12.

(*B*) *Maxima and Minima in Univariant Lines:* Attention is called at this time to certain interesting

features of Fig. 12. The maxima shown on *EC* and *FI* separate the five quaternary invariant points *H*, *G*, *D*, *E*, and *F* from all the rest of the quaternary invariant points. The maxima shown on *EC*, *CI*, and *AK* separate the quaternary invariant points *A*, *B*, and *C* from all the rest of the quaternary invariant points. The maxima shown on *AK* and *IK* separate the quaternary invariant point *K* from the rest of the quaternary invariant points shown in Fig. 12. The maxima shown on *CI*, *IK*, *FI*, and *IJ* separate the quaternary invariant point *I* from all the rest of the quaternary invariant points. The maximum on *IJ* separates the quaternary invariant point *J* from the rest of the quaternary invariant points shown in Fig. 12.

Thus is shown the importance of the maxima on these univariant lines of Fig. 12. If the positions of these maxima were known, the tetrahedron might be divided into several volumes. In each of these volumes (for all compositions within the volume) crystallization, with perfect equilibrium, would proceed toward a particular quaternary eutectic (or in one case toward a quaternary minimum with only three solid phases, all of which are solid solutions, in equilibrium with a liquid). If all the solid phases involved in the quaternary univariant lines were of fixed composition (no solid solution), the positions of these maxima could all be located without difficulty by inspection. The maximum on *AK* (Fig. 12) lies in the join anorthite–Al_2O_3–FeO at the point *N* (Fig. 8) 1393° ± 4°C. where the composition plane corundum–anorthite–hercynite (extended toward FeO) cuts the quaternary univariant line *AK* (Fig. 12). The three solid phases corundum, anorthite, and hercynite are all of fixed composition.

(*C*) *Tie Lines and Composition Planes:* In a condensed ternary system, three tie lines may divide the ternary system into a smaller ternary system. For example, in CaO–Al_2O_3–SiO_2 (Fig. 2), the three tie lines gehlenite–anorthite, gehlenite–pseudowollastonite, and anorthite–pseudowollastonite limit the smaller ternary system gehlenite–anorthite–pseudowollastonite. These tie lines cut the boundary curves between gehlenite and anorthite, gehlenite and pseudowollastonite, and anorthite and pseudowollastonite, respectively, at a point. These three points where the tie lines cut the boundary curves are temperature maxima on the respective boundary curves. In some more complex ternary systems, the maximum on the boundary curve lies where a tie line produced (prolongation or extension of the tie line) cuts the boundary curve.[44]

In a condensed quaternary system, instead of a tie line (or composition line), there is a composition[45] plane with similar properties. This composition plane is a triangle with the compositions of the three solid phases at its apices. Where this composition plane, or sometimes this plane extended, cuts the quaternary univariant line along which these three solid phases are in equilibrium, there is a maximum on the quaternary univariant line. A quaternary invariant point may be separated from the rest of the quaternary invariant points by four maxima determined by composition planes. For example, *I* (Fig. 12) is separated from the rest of the quaternary invariant points by the maxima (each determined by a composition plane) on *CI*, *IK*, *FI*, and *IJ*. The faces of the tetrahedron, however, may partially limit a quaternary invariant point. For example, the group of quaternary invariant points *A*, *B*, and *C* are separated from all the rest of the quaternary invariant points by three maxima on *EC*, *CI*, and *AK* and by portions of the two faces CaO–Al_2O_3–SiO_2 and FeO–Al_2O_3–SiO_2 in which the ternary invariant points connected to these quaternary invariant points lie.

Thus has been shown the importance of the composition planes which depend upon the compositions of each of the three solid phases. If the compositions of the solid phases are fixed (no solid solution), the problem is simple; but, at each of the quaternary eutectics *J*, *K*, *I*, and *C* of Fig. 12 and at the quaternary minimum on *HF* (Fig. 12), there is at least one crystalline solid phase whose composition might be variable (i. e., a solid solution). The location of the maxima requires a specific knowledge of the composition of the solid solutions involved.

(*D*) *Temperatures and Compositions of Eleven Quaternary Invariant Points:* The available information on the eleven quaternary invariant points shown in Fig. 12 is now presented.

POINT *A* (FIG. 12) REACTION POINT (CORUNDUM + MULLITE + ANORTHITE + HERCYNITE + LIQUID)

(1) Temperature must be below *j* (1512° ± 5°), a ternary reaction point in the system CaO–Al_2O_3–SiO_2.

(2) Temperature must be below *i* (1380° ± 5°), a ternary reaction point in the system FeO–Al_2O_3–SiO_2.

(3) Temperature must be above that of the quaternary reaction point *B* (Fig. 12).

(4) Temperature must be below *N* (Fig. 8) 1393° ± 4°, which is the maximum on *AK* (Fig. 12). *N* (Fig. 8) is the maximum on *AK* (Fig. 12) because it lies in the composition plane anorthite–Al_2O_3–FeO produced (extended) toward FeO. All compositions in the area anorthite–Al_2O_3–hercynite of Fig. 8 are completely crystalline at all temperatures below *N* (1393° ± 4°).

(5) Inasmuch as the joins SiO_2–anorthite–FeO and anorthite–Al_2O_3–FeO do not cut the primary phase volume of mullite, the composition of the point *A*

[44] For example, in the system K_2O–CaO–SiO_2 (G. W. Morey, F. C. Kracek, and N. L. Bowen, "Ternary System K_2O–CaO–SiO_2," *Jour. Soc. Glass Tech.*, **14** [54] 149–87 (1930); *Ceram. Abs.*, **9** [10] 880 (1930)), the boundary curve between the fields of $2K_2O \cdot CaO \cdot 3SiO_2$ and $K_2O \cdot CaO \cdot SiO_2$ has a maximum where the prolongation of the line joining these two compositions cuts this boundary curve.

[45] Lea and Parker (*Trans. Roy. Soc.* [London], **A234**, p. 4 (1934)) use the term conjugation line instead of tie line and speak of a conjugation plane for ternary and quaternary systems, respectively. This does not follow the usage of conjugation lines ("Konjugationslinien") by Schreinemakers (F. A. H. Schreinemakers, "Mischkristalle in Systemen dreier Stoffe, III," *Z. physik. Chem.*, **52** [5] 513–50 (1905); p. 518.). The term conjugation line has been used with a connotation different from tie line or composition line by Schreinemakers in his papers and by Osborn and Schairer (*Amer. Jour. Sci.*, **239**, p. 735 (1941)).

(Fig. 12) must lie in the volume anorthite–Al_2O_3–SiO_2–FeO.

(6) Inasmuch as in the ternary system FeO–Al_2O_3–SiO_2 all compositions in the area hercynite–mullite–Al_2O_3 are completely crystalline at all temperatures below *i* (Fig. 12) 1380° ± 5°; in the ternary system CaO–Al_2O_3–SiO_2, all compositions in the area anorthite–mullite–Al_2O_3 are completely crystalline at all temperatures below *j* (Fig. 12) 1512° ± 5°; in the join anorthite–Al_2O_3–FeO, all compositions in the area anorthite–hercynite–Al_2O_3 are completely crystalline at all temperatures below *N* (Fig. 8) 1393° ±4°; the composition of *A* (Fig. 12) cannot lie within the volume anorthite–mullite–hercynite–Al_2O_3 and all compositions within this volume must be completely crystalline at all temperatures below that of *A* (Fig. 12).

(7) Inasmuch as the composition plane anorthite–fayalite–hercynite does not cut the primary phase volume of mullite, the composition of *A* (Fig. 12) cannot lie in the volume anorthite–fayalite–hercynite–FeO.

(8) The composition of the quaternary reaction point *A* (Fig. 12) lies in the volume anorthite–mullite–SiO_2–hercynite–fayalite. It probably lies in the smaller volume anorthite–hercynite–SiO_2–fayalite.

POINT *B* (FIG. 12) REACTION POINT (MULLITE + ANORTHITE + TRIDYMITE + HERCYNITE + LIQUID)

(1) Temperature must be below *g* (1345° ± 5°), a ternary eutectic in the system CaO–Al_2O_3–SiO_2.

(2) Temperature must be below *h* (1205° ± 5°), a ternary reaction point in the system FeO–Al_2O_3–SiO_2.

(3) Temperature must be below that of the quaternary reaction point *A* (Fig. 12).

(4) Temperature must be above that of the quaternary eutectic *C* (Fig. 12).

(5) For the same reason as given in item (5) under point *A* (Fig. 12), the composition of the quaternary reaction point *B* (Fig. 12) lies in the volume anorthite–Al_2O_3–SiO_2–FeO.

(6) Inasmuch as in the ternary system FeO–Al_2O_3–SiO_2 all compositions in the area hercynite–SiO_2–Al_2O_3 are completely crystalline at all temperatures below *h* (Fig. 12) 1205° ± 5°; and in the ternary system CaO–Al_2O_3–SiO_2 all compositions in the area anorthite–Al_2O_3–SiO_2 are completely crystalline at all temperatures below *g* (Fig. 12) 1345° ± 5°; the composition of *B* (Fig. 12) cannot lie within the volume anorthite–hercynite–SiO_2–Al_2O_3, and all compositions within this volume must be completely crystalline at all temperatures below that of *B* (Fig. 12).

(7) For the same reason as given in item (7) under point *A* (Fig. 12), the composition of *B* (Fig. 12) cannot lie in the volume anorthite–fayalite–hercynite–FeO.

(8) The composition of the quaternary reaction point *B* (Fig. 12) lies in the volume anorthite–SiO_2–hercynite–fayalite.

POINT *C* (FIG. 12) EUTECTIC (ANORTHITE + TRIDYMITE + OLIVINE + HERCYNITE + LIQUID)

(1) Temperature must be below *f* (1073° ± 5°), a ternary eutectic in the system FeO–Al_2O_3–SiO_2.

(2) Temperature must be below *I* (Fig. 7) 1108° ± 4° only if *I* (Fig. 7) lies either at the maximum on *CI* (Fig. 12) or between this maximum and *C* (Fig. 12). Whether the composition of the olivine is pure fayalite or a lime–iron olivine, point *I* (Fig. 7) lies between the maximum on *CI* (Fig. 12) and *C* (Fig. 12). If the olivine is pure fayalite, the maximum on *CI* (Fig. 12) lies in the composition plane anorthite–hercynite–fayalite extended within the tetrahedron.

(3) Temperature must be below *J* (Fig. 7) 1070° ± 4° only if *J* (Fig. 7) lies either at the maximum on *EC* (Fig. 12) or between this maximum and *C* (Fig. 12). If the olivine is pure fayalite, the maximum is at *J* (Fig. 7), which also lies in the composition plane anorthite–tridymite–fayalite. If the olivine is a lime–iron olivine, *J* (Fig. 7) lies between the maximum on *EC* (Fig. 12) and *C* (Fig. 12). The temperature of *C* (Fig. 12) is therefore below 1070° ± 4°.

(4) Temperature must be below that of the quaternary reaction point *B* (Fig. 12).

(5) Because the join SiO_2–anorthite–FeO cuts *EC* (Fig. 12) either at the maximum on *EC* (Fig. 12) or between this maximum and *C* (Fig. 12); and this same join also cuts *CI* (Fig. 12) between the maximum on *CI* (Fig. 12) and *C* (Fig. 12); and all compositions within the volume anorthite–hercynite–SiO_2–Al_2O_3 are completely crystalline at all temperatures below that of *B* (Fig. 12); the composition of the quaternary eutectic *C* (Fig. 12) must lie within the volume anorthite–hercynite–SiO_2–fayalite, and all compositions within this volume become completely crystalline only below the temperature of *C* (Fig. 12).

POINT *D* (FIG. 12) REACTION POINT (PSEUDOWOLLASTONITE + WOLLASTONITE (β-$CaSiO_3$ SOLID SOLUTION) + ANORTHITE + TRIDYMITE + LIQUID)

(1) Temperature must be below *c* (1272° ± 3°), a ternary transition point in the system CaO–FeO–SiO_2. The general problem of temperature changes along a univariant line which joins a ternary and quaternary invariant point has been discussed.

(2) Temperature must be below *d* (1165° ± 5°), a ternary eutectic in the system CaO–Al_2O_3–SiO_2.

(3) Temperature must be below that of the maximum on *DG*. This maximum lies where the composition plane $CaSiO_3$–$FeSiO_3$–anorthite cuts the line *DG* (assuming only binary and no ternary solid solution in wollastonite crystals). The point *R'* (Fig. 9) lies between the maximum on *DG* (Fig. 12) and *G* (Fig. 12). The temperature of this maximum must be above that of *R'* (1186° ± 5°).

(4) Temperature must be above that of the quaternary reaction point *E*.

(5) Because the join SiO_2–anorthite–FeO does not cut the primary phase volume of wollastonite (solid solutions); and where the primary phase volume of wollastonite (solid solutions) is cut by the join $CaSiO_3$–anorthite–FeO, this primary phase volume is in contact with pseudowollastonite and anorthite at *R'* (Fig. 9) and with melilite and anorthite at *R* (Fig. 9) and with

pseudowollastonite and olivine at V' (Fig. 9) and with melilite and olivine at V (Fig. 9); the composition of the quaternary reaction point D (Fig. 12) must lie in the volume $CaSiO_3$–anorthite–SiO_2–FeO.

POINT E (FIG. 12) REACTION POINT (WOLLASTONITE (β-$CaSiO_3$ SOLID SOLUTION) + ANORTHITE + OLIVINE (SOLID SOLUTION CALLED LIME–IRON OLIVINE) + TRIDYMITE + LIQUID)

(1) Temperature must be below e (1105° ± 3°), a ternary reaction or neutral point[46] in the system CaO–FeO–SiO_2. The general problem of temperature changes along a univariant line which joins a ternary and quaternary invariant point has already been discussed.

(2) Temperature must be below that of the maximum on EC. If the olivine present at the quaternary eutectic C (Fig. 12) (already discussed as item (3) under point C) is pure fayalite, the maximum on EC (Fig. 12) is at J (Fig. 7), which lies in the composition plane anorthite–tridymite–fayalite. The temperature of J (Fig. 7) is 1070° ± 4°.

(3) Temperature must be below that of the quaternary reaction point D (Fig. 12).

(4) Temperature must be above that of the quaternary reaction point F (Fig. 12).

(5) For the same reasons as given in item (5) under D (Fig. 12), the composition of the quaternary reaction point E (Fig. 12) lies in the volume $CaSiO_3$–anorthite–SiO_2–FeO.

POINT F (FIG. 12) REACTION POINT (WOLLASTONITE (β-$CaSiO_3$ SOLID SOLUTION) + OLIVINE (SOLID SOLUTION CALLED LIME–IRON OLIVINE) + ANORTHITE + MELILITE (GEHLENITE WITH POSSIBLY ANOTHER MELILITE MOLECULE CONTAINING FeO) + LIQUID)

(1) Temperature must be below R (Fig. 9) 1125° ± 5° because R (Fig. 9) lies on GF (Fig. 12).

(2) Temperature must be below that of the maximum on FI. No data are available on the temperature of this maximum.

(3) Temperature must be below that of the quaternary reaction point E.

(4) Temperature must be above that of the minimum on HF (the quaternary minimum with only three solid phases, melilite (gehlenite with possibly another melilite molecule containing FeO), wollastonite (solid solution), and olivine (solid solution called lime–iron olivine), and liquid). The temperature of the quaternary minimum is below that of the ternary minimum 1093° ± 3° in CaO–FeO–SiO_2.

(5) For the same reasons as given in item (5) under D (Fig. 12), the composition of the quaternary reaction point F (Fig. 12) lies in the volume $CaSiO_3$–anorthite–SiO_2–FeO.

POINT G (FIG. 12) REACTION POINT (PSEUDOWOLLASTONITE + WOLLASTONITE (β-$CaSiO_3$ SOLID SOLUTION) + ANORTHITE + MELILITE (GEHLENITE WITH POSSIBLY ANOTHER MELILITE MOLECULE CONTAINING FeO) + LIQUID)

(1) Temperature must be below b (1265° ± 5°), a ternary eutectic in the system CaO–Al_2O_3–SiO_2.

(2) Temperature must be below R' (Fig. 9) 1186° ± 5°, which is between the maximum on DG (Fig. 12) and G (Fig. 12).

(3) Temperature must be above R (Fig. 9) 1125° ± 5°, which lies on the univariant line GF (Fig. 12).

(4) Temperature must be below that of the maximum on GH. No data are available on the temperature of this maximum.

(5) Because the joins $CaSiO_3$–gehlenite–FeO and gehlenite–anorthite–FeO do not cut the primary phase volume of wollastonite (solid solutions) and where the primary phase volume of wollastonite (solid solutions) is cut by the join $CaSiO_3$–anorthite–FeO, this primary phase volume is in contact with pseudowollastonite and anorthite at R' (Fig. 9) and with melilite and anorthite at R (Fig. 9) and with pseudowollastonite and olivine at V' (Fig. 9) and with melilite and olivine at V (Fig. 9); the composition of the quaternary reaction point G (Fig. 12) lies in the volume gehlenite–anorthite–$CaSiO_3$–FeO and in the portion of this volume close to the join $CaSiO_3$–anorthite–FeO and close to the compositions of R' and R (Fig. 9).

POINT H (FIG. 12) REACTION POINT (PSEUDOWOLLASTONITE + WOLLASTONITE (β-$CaSiO_3$ SOLID SOLUTION) + OLIVINE (SOLID SOLUTION CALLED LIME–IRON OLIVINE) + MELILITE (GEHLENITE WITH POSSIBLY ANOTHER MELILITE MOLECULE CONTAINING FeO) + LIQUID)

(1) Temperature must be below a (1193° ± 3°), a ternary reaction point in the system CaO–FeO–SiO_2. The general problem of temperature changes along a univariant line joining a ternary and quaternary invariant point has already been discussed.

(2) Temperature must be below V' (Fig. 9) 1188° ± 5°, which lies on aH (Fig. 12).

(3) Temperature must be below that of the maximum on GH (Fig. 12). No data are available on the temperature of this maximum except that it must be above both G and H.

(4) Temperature must be above V (Fig. 9) 1145° ± 5°, which lies on HF (Fig. 12) between the minimum in HF (Fig. 12) and H (Fig. 12).

(5) The univariant line pH (Fig. 12) connects the quaternary reaction point H with another quaternary invariant point (probably pseudowollastonite + olivine + melilite + $3CaO \cdot 2SiO_2$ + liquid) in a part of the tetrahedron not discussed in this paper. D (Fig. 11) 1178° ± 4° lies on pH (Fig. 12). No discussion of the temperature relations along pH is given here.

(6) For the same reasons as given in item (5) under G (Fig. 12), the composition of the quaternary reaction point H (Fig. 12) lies in the volume gehlenite–anorthite–$CaSiO_3$–FeO, and in the portion of the volume close to the join $CaSiO_3$–anorthite–FeO, and close to the compositions V' and V (Fig. 9).

POINT I (FIG. 12) EUTECTIC (ANORTHITE + HERCYNITE + OLIVINE (SOLID SOLUTION CALLED LIME–IRON OLIVINE) + MELILITE (GEHLENITE WITH POSSIBLY ANOTHER MELILITE MOLECULE CONTAINING FeO) + LIQUID)

[46] Point e (Fig. 12) is the point K of Bowen, Schairer, and Posnjak ("System CaO–FeO–SiO_2," *Amer. Jour. Sci.*, **26**, Fig. 19, p. 229, and discussed on p. 230); K may be either a reaction point or a neutral point whose relations are discussed in detail.

(1) Temperature must be below *Z* (Fig. 10) 1320° ± 5° only if *Z* (Fig. 10) lies at the maximum on *IK* (Fig. 12) or between this maximum and *I* (Fig. 12). The melilite at *K* (Fig. 12) is probably pure gehlenite or nearly so, and the maximum on *IK* (Fig. 12) lies where the composition plane anorthite–gehlenite–hercynite cuts this univariant line *IK* (Fig. 12). The point *Z* (Fig. 10) lies between the maximum on *IK* (Fig. 12) and *I* (Fig. 12).

(2) Temperature must be below *S* (Fig. 9) 1130° ± 5°, because *S* (Fig. 9) lies on the univariant line *IK* (Fig. 12) between *Z* (Fig. 10) and *I* (Fig. 12).

(3) Temperature must be below that of the maximum on *IJ* (Fig. 12). The point *T* (Fig. 9) lies between this maximum and *J* (Fig. 12). This maximum must be above the temperature of *T* (1118° ± 5°).

(4) Temperature must be below that of the maximum on *CI* (Fig. 12). The point *I* (Fig. 7) 1108° ± 4° lies either at the maximum on *CI* (Fig. 12) or between this maximum and *C* (Fig. 12). This has been discussed in item (2) under point *C* (Fig. 12).

(5) Temperature must be below that of the maximum on *FI*. No data are available on the temperature of this maximum (Fig. 12).

(6) Inasmuch as the joins gehlenite–anorthite–FeO and $CaSiO_3$–anorthite–FeO cut *IK* (Fig. 12) between the maximum on *IK* (Fig. 12) and *I* (Fig. 12); and the join $CaSiO_3$–anorthite–FeO cuts the line *IJ* (Fig. 12); and the join SiO_2–anorthite–FeO cuts the line *IC* (Fig. 12); the composition of *I* (Fig. 12) must lie in the volume $CaSiO_3$–anorthite–SiO_2–FeO.

POINT *J* (FIG. 12) EUTECTIC (OLIVINE (SOLID SOLUTION CALLED LIME–IRON OLIVINE) + MELILITE (GEHLENITE WITH POSSIBLY ANOTHER MELILITE MOLECULE CONTAINING FeO) + HERCYNITE + WÜSTITE + LIQUID)

(1) Temperature probably lies below *A* (Fig. 10) 1263° ± 10°, where the join gehlenite–anorthite–FeO cuts the line *oJ* (Fig. 12). The univariant line *oJ* (Fig. 12) connects the quaternary eutectic *J* and some other quaternary invariant point in the part of the tetrahedron not discussed in this paper.

(2) Temperature probably lies below *E* (Fig. 11) 1180° ± 5°, where the join $CaSiO_3$–gehlenite–FeO cuts the line *nJ* (Fig. 12). The univariant line *nJ* (Fig. 12) connects the quaternary eutectic *J* and some other quaternary invariant point in the part of the tetrahedron not discussed in this paper.

(3) Temperature must be below *l* (1148° ± 5°), a ternary eutectic in the system FeO–Al_2O_3–SiO_2.

(4) Temperature must be below *F* (Fig. 7) 1120° ± 4°, where the join SiO_2–anorthite–FeO cuts the univariant line *lJ* (Fig. 12).

(5) Temperature must be below *U* (Fig. 9) 1118° ± 5°, where the join $CaSiO_3$–anorthite–FeO cuts the univariant line *lJ* (Fig. 12). Point *U* (Fig. 9) lies between *F* (Fig. 7) and *J* (Fig. 12) in the line *lJ* (Fig. 12).

(6) Temperature must be below *T* (Fig. 9) 1118° ± 5° only if *T* (Fig. 9) lies either at the maximum on *IJ* (Fig. 12) or between the maximum and *J* (Fig. 12). The point *T* (Fig. 9) lies between this maximum and *J* (Fig. 12).

(7) Inasmuch as the join gehlenite–anorthite–FeO cuts *oJ* (Fig. 12) at *A* (Fig. 10); the join $CaSiO_3$–gehlenite–FeO cuts *nJ* (Fig. 12) at *E* (Fig. 11); the joins SiO_2–anorthite–FeO and $CaSiO_3$–anorthite–FeO cut *lJ* (Fig. 12) at *F* (Fig. 7) and *U* (Fig. 9), respectively; and the join $CaSiO_3$–anorthite–FeO cuts *IJ* (Fig. 12) at *T* (Fig. 9); the composition of the quaternary eutectic *J* (Fig. 12) must lie in the volume gehlenite–anorthite–$CaSiO_3$–FeO very near to the join $CaSiO_3$–anorthite–FeO and must lie specifically very close to the compositions of the points *U* and *T* (Fig. 9) and the temperature of the quaternary eutectic *J* (Fig. 12) must be about 1115° ± 5° (slightly below those of *U* and *T* (Fig. 9), which are both 1118° ± 5°).

POINT *K* (FIG. 12) EUTECTIC (CORUNDUM + ANORTHITE + HERCYNITE + GEHLENITE + LIQUID)

(1) Temperature must be below *k* (1380° ± 5°), a ternary eutectic in the system CaO–Al_2O_3–SiO_2.

(2) Temperature must be below *N* (Fig. 7) 1393° ± 4°. The maximum on *AK* (Fig. 12) lies where the composition plane corundum–anorthite–hercynite (produced toward FeO) cuts *AK* (Fig. 12) at the point *N* (Fig. 7).

(3) Temperature must be below that of the maximum on *IK*. The melilite at *K* is probably pure gehlenite or nearly so, and the maximum on *IK* lies where the composition plane anorthite–gehlenite–hercynite cuts this line. The temperature of the maximum on *IK* (Fig. 12) must be higher than *Z* (Fig. 10) 1320° ± 5° because *Z* (Fig. 10) lies between this maximum and *I* (Fig. 12).

(4) The univariant line *mK* (Fig. 12) connects the quaternary eutectic *K* and some other quaternary invariant point in the part of the tetrahedron not discussed in this paper. This other quaternary invariant point is probably a reaction point (there is no maximum in *mK*, but the temperature falls from this reaction point toward *K*) with corundum + melilite + hercynite + $3CaO \cdot 5Al_2O_3$ + liquid in equilibrium. The temperature of this quaternary reaction point must be higher than *K* and lower than the temperature of the ternary reaction point corundum + gehlenite + $3CaO \cdot 5Al_2O_3$ + liquid (1475° ± 5°) in the system CaO–Al_2O_3–SiO_2.

(5) Inasmuch as the joins anorthite–Al_2O_3–FeO and gehlenite–anorthite–FeO cut the lines *AK* and *IK* (Fig. 12), respectively, the composition of the quaternary eutectic *K* (Fig. 12) probably lies in the volume gehlenite–anorthite–Al_2O_3–FeO.

A broad picture of the interrelations of the ternary and quaternary invariant points may be obtained from Fig. 12. No adequate concept of their spacial relations, however, may be gained without constructing a tetrahedral model and examining the temperature and composition relations which have been presented for the five joins and for the eleven quaternary invariant points.

Anyone who is interested in the details of these relations within the quaternary system should construct a tetrahedral model—a tetrahedral frame of wood or a light metal. Each face, for convenience, should be the

size of the triangular coordinate paper used to plot the data for the limiting ternary systems. Triangular coordinate paper, 50 cm. on a side, is convenient; if a smaller size is used, the relations appear crowded.

The data for the three limiting ternary systems may be transferred to heavy drawing paper to give rigidity to the faces and may be plotted on both sides of the drawing paper in order that the faces of the tetrahedron may be viewed from within or from the outside. Because no data are available on $CaO–FeO–Al_2O_3$, this face is left open. The data for the five joins may be plotted on both sides of triangles (not equilateral) of heavy drawing paper, cut to have the proper angular relations within the tetrahedron. It is convenient to connect wires from anorthite and from gehlenite to FeO, and from these wires, four of the five joins presented may be hung by leaving a hinged edge of drawing paper on the proper side or sides of each of the joins plotted. Some people find it more convenient to use heavy transparent celluloid or plastic instead of drawing paper. The general appearance of the model (with none of the data plotted) is shown by Fig. 5 of this paper, p. 248.

(9) Crystallization

The systematic elaboration of the theory of phase separation in ternary systems where the components show no solid solution has been carried out by Geer.[47] These principles were applied to the ternary system $CaO–Al_2O_3–SiO_2$ by Rankin and Wright,[48] who discussed in detail the paths of crystallization in all portions of this ternary system.

Some theoretical cases of solid solution in ternary systems, which had been treated by Schreinemakers,[49] were discussed briefly by Bowen,[50] who elaborated the principles, defined three-phase boundaries, discussed methods for their determination, and demonstrated their importance in any discussion of crystallization in systems showing solid solution. In this paper, Bowen emphasizes the importance of two types of crystallization curves in a system in which solid solution exists. In one type, perfect fractionation occurs; the solid solution crystals as soon as formed effectively drop out of the system, that is, no reaction between liquid and solid occurs. In the other type, perfect equilibrium between liquid and crystals is maintained; solid solution crystals continuously react with the liquid and remain in equilibrium with it as long as liquid is present. Osborn and Schairer,[51] in their study of the system pseudowollastonite–akermanite–gehlenite, determined conjugation lines in the solid solution field and three-phase boundaries. They discuss crystallization in this system and in a theoretical ternary system involving a series of binary solid solutions with a minimum on the liquidus surface, and they show the relation of the conjugation line to both fractionation and equilibrium curves of crystallization. They show how curves of the other type may be constructed if curves of one type are known.[52] In this paper, they emphasize a fact sometimes overlooked in discussions of the compositions of liquids during crystallization, namely, that the composition of a liquid cannot change arbitrarily but that the path (direction of change of composition) of a liquid is merely a necessary response to subtraction from the liquid of crystals of a certain composition and amount.

The subject of crystallization in a ternary system with several solid solution series has been treated in detail for the ternary system $CaO–FeO–SiO_2$ by Bowen, Schairer, and Posnjak,[53] who present a series of isothermal diagrams that give the phases present at equilibrium and the three-phase boundaries at chosen temperatures. These isothermal planes were used as the basis for the construction of crystallization diagrams and for the discussion of crystallization of typical liquids.

The crystallization of quaternary mixtures in the system $CaO–FeO–Al_2O_3–SiO_2$ is directly related to crystallization processes in the limiting ternary systems and involves an extension of the principles developed for ternary systems. Crystallization in the two faces $CaO–Al_2O_3–SiO_2$ and $FeO–Al_2O_3–SiO_2$ that show no solid solution is quite simple. On the other hand, crystallization becomes very complex in the face $CaO–FeO–SiO_2$ with several solid solution series. The presence of solid solutions increases the complexity of crystallization processes and necessitates a large amount of experimental data on the actual compositions of the solid solutions at various temperatures.

The subject of crystallization in the quaternary mixtures cannot be thoroughly treated at this time because much necessary information has not yet been obtained. Before an adequate presentation of crystallization is possible, the temperatures and compositions of the quaternary invariant points must be known more closely. But more particularly, the exact compositions and ranges of variation of composition with temperature for the solid solutions must be known. The positions of composition planes, temperature maxima and minima on univariant lines, and many other important details are related to the composition of the solid crystalline phases. Some brief observations on crystallization in the portion of the tetrahedron bounded by the compositions anorthite, Al_2O_3, SiO_2, hercynite, and fayalite, where the solid phases have a fixed composition (no solid solution) are made in section (10) and in the discussion of the effect of both CaO and FeO on high

[47] W. C. Geer, "Crystallization in Three-Component Systems," *Jour. Phys. Chem.*, **8**, 257–87 (1904).

[48] G. A. Rankin and F. E. Wright, "Ternary System $CaO–Al_2O_3–SiO_2$," *Amer. Jour. Sci.*, **39**, pp. 51–69 (1915).

[49] F. A. H. Schreinemakers, "Mischkristalle in Systeme dreier Stoffe," *Z. physik. Chem.*, **50** [2] 169–99; **51** [5] 547–76 (1905).

[50] N. L. Bowen, "Ternary System Diopside–Forsterite–Silica," *Amer. Jour. Sci.*, **38**, 207–64 (1914).

[51] E. F. Osborn and J. F. Schairer, "Ternary System Pseudowollastonite–Akermanite–Gehlenite," *ibid.*, **239**, pp. 735–53 (1941).

[52] Additional theoretical aspects of the relations of fractionation and equilibrium curves in solid solution fields are discussed by Bowen (N. L. Bowen, "Certain Singular Points on Crystallization Curves of Solid Solutions," *Proc. Nat. Acad. Sci.*, **27** [6] 301–309 (1941)).

[53] N. L. Bowen, J. F. Schairer, and E. Posnjak, "System $CaO–FeO–SiO_2$," *Amer. Jour. Sci.*, **26**, pp. 221–58 (1933).

alumina (mullite-bearing) refractories given in section (11).

(10) Observations of Interest to the Geologist or Petrologist

Now that the approximate position within the tetrahedron of eleven quaternary invariant points has been located and their approximate temperatures and their relations to one another and to five planes (joins) within the tetrahedron have been found, their distribution may be examined and some observations may be offered on the direction of change of composition of the liquid phase during crystallization for quaternary liquids in a large part of the tetrahedron.

From data presented in section (8*D*), seven of the quaternary invariant points (*D*, *E*, *F*, *G*, *H*, *I*, *J* of Fig. 12) and also the quaternary minimum (on *HF*, Fig. 12) have their compositions in or near the same small portion of the volume $CaSiO_3$–anorthite–SiO_2–FeO. The composition of the liquid phase during crystallization for quaternary mixtures in a large portion of the tetrahedron (the portion which lies in the volume bounded by the six planes gehlenite–anorthite–SiO_2–$CaSiO_3$, gehlenite–$CaSiO_3$–FeO, gehlenite–hercynite–anorthite, anorthite–fayalite–hercynite, gehlenite–hercynite–FeO, and fayalite–hercynite–FeO) changes toward[54] the quaternary minimum (some may approach this goal by way of *D*, *E*, and *F* or by way of *G* and *F* or by way of *G* and *H*), toward the quaternary eutectic *I* (Fig. 12), or toward the quaternary eutectic *J* (Fig. 12).

All compositions in the volume anorthite–Al_2O_3–SiO_2–hercynite–fayalite (which lies between the volume just discussed and the face FeO–Al_2O_3–SiO_2 of the tetrahedron) change toward the quaternary eutectic *C* (Fig. 12). The quaternary reaction points *A* and *B* (Fig. 12) and the quaternary eutectic *C* (Fig. 12) lie in the volume anorthite–SiO_2–hercynite–fayalite. The composition of the liquid phase during crystallization for all quaternary mixtures in the volume anorthite–Al_2O_3–SiO_2–hercynite–fayalite changes toward the quaternary eutectic *C* (Fig. 12). With perfect fractionation for all mixtures in this volume, the composition of the liquid phase approaches *C* (Fig. 12). With perfect equilibrium, all mixtures in the volume anorthite–mullite–hercynite–Al_2O_3 (a portion of the larger volume) become completely crystalline below the temperature of *A* (Fig. 12) and the last liquid has the composition *A*. With perfect equilibrium, all mixtures in the volume anorthite–mullite–hercynite–SiO_2 (a portion of the larger volume) become completely crystalline below the temperature of *B* (Fig. 12) and the last liquid has the composition *B*. In all mixtures in the volume anorthite–hercynite–SiO_2–fayalite (a portion of the larger volume), the composition of the liquid phase reaches *C* (Fig. 12).

Only brief mention will be made of the volume gehlenite–anorthite–Al_2O_3–hercynite, which has little or no geological interest. The quaternary eutectic *K* (Fig. 12) lies in this volume. Another quaternary invariant point (probably a reaction point with $3CaO \cdot 5Al_2O_3$ as one of the solid phases) not discussed in this paper also lies in this volume. The composition of the liquid phase during crystallization for mixtures in this volume changes toward *K*.

In summary, it is noted that there are two general composition goals toward which quaternary liquids in this system (in regions of any geological interest) proceed during crystallization. One goal is the region[55] near the quaternary minimum on *HF* (Fig. 12) or the point *I* (Fig. 12) which lies near it. The crystalline solid phases at the minimum on *HF* (Fig. 12) are wollastonite (solid solution) + lime–iron olivine (solid solution) + melilite; at the point *I* (Fig. 12), they are anorthite + hercynite + lime–iron olivine (solid solution) + melilite. The other goal is the point *C* (Fig. 12) where one of the solid phases is silica. The solid crystalline phases at *C* (Fig. 12) are anorthite + tridymite + hercynite + fayalite (pure or nearly pure Fe_2SiO_4).

Examination of the assemblages of solid phases present at the quaternary invariant points of Fig. 12 discloses that certain combinations of solid phases are incompatible at equilibrium. Only the sixteen pairs in which the two solid phases do not coexist at equilibrium are noted here.

(1) Melilite, tridymite
(2) Corundum, tridymite
(3) Corundum, olivine
(4) Corundum, wüstite
(5) Mullite, olivine
(6) Mullite, wüstite
(7) Anorthite, wüstite
(8) Tridymite, wüstite
(9) Pseudowollastonite, hercynite
(10) Pseudowollastonite, mullite
(11) Pseudowollastonite, wüstite
(12) Pseudowollastonite, corundum
(13) Wollastonite, hercynite
(14) Wollastonite, mullite
(15) Wollastonite, wüstite
(16) Wollastonite, corundum

None of these pairs of crystalline solids should be found together in a wholly or partially crystallized melt unless there is a wide departure from equilibrium.

(11) Technologic Applications

The effects of the addition of CaO, FeO, and SiO_2 on the refractoriness of high alumina (mullite) refractories and the effects of the addition of CaO, FeO, and Al_2O_3 on silica refractories may now be examined.

In the binary system Al_2O_3–SiO_2,[56] all compositions between mullite ($3Al_2O_3 \cdot 2SiO_2$) and Al_2O_3 are completely crystalline at all temperatures below the binary reaction point at 1810° ± 10°. All compositions be-

[54] With perfect equilibrium between crystals and liquid, the composition of the liquid does not always reach the goal toward which it proceeds. The liquid may be exhausted (used up) by crystallization at some point before it reaches its goal. With perfect fractionation, only an infinitesimal portion of liquid may reach the goal.

[55] *J* (Fig. 12), which is also near *HF* and *I*, is neglected as being too iron-rich to be of geological interest. Wüstite (FeO) is one of the solid phases.

[56] See reference 6, p. 244.

tween mullite and SiO_2 are completely crystalline only below the temperature of the binary eutectic[57] 1595° ± 10°.

In the ternary system anorthite–Al_2O_3–SiO_2 (a portion of the ternary system CaO–Al_2O_3–SiO_2, Fig. 2), all compositions within the area anorthite–mullite–Al_2O_3 are completely crystalline (no liquid present) at all temperatures below that of the ternary reaction point 1512°C. All compositions within the area anorthite–mullite–SiO_2 are completely crystalline only below the temperature of the ternary eutectic 1345°.

In the ternary system FeO–Al_2O_3–SiO_2 (Fig. 4), all compositions within the area mullite–hercynite–Al_2O_3 are completely crystalline (no liquid present) at all temperatures below the ternary reaction point *J* (Fig. 4) 1380°C. All compositions within the area mullite–hercynite–SiO_2 are completely crystalline at all temperatures below the temperature of the ternary reaction point *L* (Fig. 4) 1205°C. All compositions within the area hercynite–SiO_2–fayalite are completely crystalline only at temperatures below that of the ternary eutectic *M* (Fig. 4) 1073°C.

In the tetrahedron representing the quaternary system CaO–FeO–Al_2O_3–SiO_2, all compositions within the volume anorthite–mullite–hercynite–Al_2O_3 are completely crystalline at all temperatures below the temperature of the quaternary reaction point *A* (Fig. 12). All compositions within the volume anorthite–mullite–hercynite–SiO_2 are completely crystalline only at temperatures below the temperature of the quaternary reaction point *B* (Fig. 12). All compositions within the volume hercynite–anorthite–SiO_2–fayalite are completely crystalline only at temperatures below that of the quaternary eutectic *C* (Fig. 12). These observations clearly indicate the rapid lowering in refractoriness by additions of either CaO or FeO or both to either high alumina (mullite) refractories or silica refractories.

Bowen, Schairer, and Posnjak[58] showed how the results on the system CaO–FeO–SiO_2 furnished complete information regarding the chemical, as distinct from the mechanical, aspects of the attack of slags (which contain only CaO, FeO, and SiO_2) upon silica refractory bodies including those to which some lime has been added. In a similar manner, the results obtained on the quaternary system CaO–FeO–Al_2O_3–SiO_2 show the effects of slags (which contain CaO, FeO, Al_2O_3, and SiO_2) on both high alumina (mullite bearing) and silica refractory bodies although, unfortunately, the experimental data are not so detailed and complete as were those for the ternary system CaO–FeO–SiO_2.

The results on the quaternary system CaO–FeO–Al_2O_3–SiO_2 will be of general interest to those studying the fusibility of coal-ash slags and the chemical action of these slags on refractory bodies. Under the conditions of operation, however, these slags usually have most of their iron as Fe_2O_3 and not as FeO. Attention is called to a paper by Crook[59] in which the system FeO–SiO_2 was studied in iron crucibles in air and the results compared with those of Bowen and Schairer[60] made in iron crucibles in an inert atmosphere (purified nitrogen). The results agree quite closely. The reaction between the charges (synthetic slags) and the iron crucible is very rapid and the oxidizing action of the atmosphere will have little effect other than to increase the total iron content of the charge. Any attempt to increase the Fe_2O_3 content of a ferrous silicate charge in contact (equilibrium) with metallic Fe over the equilibrium amount (small for most compositions) results only in an increase in the total iron content of the charge due to the rapid reaction between metallic Fe and any excess Fe_2O_3 over the equilibrium amount. Similar experiments made by Crook in silica crucibles (instead of iron) yield totally different results, as would be expected. The charges in this case are high in Fe_2O_3.

The writer has attempted merely to indicate here a few examples of how the results on CaO–FeO–Al_2O_3–SiO_2 might be of interest in the technical problems in the fields of ceramics and metallurgy. Many other applications suggest themselves, such as to compositions of special fluxes, welding compounds, slags in special purification operations, the composition of nonmetallic inclusions in metals, etc.

IV. Summary

The results of quenching experiments on 216 separate compositions are given. Liquidus data are complete for five joins through the tetrahedron, SiO_2–anorthite–FeO, anorthite–Al_2O_3–FeO, $CaSiO_3$–anorthite–FeO, gehlenite–anorthite–FeO, and $CaSiO_3$–gehlenite–FeO.

Although data are given for only five joins, it has been shown how these data indicate within approximate limits the temperatures and compositions of eleven quaternary invariant points and show the direction of change of composition of the liquid phase during crystallization in a large portion of the tetrahedron.

An equilibrium diagram for the ternary system FeO–Al_2O_3–SiO_2 is given, but the data on which it is based will be published in a separate paper.

Observations of interest to the geologist and petrologist are made on the direction of change of composition of the liquid phase during crystallization and on the incompatibility of certain assemblages of solid phases.

Brief mention is made of the application of the results to refractories and slags of interest to the ceramist and metallurgist.

Geophysical Laboratory
Carnegie Institution of Washington
Washington, D. C.

[57] In studies of the ternary systems Na_2O–Al_2O_3–SiO_2 and K_2O–Al_2O_3–SiO_2 by J. F. Schairer and N. L. Bowen (data complete and manuscripts in preparation), the temperatures along the cristobalite–mullite boundary curve and the isotherms indicate that the binary eutectic temperature, 1545°, is too low and the eutectic temperature must be 1595° ± 10°.

[58] N. L. Bowen, J. F. Schairer, and E. Posnjak, "Ternary System CaO–FeO–SiO_2," *Amer. Jour. Sci.*, 26, pp. 281–82 (1933).

[59] Welton J. Crook, "Series Iron Oxides–Silica," *Jour. Amer. Ceram. Soc.*, 22 [10] 322–34 (1939).

[60] N. L. Bowen and J. F. Schairer, see reference 1 (*a*).

AN IMPROVED MERCURY BALANCE VOLUMETER*

By Sidney Speil and Hewitt Wilson†

Abstract

An improved mercury balance volumeter is described, which uses a commercially available balance for the determination of the volume of small test pieces. The volume is determined indirectly by using the sample weight and the force necessary to submerge the sample in a mercury reservoir. The accuracy, manipulation, and advantages of the method are discussed.

I. Introduction

During a study of American clays at the Electrotechnical Laboratory, a great many volume measurements were necessary to determine shrinkage characteristics. A Goodner[1] mercury displacement volumeter as improved by McMahon[2] had been used for these determinations, but this apparatus was not entirely satisfactory because of difficulty in obtaining precise check readings for the mercury level. Clay-shrinkage determinations are made by taking differences between two volume measurements. Errors in the individual volumes may then be magnified in the final shrinkage value.

The requirements formulated for a satisfactory volumeter are (1) it must be accurate and precise to 0.1 cc., rapid, and practically direct-reading without detailed calculations; (2) no preliminary soaking of the specimen should be necessary; (3) it must not be necessary to refill any container to a definite level before each measurement; (4) the machine must be rugged and easily constructed; and (5) it must be capable of a large range of volumes.

Goodner[1] discussed the various volumeters in use before 1920. These employed kerosene or similar liquids and therefore required preliminary soaking. Other volumetric methods were developed by Wheeler and Kuechler[3] and Spiers.[4] Mercury, in general, is preferable to such liquids as kerosene and water as a volume-measuring fluid because it envelops the specimen without wetting it, and preliminary soaking is unnecessary. Volumetric methods usually require perfectly fitting joints and rubber connections which are a potential source of trouble. Weight determinations are usually capable of higher precision than volume measurements. An apparatus, therefore, which involves the measurement of forces would probably give a higher precision in results when it is subjected to rapid and rough handling than one which measures volume directly.

Westman[5] introduced the mercury balance to determine the volume of full-size brick, in which a brick is placed in mercury and the force necessary for complete submersion is noted. The volume is determined by means of the following formula:

$$\frac{W + W_1}{D_m} = \text{volume}.$$

W = weight of brick.
W_1 = force necessary for submersion.
D_m = density of mercury.

Westman was able to measure the volume of a full-size brick to ±0.1 cc., but the apparatus was not particularly suited for rapid determinations of the volume of small test pieces. A modification of his balance method, using a commercially available balance, has therefore been devised.

II. Description of Apparatus

The apparatus as finally assembled is shown in Figs. 1 and 2. A more sensitive balance may be substituted for the one shown if necessary, but it should be of equally rugged construction. *A* is an O'Haus double-beam balance with 20-kg. capacity and sensitive to 1 gm. At the end of the beam, in place of the usual extra-weight hanger, a special saddle, *B*, is put over the head of the beam and fastened with lock screws. Through a hole in this saddle, a vertical 2- by $^1/_2$-cm. rod, *C*, can slide in a vertical direction only, its downward descent being controlled by a stop, *D*. It is thus stopped at a definite position and screwed securely in that position by a single turn of the wing screw, *E*, which tightens the rod against the two line contacts, *F*, so that its orientation is normal to that of the beam. At the mercury level, this rod is cut down to a circular rod, 0.3 cm. in diameter, to reduce the error caused by the rise of the mercury level when the test sample is inserted. The sample holder, *G*, is made of iron wire,

* Presented at the Forty-Fourth Annual Meeting, The American Ceramic Society, Cincinnati, Ohio, April 23, 1942 (Materials and Equipment Division). Received February 20, 1942.

† The authors are, respectively, assistant nonmetals engineer and supervising engineer, Electrotechnical Laboratory, Bureau of Mines, U. S. Department of Interior, Norris, Tennessee. This paper is published by permission of the Director of the Bureau of Mines, and the work has been done in cooperation with the Tennessee Valley Authority.

[1] E. F. Goodner, "Mercury Volumeter," *Jour. Amer. Ceram. Soc.*, **4** [3] 288–305 (1921).

[2] J. F. McMahon, "Improved Goodner Mercury Volumeter," *ibid.*, **13** [5] 363–67 (1930).

[3] E. S. Wheeler and A. H. Kuechler, "New Mercury Volumeter," *ibid.*, **10** [10] 807–12 (1927).

[4] C. H. Spiers, "Direct-Reading Volumenometer for Determining Real Volume and Specific Gravity of Porous Bodies," *Jour. Sci. Instruments*, **11** [7] 216–18 (1934); *Ceram. Abs.*, **14** [2] 44 (1935).

[5] A. E. R. Westman, "Mercury Balance," *Jour. Amer. Ceram. Soc.*, **9** [5] 311–18 (1926).

welded together with one open end, and has oblique sides which cause the sample to center itself when rising to the top of the cage when it is submerged in mercury. The center of gravity of the sample is thus always the same distance from the fulcrum of the balance. The mercury is held in an iron vessel, *H*, which has a fairly small volume of mercury but a large cross section near the surface. Rod *C* has a support, *I*, on which additional weights may be placed if a weight of more than 1100 gm. is necessary for submersion.

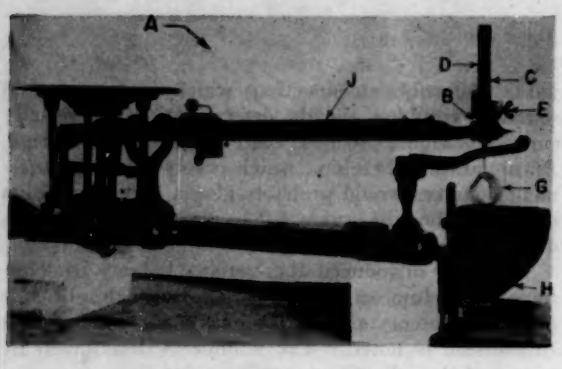

FIG 1.—Volumeter.

III. Manipulation, Calculation, and Sources of Error

With no sample in the chamber, rod *C* is pushed down to its end point as determined by *D* and clamped with the wing screw. The balance is brought to equilibrium by moving the counterbalance on the beam and is now ready for use. The sample cage is raised from the mercury, and a specimen is inserted. The rod is lowered to its end position, and equilibrium is again obtained by using sliding weights, *J*, on the beam. An additional weight, if necessary, is placed on the rod at point *I*. The few movements are simple, and the entire operation takes less than one minute.

The weight on the beam corresponds to an equal weight on the platform of the balance, but it is only proportional to the effective force at the end of the beam. The submersion force, therefore, is given by Ws/a, wherein the constant, a, may be determined by direct balance of a weight placed in the specimen holder in air.

The following equations are derived from Archimedes' principle:

$$W + \frac{Ws}{a} = V(D_m).$$

$$V = \frac{W + \frac{Ws}{a}}{D_m}.$$

Ws = beam weight.
D_m = density of mercury.
W = specimen weight.
V = specimen bulk volume.

As the method is indirect, there are several possible sources of error which will be discussed.

(1) Submersion and Specimen Weights

The measured value of the constant, a, is 4.40 for the balance tested. An error of 1 gm. in the beam weight therefore corresponds to an error of $\frac{1}{4.4 \times 13.5}$ cc. or to 0.016 cc. In a series of forty check readings, the average deviation was 0.9 gm. and the maximum was 2.5 gm., corresponding to errors of 0.015 and 0.04 cc., respectively.

With any medium sensitivity balance, the specimen weight may be determined accurately within 0.1 gm., corresponding to 0.0075 cc., which is negligible.

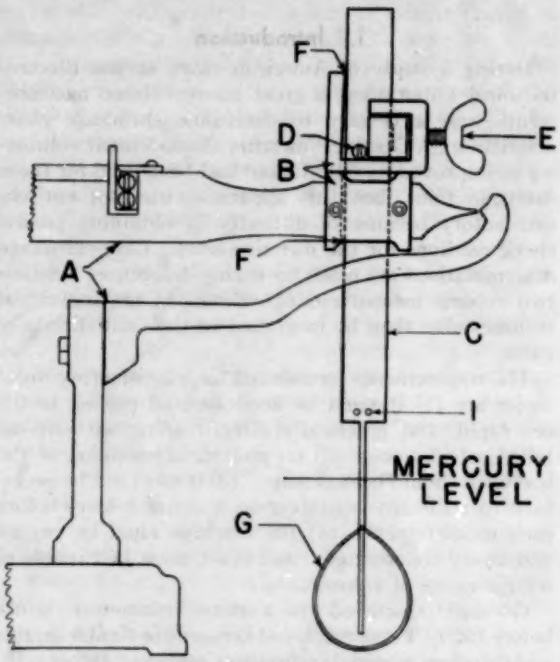

FIG. 2.—Submersion arm of volumeter.

(2) Mercury Level Rise and Temperature

When a sample is inserted, the rise in level of the mercury causes an error owing to the submergence of more of the supporting rod. The magnitude of this error in the submersion force is determined by the following ratio:

$$\frac{A_1}{A_2} \times V.$$

A_1 = rod (cross-section area) at mercury level.
A_2 = mercury surface (cross-section area).

The error in the submersion weight would then be

$$\Delta\left(\frac{Ws}{a}\right) = \frac{A_1}{A_2} \times V(D_m - D).$$

D = density of rod.

For a specimen volume of 10 cc., the volume error is

$$\Delta(V) = \frac{\Delta\left(\frac{Ws}{a}\right)}{D_m} = 0.004 \text{ cc.}$$

The density of mercury, one factor in the volume equation, varies with temperature. A variation of 5°C. from a mean of 25°C. causes an error of 0.09% or 0.009 cc. per 10-cc. volume.

IV. Nomograph

Because these errors are small, a noticeable simplification may be introduced into the calculation method. A simple alignment chart was constructed[6] with three equidistant parallel lines whose ordinates were determined as follows:

(1) $\frac{Ws}{a}$ (gm. calibrated in Ws values).

(2) $V = \frac{\frac{Ws}{a} + W}{D_{w}^{25°C.}}$ (cc.).

(3) W (gm.).

To use this nomograph, a portion of which is shown in Fig. 3, a straightedge is passed through the values of the beam weight and the sample weight on lines 1 and 3, respectively. The volume is then read directly on the center scale; for example, a specimen that weighs 35.0 gm. and requires a beam weight of 800 gm. for suspension would have a volume of 16.0 cc. Because the construction of the chart depends on the value of the constant, a, Fig. 3 cannot be used for every balance, and only a small portion is shown. Three separate charts may be made for plastic, dry, and fired samples, respectively, for convenience in use and to obtain better precision.

In the case of plastic and dry specimens, the sample weights are determined for water-of-plasticity measurements. The weight of the fired piece is necessary for absorption determinations; therefore, when a complete study of any clay is being made, no more weighings or readings are needed for this mercury balance method than for any volumetric displacement method. It is unnecessary, moreover, to repeat "zero" readings before each determination, which is necessary with most displacement volumeters.

V. Accuracy

The constant, a, was determined by balancing a known weight directly in the specimen holder (in air) with weights placed on the balance pan. The constant for this machine, 4.40, was then used to determine the volume of several steel cylinders and of fired clay bars which could be compared with their true bulk volumes as determined by weighing in air and in distilled water after soaking. All of these were in the range from 10 to 30 cc.

[6] G. W. Swett, Construction of Alignment Charts. John Wiley & Sons, Inc., New York, 1928. 89 pp.

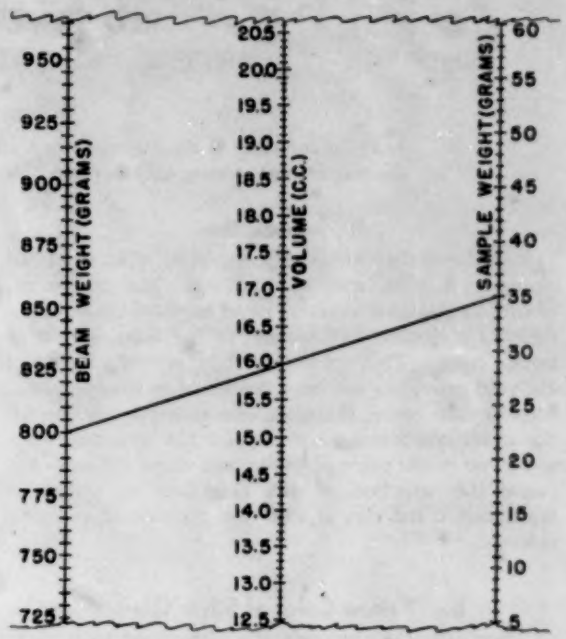

FIG. 3—Nomograph for determining volumes.

TABLE I

Specimen type	No.	Deviation (cc.) Avg.	Max.
Steel cylinder	4	0.03	0.04
Fired clay bars	10	0.02	0.04

VI. Disadvantages and Advantages

The mercury balance has the following disadvantages: (1) The initial cost for mercury is high and (2) if only the volume of a sample is desired, an extra value, that is, the weight of the piece, must also be determined. (If a complete study of the specimen is being made, the weight is determined for other tests.)

The advantages of this method are as follows: (1) The method is accurate, precise to less than 0.1 cc., and rapid; (2) the volumeter is sturdy and easily constructed from a standard commercial balance with a minor amount of machine work; (3) there are no tightly fitting joints or rubber connections which may give trouble; (4) the nomographic chart allows direct determination of volumes without any calculation; (5) no preliminary soaking is necessary because mercury does not wet the piece; and (6) possible errors in the determination of any one experimental value cause only very small errors in the final volume.

ELECTROTECHNICAL LABORATORY
U. S. BUREAU OF MINES
NORRIS, TENNESSEE

RED SILVER GLASSES *

By Edward Forst, Jr., and Norbert J. Kreidl

Abstract

At the interface of the vitreous phase and a halide precipitation forming therein, attractive red colors have been developed in glasses containing silver and halides.

I. Introduction

A study of the "striking" properties, that is, of the changes of color and opacity with heat-treatment, of various glasses containing silver revealed the development of a distinct red instead of the usual yellow or brown color. This red color, which resembled that of the gold ruby, has not been described in the literature. Experiments were therefore conducted to determine the exact conditions necessary for the formation of a silver red in the place of the known silver yellow. Because the selection of red colorants in glasses is restricted, a red tint of this type may be of practical interest.

II. Yellow Color of Silver Glasses

When silver compounds are introduced in a glass, they behave like alkali compounds as long as the relative amount of silver is below $^1/_2\%$. The silver ions (Ag^+) taking the place of alkali ions are randomly distributed in the silica network. Owing to the rather noble character of silver, a pronounced tendency to form silver atoms prevails. The elemental silver is not very soluble in glass; even under oxidizing conditions, metallic silver will therefore be precipitated as soon as the concentration of atomic silver exceeds the solubility limits. This limit depends mainly on the temperature.

In a quenched glass, the atomic silver is frozen in a condition which may be compared to the vapor state. Silver, in this state, exhibits fluorescence like the vapors of other metals, such as tin, lead, thallium, zinc, or cadmium. The glass, however, remains colorless because, in these concentrations, atomic silver like the silver ion shows no appreciable absorption in the visible part of the spectrum.

When the glass is reheated, the metal atoms aggregate to form particles of colloidal size. The glass becomes yellow, its fluorescence is shifted to longer wave lengths, and the intensity of the fluorescence decreases at the same time.[1]

Further growth of the particles causes the disappearance of fluorescence and a change of the color from yellow to brown and finally to gray. The particles are now large enough to exhibit the reflection color of silver.

III. Silver Glasses Showing a Red Color

(1) Role of Chlorine

Inasmuch as alkali-lead-silicate glasses are better solvents for silver than alkali-lime-silicate glasses, the striking properties were first encountered in lead-containing base glasses. Table I shows examples of the composition of some of these glasses, the reheating temperatures studied, and the colors obtained. Under the conditions of the experiment, all of the glasses turned red above 500°C. and became "livery," that is, a turbid, dusky brown at about 600°C. The glasses with higher lead content turned reddish more easily. A minimum addition of 2.5% of AgCl was required for the effect, which was not appreciably altered by further additions.

Because of the development of a purplish red rather than the reddish brown, which is characteristic of silver glasses containing larger particle sizes, it was considered improbable that the phenomenon was caused by the state of dispersion of the silver.

The silver used in these experiments had been introduced as the chloride, which was a possible source of the peculiarity of the coloration. Experiments, therefore, were made with silver carbonate and silver oxide instead of silver chloride. In no case was the red color observed.

Taylor[2] has described the effect of halides on the light absorption of colored glass. The color change in silver glass, however, is not comparable to that observed by Taylor because he used variations of ionic colors. Repeated experiments with lead glasses of different compositions showed that the occurrence of a red color was associated with the tendency of such a glass to develop opacity when it was reheated.

From the work of Firth and his associates,[3] chlorine ions in heavy lead glasses are known to cause the appearance of a second phase and, as a consequence, opacity. If, in the experimental lead-silver chloride glasses of the present study, the silver be omitted and the same amount of chlorine be introduced in the form of sodium chloride, opacity would occur on reheating. It is suggested that the red color is the result of a precipitation of elemental silver at the interface of the glass and an immiscible chloride.

---

* Presented at the Forty-Fourth Annual Meeting, The American Ceramic Society, Cincinnati, Ohio, April 22, 1942 (Glass Division). Received February 13, 1942.

From a thesis submitted in partial fulfillment of the requirements for the degree of Master of Science at Pennsylvania State College by the senior author.

[1] W. A. Weyl, "Contribution to Fluorescence of Glasses," *Sprechsaal*, 70 [46] 578–82 (1937); *Ceram. Abs.*, 17 [10] 326 (1938).

[2] W. C. Taylor, "New Method of Producing Colored Glass," *Glass Ind.*, 7 [4] 90–91 (1926); *Ceram. Abs.*, 5 [12] 386 (1926).

[3] (*a*) E. M. Firth, F. W. Hodkin, C. M. Muirhead, M. Parkin, and W. E. S. Turner, "Study of Some Effects of Chlorides on Melting and Working Properties of Potash-Lead Oxide-Silica Glasses," *Jour. Soc. Glass Tech.*, 10 [38] 176–98 (1926); (*b*) E. M. Firth, F. W. Hodkin, and W. E. S. Turner, "Production of Opalescence by Chlorides in Potash-Lead Oxide-Silica Glasses," *ibid.*, pp. 199–212; *Ceram. Abs.*, 5 [11] 346 (1926).

TABLE I

COLOR OF REHEATED LEAD SILICATE GLASSES CONTAINING SILVER

	Sample No. (1)	(2)	(3)	(4)	(5)	(6)
Base glass ($75SiO_2 \cdot 17Na_2O \cdot 8CaO$)	23.5	23.5	23.5	39.5	39.5	39.5
Lead silicate ($PbO \cdot SiO_2$)	75.5	75.5	75.5	59.5	59.5	59.5
KNO_3	1	1	1	1	1	1
AgCl	2.4	4	5.6	2.4	4	5.6
Reheated at (°C.)						
248	Yellow	Yellow	Brown	White	Yellow	Yellow
321	"	"	"	Light yellow	"	"
414	Reddish brown	Reddish brown	Reddish brown	Orange	Reddish orange	Orange
514	Intense red throughout					
630	Livery (dusky brown) throughout					

TABLE II

COLORS OF SILICATE GLASSES CONTAINING HALIDES AND 4% OF Ag_2CO_3*

KI	Dark purplish red	Dark brownish red	Dark purplish red	Dark purplish red	Dark purplish red	Dark purplish red	Dark purplish red
KBr	Yellow-brown†	Purplish red	Purplish red	Bright purplish red	Red	Bright purplish red	Bright purplish red
NaCl				Brown-orange†	Brown-yellow†	Brown-red spots†	
NaF						Colorless	Light green-yellow

* Reading from left to right, the concentration of halides increases; the halide addition in each column is compared on an equimolecular basis.

† Red on reheating.

(2) Role of Lead

The results of another series of experiments may be summarized by the statement that lead is not essential in producing the effect but that the lead glasses are more brilliant and the color more homogeneous. A coarser precipitation as well as heavily striated areas of different opacification are more frequently obtained in lead-free glasses. Lead-free halide opal glasses have been described by Taylor.[4]

(3) Role of Other Halides

Further experiments were made to compare the effects of the different halides, and the results are summarized in Table II.

Equimolecular amounts were increasingly effective with increasing atomic weight, that is, in the order of fluorine-chlorine-bromine-iodine. This effect may be illustrated by the following examples:

(1) A glass containing 10% of sodium fluoride develops opacity and reddish color only in limited areas and only if it is reheated to 500°C. Glasses containing less fluorine do not develop the red color as they do not strike at all. Glasses which contain the equivalent amount of sodium chloride are red. Those containing the equivalent amount of bromine are dark purplish red, and a strong tendency prevails toward the separation of a red foamy mass of bromides. The corresponding iodine glass behaves in a similar manner.

(2) A glass which contains only 2% of iodine, that is, one fifth the equivalent of example (1) is still dark red after it is cooled in the crucible. The equivalent bromine glass cools down to a yellow glass and becomes red only when it is reheated to 500°C. The corresponding fluorine glass is colorless.

The bromine glasses cool to beautiful red and purplish red colors with a marbled striation in a wide range of compositions.

[4] W. C. Taylor, "Glass Composition," U. S. Pat. 1,615,247, January 25, 1927; *Ceram. Abs.*, 6 [4] 141 (1927).

IV. Conclusion

Considering the scarcity of red colors in ceramics the practical aspects of this phenomenon deserve further study. Their main field of application would be in glazes, enamels, and vitrifiable colors in which opacity is acceptable or desirable and where red colors could be produced by the simultaneous use of silver compounds and halides, particularly the bromides. The opaque glasses described by Taylor[4] are examples of suitable base compositions.

Department of Ceramics
Pennsylvania State College
State College, Pennsylvania

EFFECT OF TIN IN GOLD RUBY GLASS*

By F. M. Veazie and W. A. Weyl

Abstract

The century-old use of tin compounds in the preparation of gold ruby, copper ruby, and silver yellow is based not on reduction phenomena but on its specific influence on the solubility of these metals in glass.

I. The Problem

Old formulas for gold ruby glasses as well as for copper ruby and silver yellow glasses contain a certain small amount of tin either in the metallic form or as a tin compound. Except in glasses rich in lead oxide, tin seems to be indispensable for the production of a satisfactory color. No explanation other than its reducing action has been offered for the effect of tin in these glasses, and this explanation cannot be accepted in the case of the gold ruby glass in which it is known that reducing or oxidizing agents have no influence. An investigation has therefore been made on the specific action of tin in gold ruby in order to obtain an explanation that might also apply to copper ruby and to silver yellow glass.

II. Reduction in Ruby Glasses

The art of making copper ruby glass consists in reducing the copper compounds into cuprous ions or elemental copper during the melt and precipitating metallic copper in the proper state of subdivision either on cooling or reheating. The melt might contain elemental copper as well as cuprous ions which decompose into metallic copper and cupric ions when they are reheated. It is essential in any case that copper ruby glasses be melted under reducing conditions. This may be accomplished by various means, the most common being the addition to the batch of organic materials such as cream of tartar. Tin compounds, however, are required, and it is not possible to replace them by an excess of cream of tartar. How important the tin is for the development of the copper ruby color may be seen from the borax bead test, in which the development of ruby formation is used to detect traces of copper and also of tin. When the blue borax bead containing cupric oxide is exposed to the reducing part of the flame, its color fades because the blue cupric ions change into colorless cuprous ions.

From such a colorless bead, a ruby color may be developed on reheating only if traces of tin are present. This experiment does not exclude the value of the reducing action of metallic tin in the glass batch, but it shows conclusively that its reducing effect does not represent the typical role of tin in ruby formation.

Metallic silver as a glass colorant is rarely used now, but before cadmium sulfide glasses were discovered, silver was widely used to obtain yellow colors. Silver glasses do not require additions of reducing agents to the batch inasmuch as this metal is noble enough to be formed merely by dissociation of the silver compounds at glassmelting temperatures. Experience has shown that reproducible yellow glasses may be obtained in heavy lead glasses or when sufficient amounts of tin have been added to the batch. Glasses free of lead and tin exhibit a tendency to develop muddy colors.

Because gold is still nobler than silver, appreciable amounts of gold ions cannot be expected to be present in the melt. Silver glasses contain atomic silver in equilibrium with ionic silver, but all of the gold compounds in gold glasses will dissociate to form elemental gold. This dissociation takes place at about 300°C. even in phosphate glasses, which allow a high concentration of silver ions to persist. Gold ruby glasses can therefore be melted under strongly oxidizing conditions, and reducing agents do not affect their color development.

III. Gold Ruby Glasses

Since the work of Faraday and Zsigmondy, it has been established that the color of gold ruby glasses is caused by metallic gold in a finely subdivided state. Small gold particles exhibit a strong absorption of green light which results in a red color. The gold compounds in the batch dissociate during melting to form elemental gold, which is soluble at a high temperature. When such a melt is cooled, a supersaturated solution is formed, and part of the gold aggregates and forms invisible nuclei. Such aggregations of about 300 gold atoms do not possess the optical properties of the compact metal, and they are colorless. When the colorless glass is reheated, gold atoms precipitate at the nuclei already formed. The most desirable ruby color is obtained when the little gold crystals reach a size of between 5 and 20 mμ.

---

* Presented at the Forty-Fourth Annual Meeting, The American Ceramic Society, Cincinnati, Ohio, April 22, 1942 (Glass Division). Received February 13, 1942.

Instead of a regular growth of the gold nuclei, the nuclei possibly collide and form clusters which cause the color of the glass to be bluish and "livery." Such an undesirable cluster formation occurs when the glass is heated to high temperatures and the nuclei become too mobile at the corresponding low viscosities.

The requirements, therefore, for producing a good ruby color are (1) high solubility of gold in the glass at the melting temperature in order to develop a deep color and (2) a low but still appreciable amount of solubility of gold in the glass in the softening range where the striking occurs. There must be some solubility because the entire gold content would otherwise be precipitated when the glass is cooled (for example, to 800°C.), and no more gold atoms would be available to cause a regular growth of the nuclei. When such a glass is reheated, it could strike only by cluster formation and would therefore produce bluish shades with brown reflectance.

This undesirable condition, in which the solubility on cooling approaches zero before the softening range is reached, is represented by curve *B* of Fig. 1. Curve *A* represents the desirable solubility behavior which permits the formation of good gold ruby because there is still appreciable solubility in the softening range.

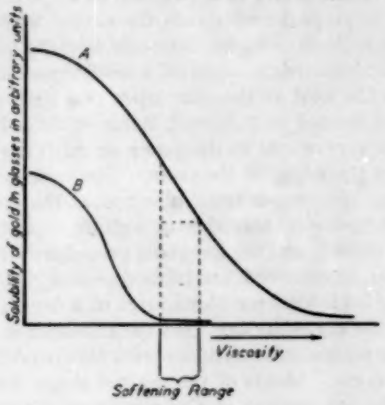

FIG. 1

The type of solubility depends on the composition of the base glass. Curve *A* of Fig. 1 characterizes a heavy lead crystal, whereas curve *B* is characteristic of low-melting borax glasses. The position of the soda-lime glasses is intermediate but seems to approach the type of curve *B*. From the study of gold ruby formation in glasses of widely differing compositions, the impression is gained that the addition of tin makes a glass of the type B approach that of type A. Such action of the tin ion would be specific and independent of the reducing effect of metallic tin.

Tin oxide is used chiefly in the ceramic industry as an opacifying agent because of its high refractive index and its low rate of solution. The latter property may be explained by the probable position which the Sn^{4+} ion would have to assume in a glass. Because of its charge and size, it may take the place of silicon and therefore enter the network proper. Such a position requires the breaking of the silicon-oxygen bond, which is the strongest bond in a glass. In a gold ruby glass, such small amounts of SnO_2 are added that they are completely dissolved. A clear glass which contains small amounts of dissolved tin dioxide, according to this theory, differs from an ordinary glass by having some $Si–O_4$ tetrahedra replaced by $Sn–O_4$ tetrahedra.

IV. Tin Ion a Stabilizer of Noble Metals

The action of tin on metallic colors is limited neither to gold nor to glasses. The protective effect of stannic hydroxide on the stability of gold hydrosols is well known in the field of colloidal chemistry. Pigments, such as MgO, $BaSO_4$, and $Ca_3(PO_4)_2$, furthermore, may be stained by gold, but stable stains are obtained only if SnO_2 is used as a basis. When MgO or similar substances are moistened with gold chloride solution and heated, the gold compounds at the surface of the crystals decompose, and the metallic gold, in its fine subdivision, imparts a pink color to the pigment. The forces which hold the gold particles to the surface of the crystal, however, are too weak to prevent aggregation by diffusion along the surface. The color of these pigments fades on additional heating because the typical ruby color is limited to a particle size ranging between 5 and 20 mμ.

Tin dioxide is the only exception. When SnO_2 is used as a basis, the precipitated gold is prevented from aggregating on further heating so that a stable purple stain, called purple of Cassius, is obtained, which finds many uses in decorating ceramic ware. The tin seems to exert strong enough forces on the gold to prevent its diffusion. Similar phenomena are known in the case of silver and platinum. The action of tin goes so far that even platinum can be made soluble in ether and similar organic solvents by using tin chloride, which is soluble in these solvents and which has sufficient residual valencies to keep platinum in solution.

V. Conclusions

These experiments on the action of tin oxide in gold ruby, especially on its striking properties, lead to the conclusion that tin exerts strong forces on the noble metals, which determine their solubility behavior in glasses and decrease their diffusion speed. The twofold action of the tin ion participates in the formation of the glass network and at the same time exerts forces on the metal by its residual valencies. Both effects result in strengthening the otherwise very weak bond between the noble elements and the silicate glass. These forces are responsible for the fact that the metal does not volatilize from the melt or precipitate completely on cooling. A certain solubility of the metal in the glass is essential to warrant proper crystal growth on reheating. This characteristic action of tin is exerted if tin compounds are present in very low concentrations. Essentially the same action has been found on the noble metals when lead oxide, zinc oxide, cadmium oxide, or bismuth oxide is introduced although far higher concentrations of these oxides are required.

DEPARTMENT OF CERAMICS
PENNSYLVANIA STATE COLLEGE
STATE COLLEGE, PENNSYLVANIA

PREPARATION OF REFRACTORY AND OF COAL-ASH TEST CONES*

By Russell J. Smith

I. Introduction

The A.S.T.M. specifications for testing the fusion of refractory materials and of coal ash stipulate the following procedures for cone preparation:

A.S.T.M. C24–35: Preparation for Test Cones

3(*a*).—The dried sample shall be thoroughly mixed and, after the addition of sufficient dextrine, glue, gum tragacanth, or other alkali-free organic binder and water, shall be formed in a truncated trigonal pyramid with its base at a small angle to the trigonal axis and of the following dimensions: Overall height (between planes perpendicular to the trigonal axis), $1^1/_{16}$ in.; length of side of the truncated tip, $^1/_{32}$ in.; length of the two longer sides of the base, $^9/_{32}$ in.; base at an external angle of 82 degrees to one face and perpendicular to the symmetry plane through the opposite edge of the pyramid.

3(*b*).—When dry, the test cones may be subjected to a preliminary firing at a temperature not exceeding 1300°C. for the purpose of sintering them into a firm condition to permit handling.

A.S.T.M. D271–40: Preparation of Cones

29.—Moisten the ignited ash with dextrine solution (10%) and work into a plastic mass with a spatula. Mold the plastic material into small triangular pyramids, $^3/_4$ in. in height and $^1/_4$ in. in width at sides of base. The pyramids are made by firmly pressing the plastic material with a steel spatula into a brass mold. Strike off the surface smooth and remove the cone from the mold by applying a small knife blade at the base. Mount the cones when dry in a refractory base composed of a mixture of equal parts of kaolin and calcined alumina. Moisten the base mixture to make it workable, and spread part of it out on a sheet-iron plate. Then mount the cone in a vertical position in a small hole made in the base, and pat base material into hole around the bottom of cone to fill the crevices and make the cone stand firmly. Usually five cones are mounted in one base. Dry the sheet-iron plate with test piece on a hot plate. Ignite the cones at a red heat for 30 minutes in an open muffle to remove the carbonaceous material.

II. Preparation of Cones of Nonplastic Material

The foregoing standard procedure for molding the cones is undoubtedly satisfactory for plastic or semi-plastic refractory materials. For nonplastic materials, however, such as silica and alumina, the preparation of cones for fusion tests requires a different procedure.

(1) Procedure

The chromium-plated cone mold (which has either (*a*) a truncated, trigonal pyramid cavity, $1^1/_{16}$ in. high and $^9/_{32}$ in. on the long sides at the base for refractory materials, or (*b*) a pyramid cavity, $^3/_4$ in. high and $^1/_4$ in. on the sides at the base for coal ash) is heated in a low Bunsen flame or on a hot plate until the mold is hot to the touch. A small camel's hair brush is used to paint the mold cavity with molten paraffin; the excess of paraffin is shaken or wiped off, and the mold is chilled on a cake of ice or cold copper plate.

The refractory material (−70-mesh, A.S.T.M.) or ignited ash (−200-mesh) is moistened with only enough 10% dextrine solution (to which has been added 10 to 15 drops of oil of wintergreen to prevent fermentation of the stock solution) to make a stiff mass when it is worked with a spatula. A spatula is held over the base of the pyramid cavity of the chilled mold, and the cone material is pressed firmly into the cavity with a small slick (made from a $^1/_8$-in. diameter brazing rod); the spatula is also used to strike off a smooth surface. The cone mold is held at the cone apex end with a pair of pliers and heated in a Bunsen flame or on a hot plate until it is very warm to the touch or until the paraffin is fluid at the edges of the cone. The cone is then removed by applying a triangular rod at the cone base; the mold cavity is cleaned with a cloth, repainted with paraffin, chilled, and the foregoing procedure is repeated. The cones, as removed, are pushed onto a glazed porcelain plate and dried for 15 minutes in a drying oven.

When the cones are dry, they are mounted in a refractory base plaque in accordance with the usual A.S.T.M. specifications. Molds of the desired shape and height aid in the preparation of the refractory plaque before the cones are mounted. A piece of paper placed under the plaque will prevent it from sticking to the refractory plate during drying and sintering.

This procedure for cone preparation has been found satisfactory for plastic and nonplastic material alike, and it is estimated that from 94 to 98% of cones thus produced are of perfect shape.

Department of Metallurgical Engineering
Michigan College of Mining and Technology
Houghton, Michigan

* Received January 31, 1942.

WAR EMERGENCIES REQUIRE

Cooperation of Technologists
Working to Increase Industrial Facilities
For War Needs and Postwar Security

THE AMERICAN CERAMIC SOCIETY

A Collaboration of Ceramists in Fact Finding and Fact Recording
A Bureau of Research Financed by Aggressive Ceramists,
Personal and Corporation, Who Know by Experience the Value of
Proved Facts Applied to Ceramic Ware Production

CERAMIC CORPORATION MEMBERSHIP IN THE AMERICAN CERAMIC SOCIETY

IS A WAR EMERGENCY

Assuring Present War Needs and Postwar Survival by Research

Personal $12.50 per year **Corporation $25.00 (minimum)**

The American Ceramic Society, 2525 North High Street, Columbus, Ohio